2018

Guest-Host Interactions To Engineer Injectable Hydrogels With Controlled Degradation And Release For Cardiac Repair

Joshua Eugene Mealy
University of Pennsylvania, mealy@seas.upenn.edu

Guest-Host Interactions To Engineer Injectable Hydrogels With Controlled Degradation And Release For Cardiac Repair

Abstract
Guest-host chemistry is an emerging tool in the preparation of biomaterials. Towards the design of hydrogels, guest-host chemistry has been used to impart unique shear-thinning and self-healing properties that allow these materials to be injected through syringes and catheters as a single component, avoiding complications associated with traditional covalent systems. As a treatment for myocardial infarction, injectable guest-host hydrogels may be injected directly into the myocardial wall and have shown therapeutic benefit in a number of strategies, including drug delivery, cell delivery, and tissue bulking. As delivery systems, injectable hydrogels provide controlled release of payloads that attenuate maladaptive remodeling of the left ventricle, by inhibiting expression of proteases, recruiting cells to the region, or otherwise stimulating therapeutic biological processes such as angiogenesis. Guest-host biomaterials must be refined and advanced to overcome challenges associated with delivering therapeutics in these areas, as well as to provide novel materials platforms for investigating therapeutic delivery in the future. This dissertation describes the engineering of two injectable hydrogel platforms that address challenges in the delivery of therapeutics after myocardial infarction. Each of these systems is investigated both in vitro for an understanding of material properties and the parameters that tune them, as well as in vivo, in a number of clinically relevant animal models and therapeutic targets. In the first aim of this thesis, isotropic guest-host hydrogels are designed for the sustained release of a variety of small molecules. Through the control of small molecule binding with cyclodextrin host moieties engineered in the hydrogel, we show that both cyclodextrin content and molecule affinity for cyclodextrin are critical factors that provide tunable release of small molecules from these systems. Furthermore, we demonstrate that this system is broadly applicable to the release of a number of pharmaceutical small molecule payloads. In the second aim of this thesis, isotropic guest-host hydrogels are specifically formulated for the delivery of the small molecule protease inhibitor SD-7300, a therapeutic requiring local delivery after myocardial infarction. Here we demonstrate that the engineered guest-host hydrogels provide sustained release and retain activity of this molecule, which in turn provides improved functional and biological outcomes in a large-animal model of myocardial infarction. In the third aim of this thesis, guest-host chemistry is utilized to assemble microstructured granular hydrogels for the design of multifunctional material platforms. Granular hydrogels are demonstrated to have disease responsivity in myocardial infarction, and functional benefit through the delivery of the chemokine SDF-1α.

Degree Type
Dissertation

Degree Name
Doctor of Philosophy (PhD)

Graduate Group
Bioengineering

First Advisor
Jason A. Burdick

Keywords
drug delivery, guest-host chemistry, hyaluronic acid, hydrogel, microparticle, myocardial infarction

GUEST-HOST INTERACTIONS TO ENGINEER INJECTABLE HYDROGELS WITH CONTROLLED DEGRADATION AND RELEASE FOR CARDIAC REPAIR

Joshua E. Mealy

A DISSERTATION

in

Bioengineering

Presented to the Faculties of the University of Pennsylvania

in

Partial Fulfillment of the Requirements for the

Degree of Doctor of Philosophy

2018

Supervisor of Dissertation

_____

Jason A. Burdick, Ph.D. Professor of Bioengineering

Graduate Group Chairperson

_____

Ravi Radhakrishnan, Ph.D. Professor of Bioengineering

Dissertation Committee

David Issadore, Ph.D. Professor of Bioengineering

Robert Mauck, Ph.D. Professor of Orthopedic Surgery

Robert Gorman M.D. Professor of Surgery

ACKNOWLEDGEMENTS

Like many, my journey through graduate school has been filled with successes and failures, serendipity and bad luck, and emotional highs and lows. Throughout this odyssey, I have had an incredible group to support me scientifically and personally in a way that I do not believe many receive. For that, I want to acknowledge and thank everyone who has contributed to my career so far, and say that it has been truly special to know each and every one of you.

Immediately, I would like to thank my committee members, Professor David Issadore, Professor Robert Mauck, and Professor Robert Gorman, who have provided guidance and perspective reviewing this work over the past few years. I would like to thank Jason Burdick, my thesis advisor and mentor who has guided me throughout my academic and personal growth during my PhD. I was originally drawn to conducting my thesis work in Jason's lab because of the combination of academically interesting science with translational motivation but also because of Jason's personal qualities. What I suspected when I chose to come here, and have found to be true every day since, is that in addition to being an excellent scientist, Jason is truly a wonderful mentor and friend.

I would also like to thank the past and present members of the Burdick lab for their contribution to my work. The Burdick lab has some of the best people in the world, and every one is better than the last. Having a group of colleagues and friends such as these to work with has truly been blessing, and the camaraderie here has been a continual source of support throughout my dissertation work. I'd like to especially mention Dr. Chris Rodell and Dr. Chris Highly, who have both been wonderful scientific contributors and personal friends to me. I would be so lucky to have a group like this at the next stage of my career.

Next I would like to thank the collaborators who have assisted me in this work. Contributions from Dr. Chris Rodell, Dr. Heon-Ho Jeong, Dr. David Issadore, Dr. Daeyeon Lee, as well as my mentee students James Howard and Justin Morena have made it possible for me to advance the materials science and chemistry of my work. Furthermore, why I believe this work is so special, is because of collaborations with surgical groups that can implement these systems in translational scenarios. Of this group, I would like to especially thank Dr. Jenn Chung, Dr. Pavan Atluri, and Dr. Frank Spinale and his team for their tireless efforts in providing surgical support and expertise for these projects.

Personally, I would like to thank my family, immediate and extended, for seeing me to this point in my life. I want to thank my mom, Dana, and dad, Darryl, who have always believed in me, loved me, and given me every tool I needed to be a successful scientist and good person. I want to thank my brother, whose fearlessness is a continual source of inspiration and whose friendship is priceless. I love you all.

Finally, I want to thank my fiancée Brittany Weikel, the most loving and caring person that I have ever known. In addition to pouring her heart and soul into caring for the neediest children in Philadelphia, she found time to help support one more person. Whether comforting me while times were tough, giving me assistance while I was busy and stressed, or sharing in the joys of my success, she is a wonderful partner and the rock that I have relied on throughout this work.

Thank you all, I couldn’t have done it without you.

ABSTRACT

GUEST-HOST INTERACTIONS TO ENGINEER INJECTABLE HYDROGELS WITH CONTROLLED DEGRADATION AND RELEASE FOR CARDIAC REPAIR

Joshua E. Mealy

Jason A. Burdick, Ph.D.

Guest-host chemistry is an emerging tool in the preparation of biomaterials. Towards the design of hydrogels, guest-host chemistry has been used to impart unique shear-thinning and self-healing properties that allow these materials to be injected through syringes and catheters as a single component, avoiding complications associated with traditional covalent systems. As a treatment for myocardial infarction, injectable guest-host hydrogels may be injected directly into the myocardial wall and have shown therapeutic benefit in a number of strategies, including drug delivery, cell delivery, and tissue bulking. As delivery systems, injectable hydrogels provide controlled release of payloads that attenuate maladaptive remodeling of the left ventricle, by inhibiting expression of proteases, recruiting cells to the region, or otherwise stimulating therapeutic biological processes such as angiogenesis. Guest-host biomaterials must be refined and advanced to overcome challenges associated with delivering therapeutics in these areas, as well as to provide novel materials platforms for investigating therapeutic delivery in the future.

This dissertation describes the engineering of two injectable hydrogel platforms that address challenges in the delivery of therapeutics after myocardial infarction. Each of these systems is investigated both *in vitro* for an understanding of material properties and the parameters that tune them, as well as *in vivo,* in a number of clinically relevant

animal models and therapeutic targets.

In the first aim of this thesis, isotropic guest-host hydrogels are designed for the sustained release of a variety of small molecules. Through the control of small molecule binding with cyclodextrin host moieties engineered in the hydrogel, we show that both cyclodextrin content and molecule affinity for cyclodextrin are critical factors that provide tunable release of small molecules from these systems. Furthermore, we demonstrate that this system is broadly applicable to the release of a number of pharmaceutical small molecule payloads.

In the second aim of this thesis, isotropic guest-host hydrogels are specifically formulated for the delivery of the small molecule protease inhibitor SD-7300, a therapeutic requiring local delivery after myocardial infarction. Here we demonstrate that the engineered guest-host hydrogels provide sustained release and retain activity of this molecule, which in turn provides improved functional and biological outcomes in a large-animal model of myocardial infarction.

In the third aim of this thesis, guest-host chemistry is utilized to assemble microstructured granular hydrogels for the design of multifunctional material platforms. Granular hydrogels are demonstrated to have disease responsivity in myocardial infarction, and functional benefit through the delivery of the chemokine SDF-1α.

Table of Contents

LIST OF FIGURES AND TABLES

CHAPTER 1

INTRODUCTION

1.1. SIGNIFICANCE

Cardiovascular disease accounts for 17.3 million deaths annually and is the leading cause of death across the globe; within cardiovascular diseases, ischemic heart disease is the most deadly.[1,2] Specifically, almost one in four deaths in the United States, or 610,000 individuals die every year of heart disease.[3] Myocardial infarction (MI) is among the most prominent and lethal types of heart disease, affecting 735,000 Americans annually. MI occurs after an occlusion of the coronary artery disrupts the normal perfusion of the myocardium (**Figure 1.1**). This ischemic event leads to cell necrosis and inflammation, including the loss of cardiomyocytes - the contractile cell of the heart.

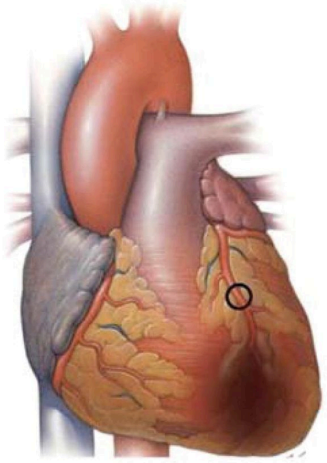

Figure 1.1. Schematic representation of myocardial infarction. Plaque buildup within a coronary artery ruptures, leading to thrombus formation and occlusion of the vessel. Ischemia as a result of this occlusion leads to muscle damage in the myocardial tissue. Adapted from Bax et al.[4]

As an immediate treatment, interventions are focused on restoring blood flow (i.e. repurfusion) to the myocardium through biochemical approaches such as fibrinolytics or

thrombolytics, or through minimally invasive surgical approaches such as coronary angioplasty.[5] In the case of damage to the coronary arteries, blood flow may be restored through bypass surgery.[6] These treatments are effective in improving the initial patient survival after infarction; however, they fail to address the long-term biological and structural changes that occur with MI. Ultimately, many patients with an MI proceed to develop heart failure in the long-term, with nearly a 50% mortality rate at 5 years after hospitalization.[1]

Managing heart failure currently involves pharmacologic interventions to increase blood flow to the myocardium and to reduce stress on the heart by reducing heart rate and blood pressure (beta blockers and ACE inhibitors).[5] Currently, the only way to return to stable, healthy cardiac function in those with end-stage heart failure is through transplant, where donor hearts are very limited.[7] Mechanical interventions such as left ventricular assist devices (LVADs) provide a temporary solution to induce systemic blood flow; however, LVADs are not currently seen as a permanent solution for patients with heart failure.[8,9] Collectively, while these treatments are effective in mitigating the issues associated with heart failure after MI, they fail to directly address the underlying biological processes involved early on in the progression of the disease.

1.2. DISEASE PROGRESSION AND LEFT VENTRICULAR REMODELING AFTER MI

The initial ischemic event that leads to MI is followed by a three-phase wound healing response consisting of inflammatory, proliferative, and maturation phases (**Figure 1.2**).[10] During the inflammatory phase, monocytes infiltrate the infarct region and differentiate into macrophages, which serve to phagocytose cellular debris, secrete a variety of inflammatory proteins, and stimulate fibroblasts towards the secretion of proteases, which degrade the local environment. These protease levels remain elevated,

and along with a concurrent decrease in the endogenous inhibitors (tissue inhibitors of metalloproteinases, TIMPs), contribute to an overall increase in proteolytic activity and a general loss of integrity of the extracellular matrix in the infarcted myocardium.[11-14] During the proliferative phase, fibroblasts begin to deposit fibrous tissue and in the maturation phase, matrix crosslinking and further apoptosis of myofibroblasts leads to the formation of a fibrous scar. Generally, the beginning of cardiomyocyte death and the inflammatory phase commences within hours of the initial infarct, and can last for several days to a week after infarction. The proliferation of myofibroblasts follows, as well as the upregulation of protease activity and can last for several weeks. Finally, in the following weeks to months after these phases, scar tissue matures.[10] While these phases give a general outline of the biological changes after MI, they are not necessarily sequential, as things such as protease activity and cardiomyocyte death are progressive with time, and often continue for months after an MI.

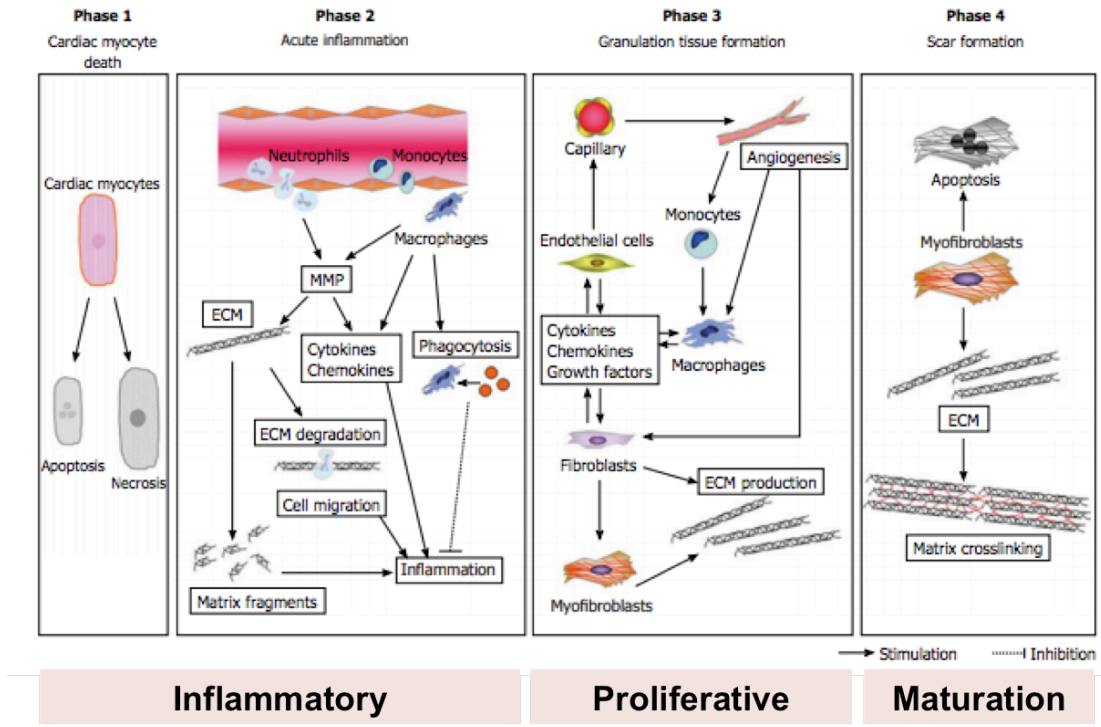

Figure 1.2. Phases of wound healing after myocardial infarction and their underlying biological processes. The initial ischemic event as part of myocardial infarction is followed by three distinct phases with unique underlying biological processes. During the inflammatory phase, cardiomyocytes undergo apoptosis and necrosis, leading to an immediate loss of the functional cell type in the infarcted region. This is followed by an invasion of neutrophils and monocytes that directly and indirectly contribute to an elevation in MMP activity, phagocytosis, and general degradation of the extracellular matrix. This phase is followed by a proliferative phase during which fibroblasts differentiate into myofibroblasts and commence production of collagenous matrix, while endothelial cells contribute to angiogenesis and the production of new vessels. Finally, in the maturation phase, matrix is crosslinked into a dense collagenous scar. Adapted from Matsui et al. [10]

Concomitant with these biological changes, global changes occur in the left ventricle (LV) known as left ventricular remodeling.[15] During LV remodeling, the LV transitions to a dilated state, which includes expansion of the initial infarct region and thinning of the myocardial wall (**Figure 1.3**).[12,15] These changes result in a loss of pumping efficiency in the heart and ultimately contribute to the progression of long-term heart failure and mortality.[12,15,16]

The elevation of matrix metalloproteinases (MMPs) and subsequent loss of matrix mechanics has largely been implicated in LV remodeling.[11-14,16-19] These

proteinases are secreted by a variety of cells, including endogenous cardiac fibroblasts and cardiomyocytes as well as invading cells mobilizing as part of the inflammatory response. Of key importance after MI, are MMP-1, MMP-2, MMP-3, MMP-7, MMP-8, MMP-9, and MMP-14, which have been shown to increase after MI.[20] This activity often persists long after the development of an infarction (**Figure 1.4**). Directly, this family of proteins is responsible for degradation of highly specific peptide sequences in the ECM. This proteolytic activity alters a number of downstream processes in the infarcted myocardium, including tissue mechanics, inflammation, cell invasion, and even direct feed-forward regulation of other subtypes of MMPs.[20,21] Ultimately, elevation of MMPs has been correlated with a loss of function in the myocardium.

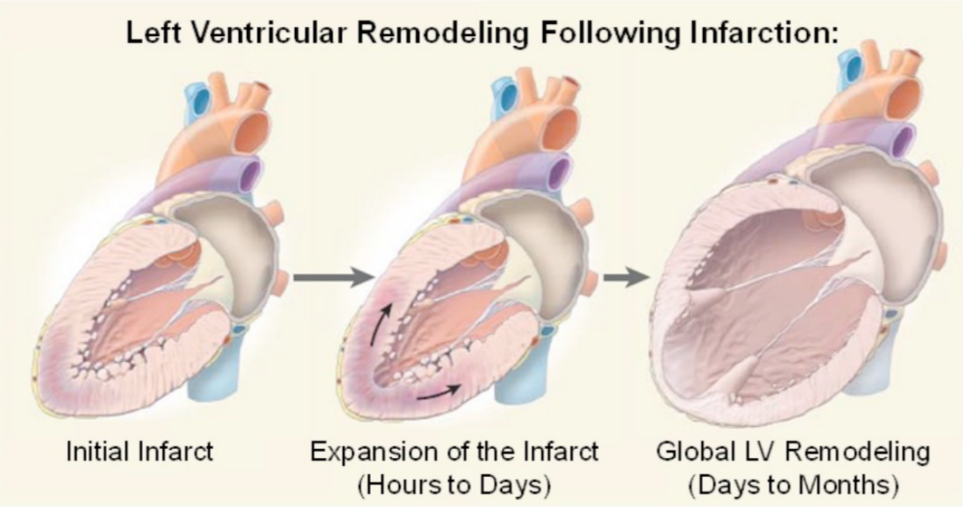

Figure 1.3. Ventricular remodeling after acute MI. After initial infarction, the portion of the myocardium affected by the infarct begins to expand during the initial hours to days. Within days to months, there is global remodeling in the LV that leads to a decrease in systolic function, ventricular dilation, and thinning of the myocardial wall, all of which contribute to the progression of long term heart failure. Adapted from Jessup et al.[23]

In addition to the elevation of proteinases after MI, a subsequent down-regulation of their endogenous inhibitors, TIMPs, also contributes to the net effect of this proteolytic activity. Because of the disruption of this balance, experimental interventions restoring MMP inhibitory action in the myocardium through the delivery of exogenous inhibitors

have proven effective in improving functional outcomes.[19,22] Indeed, it has even been hypothesized that currently administered clinical therapeutics may have partial benefit due to their influence on MMP activity and regulation in the myocardium.[20]

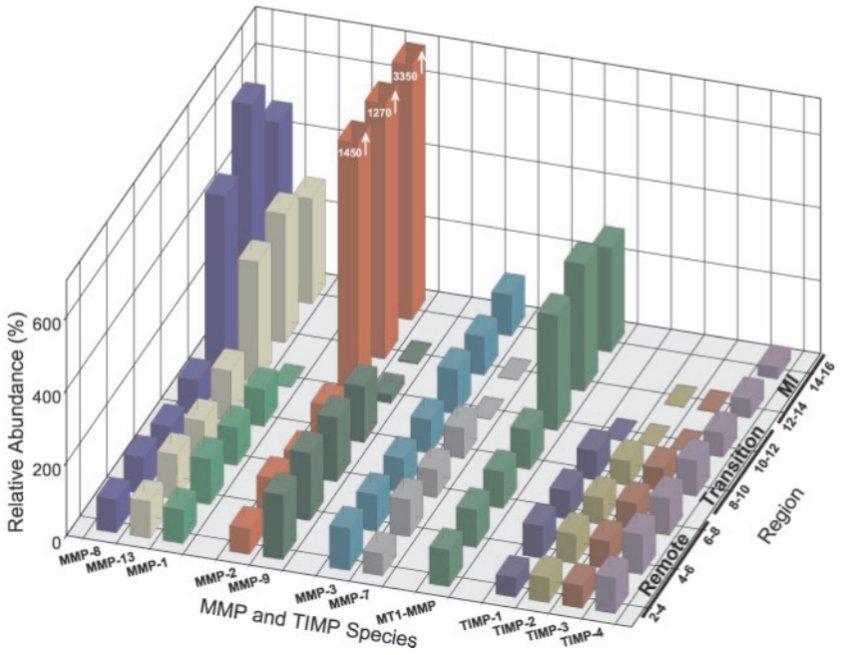

Figure 1.4. Relative activity of MMP subtypes and TIMP subtypes in various regions of the myocardium. Analyzed at 8 weeks after infarction in an ovine model of MI, researchers observed an elevation of MMP activity most strongly in the infarct region in the MMP-2, MMP-8, MMP-13, and MT1-MMP subtypes. This was coupled with a relative decrease in TIMP-1,-2, and -3 subtypes in the infarct region. Adapted from Wilson et al.[11]

Ultimately, this collection of maladaptive changes presents a number of crucial barriers that prohibit the healing of the myocardium and a return to the pre-MI healthy tissue state. First, an acute loss of matrix integrity contributes to infarct expansion and global LV remodeling. Furthermore, necrosis of cardiomyocytes provides an irreversible loss in contractility, as these cells have little innate regenerative capacity. Finally, in the long term, the infarcted tissue transitions to a collagen-dense non-contractile tissue with little vascularization. Despite these challenges, understanding of the remodeling

processes can help guide new patient therapies. For example, blocking of early increases in MMP activity to salvage matrix mechanics or regenerative approaches revascularizing or inducing cardiomyocyte proliferation in the infarct may improve clinical outcomes. Often, these approaches require localization to the myocardium, and are facilitated through the use of biomaterials.

1.3. HYDROGELS IN CARDIAC REMODELING

Biomaterials have recently become a strategy to address the barriers to recovery that are faced after an infarction.[24] Initially, mechanical restriction of the left ventricle using epicardial wraps was shown to be effective in attenuating LV dilation and infarct expansion.[25-27] These studies were followed by the use of commercially available dermal fillers as direct injections into the myocardial wall, which were also successful in attenuating LV remodeling and promoting improved functional outcomes.[28]

In addition to polymeric meshes, hydrogels have also been used as therapies to the heart after MI. Hydrogels are water-swollen polymer networks that can be made from synthetic or natural polymers, and are cross-linked in either covalent or non-covalent manners. Early work investigating the utility of hydrogels in the myocardium began with Christman et al and the use of fibrin glues.[29] This field has evolved and numerous types of hydrogels have now been investigated after MI.[24] Synthetic materials such as pNIPAAM and PEG have been explored, as well as a wide range of natural materials including alginate, collagen, chitosan, hyaluronic acid, as well as extracellular matrix products.[30-38] These materials have been crosslinked utilizing a variety of mechanisms, including covalent mechanisms, thermo-responsive gelation, ionic crosslinking, enzymatic crosslinking, as well as self-assembly. Hydrogels are most commonly

delivered directly into the myocardial wall, which has been done through direct epicardial intramuscular injections, as well as intra-coronary and endocardial approaches.

Recently, these approaches have resulted in the formation of several products in early phase clinical trials. VentriGel, a product of Ventrix, is a porcine ECM product that is delivered via an endocardial catheter based approach and is in Phase 1 clinical trials (NCT02305602). Algisyl, a product of LoneStar Heart Inc., is an alginate product that is directly injected into the myocardium. Algisyl has shown efficacy in improving aerobic capacity of patients presenting heart failure, where hydrogel injections are applied concurrently with other standard treatment procedures such as valve replacement or bypass grafts.[39,40] In short, hydrogels have developed into a robust tool to address LV remodeling that is beginning to see clinical translation.

Mechanistically, these pre-clinical and clinical hydrogels are thought to impact remodeling by altering the mechanical forces experienced by the heart through bulking the myocardial wall.[24] The law of Laplace states that the wall stress experienced by the LV is inversely proportional to the thickness of the myocardial wall. By increasing the wall thickness with hydrogel injections, wall stress can be reduced (**Figure 1.5**). Both modeling and empirical approaches have shown the effect of alterations in injection volume and material mechanics on the mechanical forces acting on the myocardium.[37,41] While it is likely that the functional improvements observed are a result of direct mechanical alterations in the myocardium, a number of biological pathways persist that are not targeted by hydrogel mechanics alone. For example, biomaterials through their innate or designed inflammatory response may lead to alterations in local collagen production that can act to stabilize the tissue.

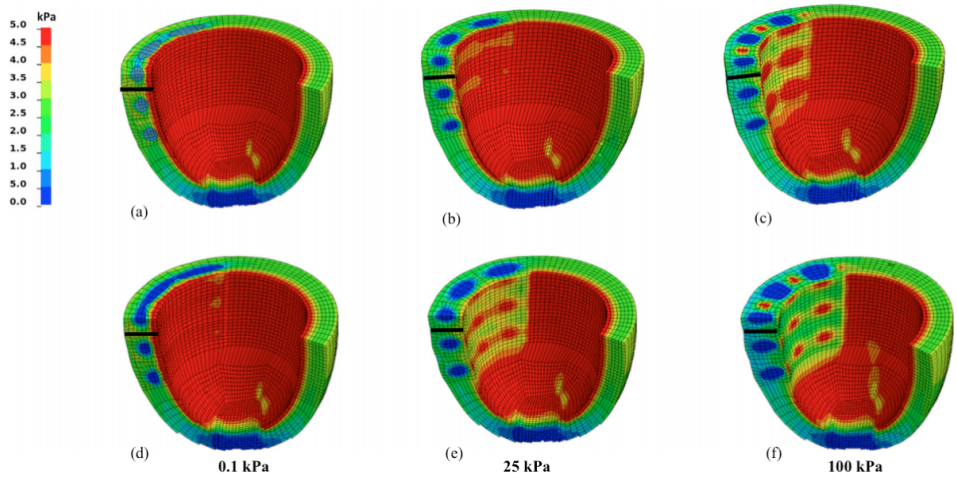

Figure 1.5. Finite element model of hydrogel injection into the myocardial wall. Nine injection sites of 150 µL hydrogel volumes at 0.1 kPa (a), 25 kPa (b), and 100 kPa (c) or using 300 µL volumes at 0.1 kPa (d), 25 kPa (e), and 100 kPa (f). Myocardial wall stress (represented by the colorimetric scale) is reduced proportionally to hydrogel stiffness and volume of injection. Adapted from Wang et al. [41]

In addition to providing mechanical intervention, hydrogels have the capacity to provide numerous other therapeutic strategies in MI. As lack of innate cellular regeneration is a significant barrier to restoration of normal function in the myocardium, cellular delivery is one approach to improving cardiac function. Numerous clinical trials have been investigated on the delivery of a variety of cell types (bone marrow derived stem cells, mesenchymal stem cells, endothelial progenitor cells, and cardiac stem cells) to the myocardium.[42] Clinical efficacy of these trials has been mixed and have largely been dependent on both cell lineage, viability, and retention in the myocardium.

As direct injections of cells alone often result in significant cell death, hydrogels have been designed as carriers for a variety of cell types to optimize cell viability, retention, and cell-material interactions at the injection site.[29,43,44] While these strategies have been effective, it is often difficult to pinpoint mechanistically the effect of cell delivery as their interactions are often complex. Additionally, logistical concerns of cell source and quality are often a concern when translating these therapies.

1.4. HYDROGELS FOR DRUG DELIVERY IN THE MYOCARDIUM

Towards more controlled biological interventions, hydrogels have also been used as drug delivery vehicles for a wide variety of payloads. From a design perspective, hydrogels have numerous features that can be tailored to influence drug release across a range of size scales (**Figure 1.6**). At the largest scale, hydrogel size can influence drug release, as smaller sizes and increasing surface area contact with the environment will lead to more rapid release.[45] At the meso scale, hydrogels can be designed as either non-porous materials or to be macroporous, with an increasing porosity often associated with more rapid drug release.[45]

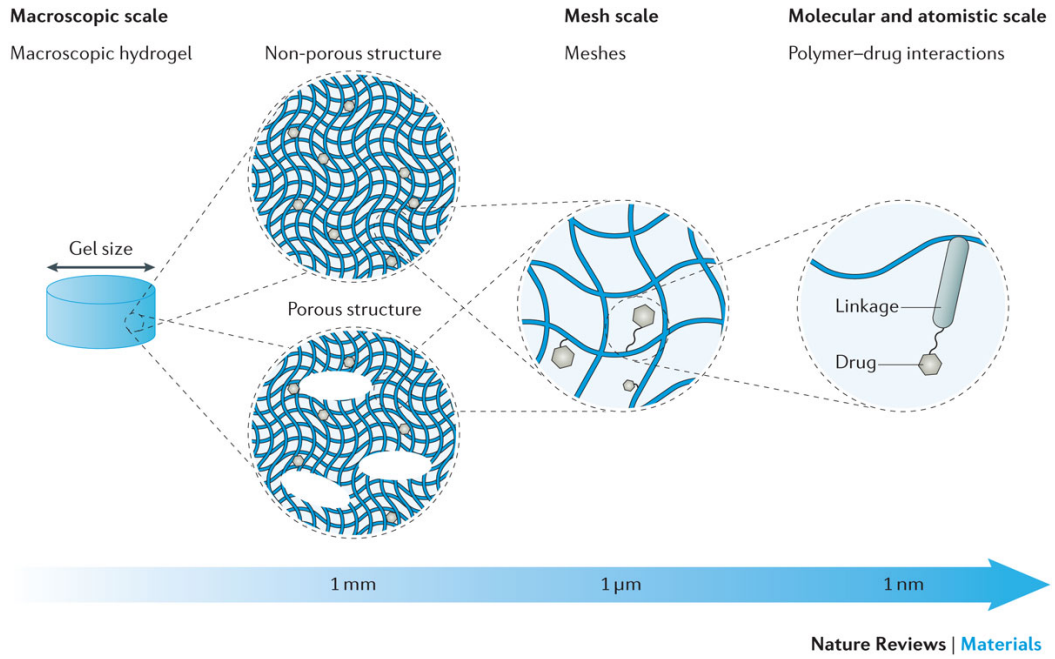

Figure 1.6. Overview of hydrogel design parameters influencing drug release. Hydrogel size, porosity, mesh-size, and chemical linkers all contribute to the controlled release of encapsulate payloads. Adapted from Li et al. [45]

At the micro- and nano-scales, hydrogel mesh size is also a key influencer of drug release properties. This property may be influenced through a variety of factors including polymer concentration, crosslinking density, and crosslinker degradability (**Figure 1.7**).[45] This mesh size can be largely static, or increase through hydrogel

swelling and degradation (**Figure 1.7**). Furthermore, the relative relationship of mesh size to drug size also contributes to release behavior of drugs from hydrogels, with meshes much larger than the drug providing rapid diffusive mediated release of drug molecules and meshes on the same or smaller size scale than drugs being mediated primarily through degradation or slow diffusive release.[45] Because of this, as a handle for tuning drug release, hydrogel mesh size is often restricted for utilization with large molecules such as proteins or plasmids.

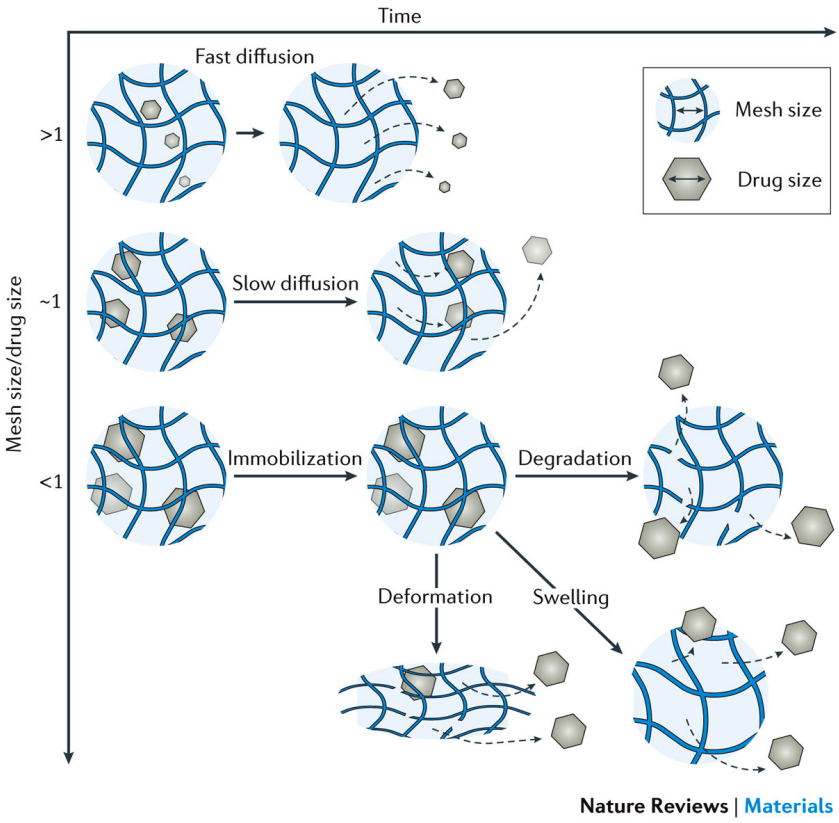

Figure 1.7. Influence of mesh size on encapsulated drug release from hydrogels. Hydrogel mesh size influences drug release by exerting an effect on diffusive, degradation, or swelling mediated drug release. The degree to which hydrogel mesh influences drug retention/release is largely dependant on the relative size scales of the mesh size and drug payload. Adapted from Li et al.[45]

Finally, drug release may be influenced at the nano scale through control of payload interactions with the hydrogel. Covalent conjugation strategies may be utilized to directly immobilize therapeutics on the hydrogel, with linkages being designed to be

stable or cleavable under a variety of conditions (**Figure 1.8**).[46] Furthermore, non-covalent interactions, such as electrostatic or hydrophobic interactions may also be used to introduce an affinity of therapeutics to the hydrogel, and subsequent slower release properties.[45] While these strategies may be used for large molecule therapeutics, they are almost exclusively used to manipulate the release of small molecules from hydrogel materials.

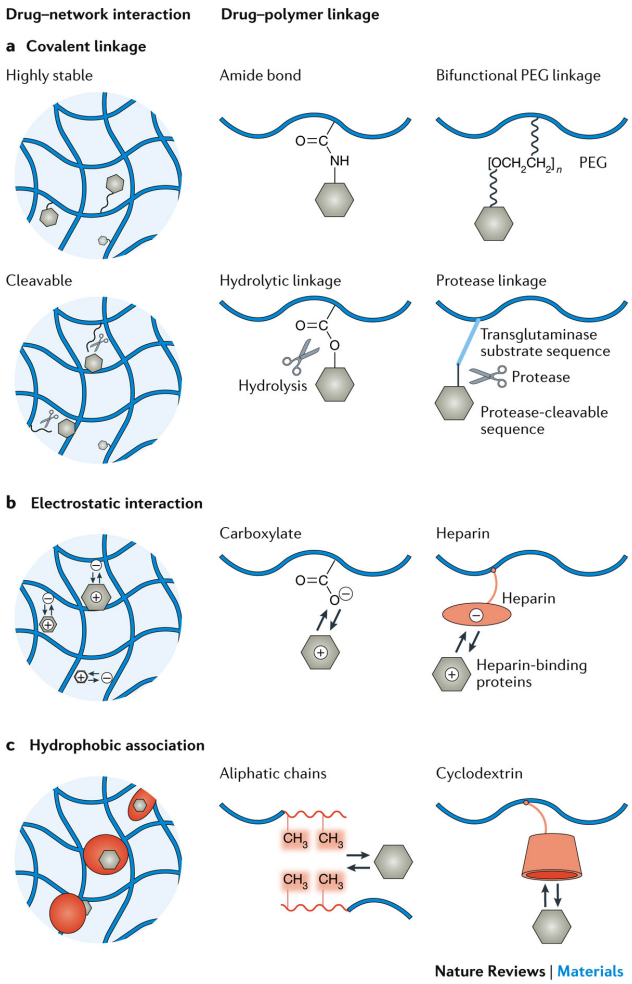

Figure 1.8. Chemical interactions between payload and hydrogel may influence drug release properties. Designing chemical interactions into the hydrogel provides another mechanism for controlling drug release properties. This may be achieved through covalent conjugation of drugs to the hydrogel, or by designing electrostatic or hydrophobic interaction into the hydrogel material to provide affinity to the hydrogel for the payload molecule.

A variety of protein-based payloads have been delivered to the heart, targeting a number of biological steps after MI.[47] In one approach, hydrogels were used to deliver anti-apoptotic molecules in order to attenuate cell death following MI.[48] In one study, Ruvinov et al. developed alginate microspheres encapsulating insulin-like growth factor 1 (IGF-1) and hepatocyte growth factor (HGF).[48] IGF-1 is a cytoprotective factor while HGF has angiogenic and anti-fibrotic properties. These microspheres were administered to the infarct to provide a sustained release of both drugs, with the hypothesis that there would be a cumulative effect from both factors. Injection of these microspheres after MI showed improvements in key markers such as reduction in fibrotic area, improvement in apoptotic cells, increased vessel densities and proliferation of cardiomyocytes at 4 weeks after injection, as compared to factors injected in saline and blank microspheres.

IGF-1 has also been used in other classes of hydrogels, such as a self-assembling peptide based hydrogel designed by Davis et al.[49] This material utilized streptavidin-biotin binding to provide long-term release of IGF-1 (84 days) and showed significant functional benefits when the hydrogels were utilized to co-deliver IGF-1 and neonatal cardiomyocytes. IGF has also been delivered using a PEG-based self-assembling block copolymer system that can be administered using catheter-based approaches. This material has shown efficacy in improving functional outcomes such as ejection fraction, as well as improvement in tissue-level outcomes such as the formation of new cardiomyocytes, and increased vascularization.[50]

In addition to targeting cytoprotection, hydrogels have been widely used for the delivery of angiogenic proteins, as a means to promote neovascular formation in the ischemic myocardium. One factor, fibroblast growth factor (FGF) has been used as a payload in a variety of hydrogel systems[51-56]. While FGF is a potent stimulator of angiogenesis, it suffers from a very short half-life in-vivo. As a means to address this limitation, Sakakibara et al utilized gelatin hydrogel microspheres as a delivery vehicle

for FGF, and showed through radiolabeling studies that effective doses of FGF could be sustained in the myocardium.[52] Furthermore, this corresponded to improvements in LV remodeling and neovasculature formation at 4 weeks after MI. This growth factor has also been delivered from a variety of other hydrogels, including thermoresponsive chitosan hydrogels.[51]

Vascular endothelial growth factor (VEGF), a stimulator of proliferation and migration in endothelial cells, has frequently been delivered to stimulate the growth of new vessels. While this is a key component in angiogenesis, often vessels require the recruitment and proliferation of smooth muscle cells to provide appropriate maturation. This dual delivery approach has been conducted using simple alginate hydrogels, as well as coacervates to provide for further control of release timing for each of these molecules.[57,58] These approaches have shown success in the generation of αSMA positive vessels over either growth factor individually, as well as benefits to cardiac function. In addition to delivering these factors as freely soluble components, other groups have immobilized angiogenic factors on hydrogel surfaces to provide a sustained effect after injection. For example, Wu et al. immobilized VEGF to PEG block copolymers using NHS chemistry.[59] These VEGF modified block copolymers were thermoresponsive, to provide a gelation mechanism after injection into the myocardium. Results from this study showed improved cardiac function and tissue morphology (scar fraction, capillary density) in hydrogels modified with VEGF as opposed to unmodified hydrogels, suggesting that immobilized proteins are also an effective strategy for inducing biological responses in the myocardium.

Other recent strategies focus on delivering therapeutics that manipulate cell recruitment and cell proliferation in the myocardium. In one strategy, stromal derived factor-1 alpha (SDF-1α) was utilized for its ability to recruit progenitor cells. SDF-1α has been delivered via covalent immobilization to self-assembling peptide hydrogels, as well

as encapsulation in hyaluronic acid hydrogels.[60-62] These strategies have shown structural benefits, including an increase in progenitor cells possessing the receptor for SDF and a concomitant increase in capillary density, as well as benefits in cardiac function. Furthermore, other SDF analogs have been delivered in order to improve the stability of the chemokine signal, as SDF is susceptible to protease degradation.[61] Other strategies focus on directly improving proliferation of non-proliferative cardiomyocytes. Mir-302, a micro RNA influencing transcription along the Hippo pathway, was delivered using an injectable hyaluronic acid hydrogel.[63] Utilizing a confetti mouse model, the study showed the ability for this payload to stimulate clonal expansion of cardiomyocytes, which contributed to overall improvements in cardiac function.

One final strategy that hydrogels have employed for drug delivery is the delivery of inhibitors for MMPs. Proteases are maladaptively upregulated in the infarct tissue, and inhibition of this activity has lead to improved outcomes through the use of systemically administered protease inhibitors.[22,64-67] Local delivery with hydrogels, however, attenuates off-target effects of these inhibitors on normal matrix turnover, which is important to mitigating harmful side effects of these molecules during systemic administration. TIMPs are protein-based inhibitors that the body uses to regulate MMP activity. As a strategy for local MMP inhibition, TIMP-3 has been delivered locally from injectable hydrogels in pig studies.[68] As a means to provide different mechanisms of control, TIMP-3 was delivered passively using covalently crosslinked hydrogels, or in response to protease degradation in protease cleavable hydrogels.[68,69] These systems showed the benefit of TIMP-3 payload in hydrogels on local MMP activity as well as ventricular geometry and function. This strategy has also been employed utilizing peptide-based inhibitors delivered using a thermogelling system based on NIPAAM, which showed an ability to decrease MMP activity and improvements in ventricular structure and function. [70]

1.5 CONCLUSIONS

MI is a widely prevalent condition that leads to an array of progressive changes in the heart, which ultimately may contribute to long-term heart failure. Current treatment methods fail to address the underlying biological changes that occur after an infarction at the acute time points, driving a need for improved therapies. As a result, injectable hydrogels have developed into a burgeoning field of cardiac intervention, providing mechanical support in the left ventricle after MI. These materials have subsequently been used to further address the underlying biology as drug delivery vehicles, delivering a variety of payloads locally that can attenuate cell death, promote cell recruitment and proliferation, generate new vasculature, or provide inhibition of MMPs.

1.6 REFERENCES

1. Benjamin EJ, Blaha MJ, Chiuve SE, Cushman M, Das SR, Deo R, et al. Heart disease and stroke statistics-2017 update: a report from the American Heart Association. Circulation. 2017;135(10):e146-e603.
2. Mozaffarian. Heart Disease and Stroke Statistics-2015 Update: A Report From the American Heart Association (vol 131, pg e29, 2015). Circulation. 2015;131(24):E535-E.
3. Heart Disease Facts and Statistics cdc.gov: Center for Disease Control and Prevention. Available from: https://http://www.cdc.gov/heartdisease/facts.htm.
4. Bax JJ, Baumgartner H, Ceconi C, Dean V, Fagard R, Funck-Brentano C, et al. Third universal definition of myocardial infarction. J Am Coll Cardiol. 2012;60(16):1581-98.

5. White HD, Chew DP. Acute myocardial infarction. The Lancet. 2008;372(9638):570-84.
6. H. Michael Bolooki AA. Acute Myocardial Infarction Cleveland Clinic: Center for Continuing Education2010. Available from: https://teachmemedicine.org/cleveland-clinic-acute-myocardial-infarction/.
7. Alraies MC, Eckman P. Adult heart transplant: indications and outcomes. Journal of thoracic disease. 2014;6(8):1120-8.
8. Patel S, Nicholson L, Cassidy CJ, Wong KY. Left ventricular assist device: a bridge to transplant or destination therapy? Postgraduate medical journal. 2016;92(1087):271-81.
9. Holley CT, Harvey L, John R. Left ventricular assist devices as a bridge to cardiac transplantation. Journal of thoracic disease. 2014;6(8):1110-9.
10. Matsui Y, Morimoto J, Uede T. Role of matricellular proteins in cardiac tissue remodeling after myocardial infarction. World journal of biological chemistry. 2010;1(5):69.
11. Wilson EM, Moainie SL, Baskin JM, Lowry AS, Deschamps AM, Mukherjee R, et al. Region- and type-specific induction of matrix metalloproteinases in post-myocardial infarction remodeling. Circulation. 2003;107(22):2857-63.
12. Vanhoutte D, Schellings M, Pinto Y, Heymans S. Relevance of matrix metalloproteinases and their inhibitors after myocardial infarction: a temporal and spatial window. Cardiovasc Res. 2006;69(3):604-13.
13. Phatharajaree W, Phrommintikul A, Chattipakorn N. Matrix metalloproteinases and myocardial infarction. Can J Cardiol. 2007;23(9):727-33.
14. Wagner DR, Delagardelle C, Ernens I, Rouy D, Vaillant M, Beissel J. Matrix metalloproteinase-9 is a marker of heart failure after acute myocardial infarction. J Card Fail. 2006;12(1):66-72.

15. French BA, Kramer CM. Mechanisms of Post-Infarct Left Ventricular Remodeling. Drug discovery today Disease mechanisms. 2007;4(3):185-96.

16. Tao ZY, Cavasin MA, Yang F, Liu YH, Yang XP. Temporal changes in matrix metalloproteinase expression and inflammatory response associated with cardiac rupture after myocardial infarction in mice. Life sciences. 2004;74(12):1561-72.

17. Rohde LE, Ducharme A, Arroyo LH, Aikawa M, Sukhova GH, Lopez-Anaya A, et al. Matrix metalloproteinase inhibition attenuates early left ventricular enlargement after experimental myocardial infarction in mice. Circulation. 1999;99(23):3063-70.

18. Yabluchanskiy A, Li Y, J Chilton R, L Lindsey M. Matrix metalloproteinases: drug targets for myocardial infarction. Current drug targets. 2013;14(3):276-86.

19. Mukherjee R, Brinsa TA, Dowdy KB, Scott AA, Baskin JM, Deschamps AM, et al. Myocardial infarct expansion and matrix metalloproteinase inhibition. Circulation. 2003;107(4):618-25.

20. Yabluchanskiy A, Li Y, Chilton RJ, Lindsey ML. Matrix metalloproteinases: drug targets for myocardial infarction. Curr Drug Targets. 2013;14(3):276-86.

21. Phatharajaree W, Phrommintikul A, Chattipakorn N. Matrix metalloproteinases and myocardial infarction. Can J Cardiol. 2007;23(9):727-33.

22. Rohde LE, Ducharme A, Arroyo LH, Aikawa M, Sukhova GH, Lopez-Anaya A, et al. Matrix metalloproteinase inhibition attenuates early left ventricular enlargement after experimental myocardial infarction in mice. Circulation. 1999;99(23):3063-70.

23. Jessup M, Brozena S. Medical progress: Heart failure. New Engl J Med. 2003;348(20):2007-18.

24. Tous E, Purcell B, Ifkovits JL, Burdick JA. Injectable acellular hydrogels for cardiac repair. J Cardiovasc Transl Res. 2011;4(5):528-42.

25. Kelley ST, Malekan R, Gorman JH, 3rd, Jackson BM, Gorman RC, Suzuki Y, et al. Restraining infarct expansion preserves left ventricular geometry and function after acute anteroapical infarction. Circulation. 1999;99(1):135-42.

26. Pilla JJ, Blom AS, Gorman JH, 3rd, Brockman DJ, Affuso J, Parish LM, et al. Early postinfarction ventricular restraint improves borderzone wall thickening dynamics during remodeling. Ann Thorac Surg. 2005;80(6):2257-62.

27. Moainie SL, Guy TS, Gorman JH, 3rd, Plappert T, Jackson BM, St John-Sutton MG, et al. Infarct restraint attenuates remodeling and reduces chronic ischemic mitral regurgitation after postero-lateral infarction. Ann Thorac Surg. 2002;74(2):444-9; discussion 9.

28. Ryan LP, Matsuzaki K, Noma M, Jackson BM, Eperjesi TJ, Plappert TJ, et al. Dermal Filler Injection: A Novel Approach for Limiting Infarct Expansion. Ann Thorac Surg. 2009;87(1):148-55.

29. Christman KL, Fok HH, Sievers RE, Fang Q, Lee RJ. Fibrin glue alone and skeletal myoblasts in a fibrin scaffold preserve cardiac function after myocardial infarction. Tissue Eng. 2004;10(3-4):403-9.

30. Seif-Naraghi SB, Singelyn JM, Salvatore MA, Osborn KG, Wang JJ, Sampat U, et al. Safety and efficacy of an injectable extracellular matrix hydrogel for treating myocardial infarction. Science translational medicine. 2013;5(173).

31. Rodell CB, MacArthur JW, Dorsey SM, Wade RJ, Wang LL, Woo YJ, et al. Shear-Thinning Supramolecular Hydrogels with Secondary Autonomous Covalent Crosslinking to Modulate Viscoelastic Properties In Vivo. Adv Funct Mater. 2015;25(4):636-44.

32. Leor J, Tuvia S, Guetta V, Manczur F, Castel D, Willenz U, et al. Intracoronary injection of in situ forming alginate hydrogel reverses left ventricular remodeling after myocardial infarction in Swine. J Am Coll Cardiol. 2009;54(11):1014-23.

33. Dai W, Wold LE, Dow JS, Kloner RA. Thickening of the infarcted wall by collagen injection improves left ventricular function in rats: a novel approach to preserve cardiac function after myocardial infarction. J Am Coll Cardiol. 2005;46(4):714-9.

34. Kofidis T, de Bruin JL, Hoyt G, Lebl DR, Tanaka M, Yamane T, et al. Injectable bioartificial myocardial tissue for large-scale intramural cell transfer and functional recovery of injured heart muscle. J Thorac Cardiovasc Surg. 2004;128(4):571-8.

35. Singelyn JM, Sundaramurthy P, Johnson TD, Schup-Magoffin PJ, Hu DP, Faulk DM, et al. Catheter-deliverable hydrogel derived from decellularized ventricular extracellular matrix increases endogenous cardiomyocytes and preserves cardiac function post-myocardial infarction. J Am Coll Cardiol. 2012;59(8):751-63.

36. Lu WN, Lu SH, Wang HB, Li DX, Duan CM, Liu ZQ, et al. Functional improvement of infarcted heart by co-injection of embryonic stem cells with temperature-responsive chitosan hydrogel. Tissue engineering Part A. 2009;15(6):1437-47.

37. Rodell CB, Lee ME, Wang H, Takebayashi S, Takayama T, Kawamura T, et al. Injectable Shear-Thinning Hydrogels for Minimally Invasive Delivery to Infarcted Myocardium to Limit Left-Ventricular Remodeling. Circulation Cardiovascular interventions. 2016;9(10).

38. Fujimoto KL, Ma Z, Nelson DM, Hashizume R, Guan J, Tobita K, et al. Synthesis, characterization and therapeutic efficacy of a biodegradable, thermoresponsive hydrogel designed for application in chronic infarcted myocardium. Biomaterials. 2009;30(26):4357-68.

39. Mann DL, Lee RJ, Coats AJ, Neagoe G, Dragomir D, Pusineri E, et al. One-year follow-up results from AUGMENT-HF: a multicentre randomized controlled

clinical trial of the efficacy of left ventricular augmentation with Algisyl in the treatment of heart failure. European journal of heart failure. 2016;18(3):314-25.

40. Anker SD, Coats AJ, Cristian G, Dragomir D, Pusineri E, Piredda M, et al. A prospective comparison of alginate-hydrogel with standard medical therapy to determine impact on functional capacity and clinical outcomes in patients with advanced heart failure (AUGMENT-HF trial). European heart journal. 2015;36(34):2297-309.

41. Wang H, Rodell CB, Lee ME, Dusaj NN, Gorman JH, Burdick JA, et al. Computational sensitivity investigation of hydrogel injection characteristics for myocardial support. J Biomech. 2017;64:231-5.

42. Hastings CL, Roche ET, Ruiz-Hernandez E, Schenke-Layland K, Walsh CJ, Duffy GP. Drug and cell delivery for cardiac regeneration. Adv Drug Deliver Rev. 2015;84:85-106.

43. Martens TP, Godier AFG, Parks JJ, Wan LQ, Koeckert MS, Eng GM, et al. Percutaneous Cell Delivery Into the Heart Using Hydrogels Polymerizing In Situ. Cell transplantation. 2009;18(3):297-304.

44. Gaffey AC, Chen MH, Venkataraman CM, Trubelja A, Rodell CB, Dinh PV, et al. Injectable shear-thinning hydrogels used to deliver endothelial progenitor cells, enhance cell engraftment, and improve ischemic myocardium. J Thorac Cardiovasc Surg. 2015;150(5):1268-76.

45. Li J, Mooney DJ. Designing hydrogels for controlled drug delivery. Nature Reviews Materials. 2016;1(12):16071.

46. Hoare TR, Kohane DS. Hydrogels in drug delivery: Progress and challenges. Polymer. 2008;49(8):1993-2007.

47. Ifkovits JL, Tous E, Minakawa M, Morita M, Robb JD, Koomalsingh KJ, et al. Injectable hydrogel properties influence infarct expansion and extent of

postinfarction left ventricular remodeling in an ovine model. Proc Natl Acad Sci U S A. 2010;107(25):11507-12.

48. Ruvinov E, Leor J, Cohen S. The promotion of myocardial repair by the sequential delivery of IGF-1 and HGF from an injectable alginate biomaterial in a model of acute myocardial infarction. Biomaterials. 2011;32(2):565-78.

49. Davis ME, Hsieh PCH, Takahashi T, Song Q, Zhang S, Kamm RD, et al. Local myocardial insulin-like growth factor 1 (IGF-1) delivery with biotinylated peptide nanofibers improves cell therapy for myocardial infarction. Proceedings of the National Academy of Sciences. 2006;103(21):8155-60.

50. Koudstaal S, Bastings MMC, Feyen DAM, Waring CD, van Slochteren FJ, Dankers PYW, et al. Sustained Delivery of Insulin-Like Growth Factor-1/Hepatocyte Growth Factor Stimulates Endogenous Cardiac Repair in the Chronic Infarcted Pig Heart. Journal of Cardiovascular Translational Research. 2014;7(2):232-41.

51. Wang H, Zhang X, Li Y, Ma Y, Zhang Y, Liu Z, et al. Improved myocardial performance in infarcted rat heart by co-injection of basic fibroblast growth factor with temperature-responsive chitosan hydrogel. The Journal of Heart and Lung Transplantation. 2010;29(8):881-7.

52. Sakakibara Y, Yamamoto M, Nishimura K, Nishina T, Miwa S, Handa N, et al. Prevasculrization using gelatin microsphere containing basic-fibroblast growth factor enhances the benefits of cardiomyocytes transplantation in rats with ischemic cardiomyopathy. 2000.

53. Yamamoto T, Suto N, Okubo T, Mikuniya A, Hanada H, Yagihashi S, et al. Intramyocardial delivery of basic fibroblast growth factor-impregnated gelatin hydrogel microspheres enhances collateral circulation to infarcted canine myocardium. Japanese circulation journal. 2001;65(5):439-44.

54. Iwakura A, Fujita M, Kataoka K, Tambara K, Sakakibara Y, Komeda M, et al. Intramyocardial sustained delivery of basic fibroblast growth factor improves angiogenesis and ventricular function in a rat infarct model. Heart and vessels. 2003;18(2):93-9.

55. Liu Y, Sun L, Huan Y, Zhao H, Deng J. Effects of basic fibroblast growth factor microspheres on angiogenesis in ischemic myocardium and cardiac function: analysis with dobutamine cardiovascular magnetic resonance tagging. European journal of cardio-thoracic surgery. 2006;30(1):103-7.

56. Fujita M, Ishihara M, Morimoto Y, Simizu M, Saito Y, Yura H, et al. Efficacy of photocrosslinkable chitosan hydrogel containing fibroblast growth factor-2 in a rabbit model of chronic myocardial infarction. Journal of Surgical Research. 2005;126(1):27-33.

57. Hao X, Silva EA, Månsson-Broberg A, Grinnemo K-H, Siddiqui AJ, Dellgren G, et al. Angiogenic effects of sequential release of VEGF-A165 and PDGF-BB with alginate hydrogels after myocardial infarction. Cardiovasc Res. 2007;75(1):178-85.

58. Awada HK, Johnson NR, Wang Y. Sequential delivery of angiogenic growth factors improves revascularization and heart function after myocardial infarction. J Control Release. 2015;207:7-17.

59. Wu J, Zeng F, Huang X-P, Chung JCY, Konecny F, Weisel RD, et al. Infarct stabilization and cardiac repair with a VEGF-conjugated, injectable hydrogel. Biomaterials. 2011;32(2):579-86.

60. Segers VFM, Tokunou T, Higgins LJ, MacGillivray C, Gannon J, Lee RT. Local delivery of protease-resistant stromal cell derived factor-1 for stem cell recruitment after myocardial infarction. Circulation. 2007;116(15):1683-92.

61. MacArthur JW, Jr., Purcell BP, Shudo Y, Cohen JE, Fairman A, Trubelja A, et al. Sustained release of engineered stromal cell-derived factor 1-alpha from injectable hydrogels effectively recruits endothelial progenitor cells and preserves ventricular function after myocardial infarction. Circulation. 2013;128(11 Suppl 1):S79-86.

62. Purcell BP, Elser JA, Mu A, Margulies KB, Burdick JA. Synergistic effects of SDF-1α chemokine and hyaluronic acid release from degradable hydrogels on directing bone marrow derived cell homing to the myocardium. Biomaterials. 2012;33(31):7849-57.

63. Wang LL, Liu Y, Chung JJ, Wang T, Gaffey AC, Lu M, et al. Sustained miRNA delivery from an injectable hydrogel promotes cardiomyocyte proliferation and functional regeneration after ischaemic injury. Nature Biomedical Engineering. 2017;1(12):983.

64. Matsumura S, Iwanaga S, Mochizuki S, Okamoto H, Ogawa S, Okada Y. Targeted deletion or pharmacological inhibition of MMP-2 prevents cardiac rupture after myocardial infarction in mice. J Clin Invest. 2005;115(3):599-609.

65. Mukherjee R, Mingoia JT, Bruce JA, Austin JS, Stroud RE, Escobar GP, et al. Selective spatiotemporal induction of matrix metalloproteinase-2 and matrix metalloproteinase-9 transcription after myocardial infarction. Am J Physiol-Heart C. 2006;291(5):H2216-H28.

66. Spinale FG, Coker ML, Heung LJ, Bond BR, Gunasinghe HR, Etoh T, et al. A matrix metalloproteinase induction/activation system exists in the human left ventricular myocardium and is upregulated in heart failure. Circulation. 2000;102(16):1944-9.

67. Yarbrough WM, Mukherjee R, Escobar GP, Mingoia JT, Sample JA, Hendrick JW, et al. Selective targeting and timing of matrix metalloproteinase inhibition in post-myocardial infarction remodeling. Circulation. 2003;108(14):1753-9.

68. Eckhouse SR, Purcell BP, McGarvey JR, Lobb D, Logdon CB, Doviak H, et al. Local hydrogel release of recombinant TIMP-3 attenuates adverse left ventricular remodeling after experimental myocardial infarction. Science translational medicine. 2014;6(223):223ra21-ra21.

69. Purcell BP, Lobb D, Charati MB, Dorsey SM, Wade RJ, Zellars KN, et al. Injectable and bioresponsive hydrogels for on-demand matrix metalloproteinase inhibition. Nat Mater. 2014;13(6):653-61.

70. Fan Z, Fu M, Xu Z, Zhang B, Li Z, Li H, et al. Sustained Release of a Peptide-Based Matrix Metalloproteinase-2 Inhibitor to Attenuate Adverse Cardiac Remodeling and Improve Cardiac Function Following Myocardial Infarction. Biomacromolecules. 2017;18(9):2820-9.

CHAPTER 2

RESEARCH OVERVIEW

2.1 SPECIFIC AIMS

It is clear that biomaterials are emerging to have an important role in the treatment of various cardiac diseases and conditions.[1-7] Specifically, hydrogels (water-swollen polymer networks) are being developed to treat patients after myocardial infarction (MI), due to their tunable properties and potential for percutaneous delivery to the heart.[6] Hydrogels are comprised of either natural or synthetic polymers and can be used to influence mechanical properties in the myocardium or as a delivery vehicle to improve the retention and viability of cells or the sustained delivery of therapeutics.[6,8-10]

Self-assembled hydrogels, formed using reversible, non-covalent bonds as crosslinks, are one class of hydrogels that possess a number of unique properties that make them highly amenable for clinical translation in myocardial applications.[11] Specifically, these materials are shear-thinning and self-healing, allowing them to be easily injected.[12,13] This is often advantageous when compared to traditional covalent systems that suffer from issues associated with reaction times that can lead to difficulty in handling by clinicians (e.g., clogging of delivery devices), as well as the potential for extravasation when injected into tissue.[11] In comparison, shear-thinning allows for injection through a variety of syringes and catheters, while self-healing allows hydrogels to re-form when they reach the desired tissue site.

Our lab has recently developed a two-component hydrogel system based on hyaluronic acid (HA) that has been engineered for injection into the myocardium.[4,13] HA is a highly useful polymer for hydrogel design, as it is a naturally occurring component of the extracellular matrix and is easily amenable to orthogonal chemical modification.[14] This developed hydrogel is crosslinked through the directed self-assembly or guest-host

(GH) chemistry between the hydrophobic cavity of β-cyclodextrin (CD) and the hydrophobic small molecule adamantane (Ad). Simply, HA is modified with either CD or Ad (CD-HA, Ad-HA) and gelation occurs when the two solutions of CD-HA and Ad-HA are mixed, to form a hydrogel with shear-thinning and self-healing behavior.[13]

Although this general hydrogel system has been explored previously to alter myocardial mechanics and for the delivery of several molecules (e.g., microRNA, extracellular vesicles), there is still much work to expand the hydrogel to the widespread therapeutics that are of interest to treat patients after MI. [4,5,15,16] To address this, the overarching objective of this thesis is to advance GH assembled materials for the delivery of small molecule therapeutics, as well as to design new GH assembled materials with complex multifunctional properties. The following aims serve to guide this objective, investigating material structure and properties that govern their therapeutic efficacy in influencing the remodeling myocardium after an infarction.

Aim 1: Design an easily injectable guest-host hydrogel formulation for sustained small molecule delivery

Hypothesis: The host molecule (CD) within GH hydrogels will bind to encapsulated small molecules to sustain and control their release behavior from hydrogels.

Hydrogels are often unable to serve as a delivery platform for small molecules, as their large mesh sizes lead to the rapid diffusion of small molecules.[17] Specifically, hydrogels are inherently highly swollen in nature, providing minimal diffusive barriers for encapsulated small molecule drugs, as their molecular mesh size is often much greater than the entrapped molecule. This rapid diffusion limits the sustained release potential for small molecule drugs from hydrogels. CD, with its cyclic structure and hydrophobic core, is known to bind to many small hydrophobic molecules and has been used

frequently as an excipient in the pharmaceutical industry to improve solubility and absorption of hydrophobic small molecules.[18,19] Given this broad affinity for small molecules, we design hydrogels through GH assembly, leveraging CD for both hydrogel formation and to retain small molecules within hydrogels. Molecule binding, diffusivity, and release when encapsulated are explored as a function of hydrogel composition (e.g., ratio of Ad:CD, polymer concentration). These studies expand our knowledge of drug binding to sustain release from hydrogels and point to specific formulations that may be investigated for treating MI.

Aim 2: Release a small molecule protease inhibitor from an injectable GH hydrogel for treatment of MI

Hypothesis: A small molecule protease inhibitor SD-7300 can be released in a sustained manner from GH hydrogels to improve functional and biological outcomes after MI when compared to hydrogels alone or saline treatment.

Spatial inhibition of MMPs throughout the body, targeting of MMP subtypes, and timing of MMP inhibition have been shown to play key roles in therapeutic benefit of targeting MMP activity for therapeutics.[20-25] This paradigm has translated to the development of numerous small molecule inhibitors; however, off-target effects related to the systemic delivery of broad-spectrum MMP knockdown has limited their translation. For example, SD-7300, an MMP-1 sparing small molecule inhibitor (Pfizer), has shown pre-clinical potential as an MI therapeutic, but only with off-target effects. Thus, the local delivery of SD-7300 may overcome these limitations. To address this, we develop a specific injectable GH hydrogel formulation, where interactions with CD lead to sustained release. Further, a large animal model of ischemia-reperfusion in swine is used to demonstrate the ability of the injectable hydrogel delivering SD-7300 to alter remodeling

outcomes and improve functional outcomes. These studies provide an innovative approach for targeted, localized MMP inhibition in the infarcted myocardium with broad impacts on evolving strategies for pharmaceutical MMP inhibitor therapies.

Aim 3: Develop an injectable granular hydrogel system for treatment of MI

Hypothesis: Shear-thinning hydrogels can be assembled through the GH interactions of polymers and microgel components with properties of degradation, molecule release, and cell invasion based on microgel design.

Towards designing material systems for application in the myocardium, it is important to consider multifunctional behavior including drug release, cell invasion, and microstructure. These properties are difficult to integrate into a single injectable material, limiting the scope of biomaterial-based approaches in MI interventions. Emerging classes of materials with potential to design modular, multi-therapeutic release systems include granular hydrogels, where microgels are assembled into a bulk hydrogel. [26-28] As GH chemistry provides a directed and highly controllable mechanism of self-assembly, we engineer unique materials based on the assembly of covalently-crosslinked microgels modified with Ad with CD-HA polymers. We investigate the rheological properties of these materials, as well as the degradation and release behavior of granular hydrogels assembled through microgels crosslinked with either stable or protease-degradable crosslinks. Further, these materials are investigated after injection into a rat model of MI, where features such as microgel erosion and the ability to alter remodeling outcomes are investigated. Thus, this aim designs innovative, multi-scale materials using the self-assembly of microgel components to provide multi-functional benefit in the infarcted myocardium.

2.2 CHAPTER OUTLINE

Chapter 1 provides an in depth overview of MI and a summary of the biological mechanisms behind left ventricular remodeling. Further, the various hydrogel approaches and specific systems that have been pursued for treating MI, including through mechanical intervention, cell delivery, and drug delivery are summarized. Chapter 3 shows a more focused review of GH assembled biomaterials, including the various GH pairs that have been explored in the development of biomaterials and their role in drug delivery and other therapeutic applications.

Chapter 4 describes the scientific research proposed in Aim 1, outlining the tunable parameters in GH hydrogels for the sustained release of a variety of therapeutic small molecules payloads. Chapter 5 describes the scientific research proposed in Aim 2, outlining the development of a GH formulation suitable for the delivery of SD-7300 and its application in a porcine model for MI. Chapter 6 describes the scientific research proposed in Aim 3, outlining the development of a multifunctional granular hydrogel and its application in a rat model for MI.

Finally, Chapter 7 provides a summary of the work presented, illuminating the overall impact of GH hydrogel systems for the delivery of therapeutics after MI. Limitations of these material systems are discussed, and potential future directions are proposed that may further expand the application of these hydrogels.

2.3 REFERENCES

1. Hastings CL, Roche ET, Ruiz-Hernandez E, Schenke-Layland K, Walsh CJ, Duffy GP. Drug and cell delivery for cardiac regeneration. Adv Drug Deliver Rev. 2015;84:85-106.

2. Purcell BP, Lobb D, Charati MB, Dorsey SM, Wade RJ, Zellars KN, et al. Injectable and bioresponsive hydrogels for on-demand matrix metalloproteinase inhibition. Nat Mater. 2014;13(6):653-61.
3. Purcell BP, Lobb D, Charati MB, Wade RJ, Zellers KN, Doviak H, et al. On-demand Delivery of TIMP-3 From Matrix Metalloproteinase Degradable Hydrogels Attenuates Post Myocardial Infarction Remodeling. Circulation. 2013;128(22).
4. Rodell CB, Lee ME, Wang H, Takebayashi S, Takayama T, Kawamura T, et al. Injectable Shear-Thinning Hydrogels for Minimally Invasive Delivery to Infarcted Myocardium to Limit Left-Ventricular Remodeling. Circulation Cardiovascular interventions. 2016;9(10).
5. Rodell CB, MacArthur JW, Dorsey SM, Wade RJ, Wang LL, Woo YJ, et al. Shear-Thinning Supramolecular Hydrogels with Secondary Autonomous Covalent Crosslinking to Modulate Viscoelastic Properties In Vivo. Adv Funct Mater. 2015;25(4):636-44.
6. Tous E, Purcell B, Ifkovits JL, Burdick JA. Injectable acellular hydrogels for cardiac repair. J Cardiovasc Transl Res. 2011;4(5):528-42.
7. Eckhouse SR, Purcell BP, McGarvey JR, Lobb D, Logdon CB, Doviak H, et al. Local hydrogel release of recombinant TIMP-3 attenuates adverse left ventricular remodeling after experimental myocardial infarction. Science translational medicine. 2014;6(223):223ra21-ra21.
8. Gaffey AC, Chen MH, Venkataraman CM, Trubelja A, Rodell CB, Dinh PV, et al. Injectable shear-thinning hydrogels used to deliver endothelial progenitor

cells, enhance cell engraftment, and improve ischemic myocardium. J Thorac Cardiovasc Surg. 2015;150(5):1268-76.

9. Ifkovits JL, Tous E, Minakawa M, Morita M, Robb JD, Koomalsingh KJ, et al. Injectable hydrogel properties influence infarct expansion and extent of postinfarction left ventricular remodeling in an ovine model. Proc Natl Acad Sci U S A. 2010;107(25):11507-12.

10. Johnson TD, Christman KL. Injectable hydrogel therapies and their delivery strategies for treating myocardial infarction. Expert opinion on drug delivery. 2013;10(1):59-72.

11. Rodell CB, Mealy JE, Burdick JA. Supramolecular guest–host interactions for the preparation of biomedical materials. Bioconjugate chemistry. 2015;26(12):2279-89.

12. Foo CTSWP, Lee JS, Mulyasasmita W, Parisi-Amon A, Heilshorn SC. Two-component protein-engineered physical hydrogels for cell encapsulation. P Natl Acad Sci USA. 2009;106(52):22067-72.

13. Rodell CB, Kaminski AL, Burdick JA. Rational design of network properties in guest-host assembled and shear-thinning hyaluronic acid hydrogels. Biomacromolecules. 2013;14(11):4125-34.

14. Burdick JA, Prestwich GD. Hyaluronic acid hydrogels for biomedical applications. Adv Mater. 2011;23(12):H41-56.

15. Chen CW, Wang LL, Zaman S, Gordon J, Arisi MF, Venkataraman CM, et al. Sustained release of endothelial progenitor cell-derived extracellular vesicles

from shear-thinning hydrogels improves angiogenesis and promotes function after myocardial infarction. Cardiovasc Res. 2018;114(7):1029-40.

16. Wang LL, Liu Y, Chung JJ, Wang T, Gaffey AC, Lu M, et al. Sustained miRNA delivery from an injectable hydrogel promotes cardiomyocyte proliferation and functional regeneration after ischaemic injury. Nature Biomedical Engineering. 2017;1(12):983.

17. Hoare TR, Kohane DS. Hydrogels in drug delivery: Progress and challenges. Polymer. 2008;49(8):1993-2007.

18. Loftsson T, Brewster ME. Pharmaceutical applications of cyclodextrins: basic science and product development. J Pharm Pharmacol. 2010;62(11):1607-21.

19. Rekharsky MV, Inoue Y. Complexation Thermodynamics of Cyclodextrins. Chem Rev. 1998;98(5):1875-918.

20. Mukherjee R, Mingoia JT, Bruce JA, Austin JS, Stroud RE, Escobar GP, et al. Selective spatiotemporal induction of matrix metalloproteinase-2 and matrix metalloproteinase-9 transcription after myocardial infarction. Am J Physiol-Heart C. 2006;291(5):H2216-H28.

21. Su H, Spinale FG, Dobrucki LW, Song J, Hua J, Sweterlitsch S, et al. Noninvasive targeted imaging of matrix metalloproteinase activation in a murine model of postinfarction remodeling. Circulation. 2005;112(20):3157-67.

22. Fingleton B. Matrix metalloproteinases as valid clinical target. Current pharmaceutical design. 2007;13(3):333-46.

23. Matsumura S, Iwanaga S, Mochizuki S, Okamoto H, Ogawa S, Okada Y. Targeted deletion or pharmacological inhibition of MMP-2 prevents cardiac rupture after myocardial infarction in mice. J Clin Invest. 2005;115(3):599-609.

24. Mukherjee R, Brinsa TA, Dowdy KB, Scott AA, Baskin JM, Deschamps AM, et al. Myocardial infarct expansion and matrix metalloproteinase inhibition. Circulation. 2003;107(4):618-25.

25. Phatharajaree W, Phrommintikul A, Chattipakorn N. Matrix metalloproteinases and myocardial infarction. Can J Cardiol. 2007;23(9):727-33.

26. Appel EA, Tibbitt MW, Webber MJ, Mattix BA, Veiseh O, Langer R. Self-assembled hydrogels utilizing polymer–nanoparticle interactions. Nat Commun. 2015;6:6295.

27. Griffin DR, Weaver WM, Scumpia P, Di Carlo D, Segura T. Accelerated wound healing by injectable microporous gel scaffolds assembled from annealed building blocks. Nature materials. 2015;14(7):737.

28. Wang HA, Hansen MB, Lowik DWPM, van Hest JCM, Li YB, Jansen JA, et al. Oppositely Charged Gelatin Nanospheres as Building Blocks for Injectable and Biodegradable Gels. Adv Mater. 2011;23(12):H119-H24.

CHAPTER 3

SUPRAMOLECULAR GUEST-HOST INTERACTIONS FOR THE PREPARATION OF BIOMEDICAL MATERIALS

Adapted from:

Rodell CB, Mealy JE, Burdick JA. Supramolecular guest–host interactions for the preparation of biomedical materials. Bioconjugate chemistry. 2015 Oct 16;26(12):2279-89.

3.1. INTRODUCTION

While chemists have traditionally focused on methods of assembling atoms and molecules through the formation and rearrangement of covalent bonds, it has been elegantly noted that this strategy pales in comparison to the array of possible interactions utilized in nature to develop large, complex molecular structures through non-covalent bonds.[1] These interactions are encompassed within the field of supramolecular chemistry, which includes electrostatics, hydrogen bonding, van der Waals forces, π-π interactions, and hydrophobic or hydrophilic attraction for molecular assembly.[2] While such interactions have long been known, the field has continued to rapidly expand since the 1987 Nobel Prize was awarded to Pedersen,[3] Cram,[4] and Lehn[5] for their pioneering work in formalizing synthetic methods in this area.

Lehn described the concept of supramolecular assembly as "chemistry beyond the molecule." [5] This is because the non-covalent nature of supramolecular bonds renders them inherently weaker than covalent bonds and they may therefore exhibit thermodynamic or forcefully induced rearrangement. As a result, supramolecular bonds display a capacity for directed assembly at length scales far exceeding that of single

atoms or molecules, such as with the formation of higher order structures in biological proteins and tissues. The capacity for spontaneous and reversible binding between molecular species is likewise a driving force in the development of structured,[6-8] dynamic,[9] and self-healing[10] materials, as well as in pharmaceutical applications[11-13] and directed cell-material interactions which will be discussed herein.

One particular subset of supramolecular chemistry, namely guest-host interactions, is of particular interest toward the biomedical community. These bonds are based on the transient association of a molecule containing a cavity (i.e. a cavitand) with suitable molecular guests. The family of cavitands includes both naturally-derived (e.g. cyclodextrin) and synthetic (e.g. cucurbit[n]urils, calix[n]arenes, and pillar[n]arenes) macrocycles.[12,14-16] The criteria for a guest-host pair involves complementary size of the host cavity and guest molecule, as well as their specific interactions (predominantly through hydrophobic attraction).[17,18] These broad criteria lend themselves to the pairing of macrocycles with numerous potential guests, which may be inert or stimuli-responsive molecules, pharmaceuticals, biomolecules (i.e. peptides, proteins), polymers, or other chemical species. Owing to the array of guest and host molecules and their synthetic flexibility, incorporation of these groups into polymeric materials may be easily achieved for a diverse range of biomedical applications. Despite recent developments in polymeric guest-host materials, there remains a tremendous capacity for growth in the biomaterial utilization of these unique chemistries. Toward elucidating these future directions, this review will highlight recent advances in both our understanding and application of materials and interactions mediated by guest-host macrocycle assembly.

3.2. MECHANISMS OF SELF-ASSEMBLY

3.2.1. DIRECT MOLECULAR RECOGNITION

Supramolecular assembly may be ambiguous, with non-specific interactions between numerous groups. Examples of such interactions in material assembly include the formation of hydrophobic crystalline domains or charge-based assembly of polyelectrolyte or polyampholyte polymers. These interactions may be preferable in some cases, such as to facilitate incorporation of hydrophobic[19,20] or charged drugs[21,22]. However, such assembly processes involve development of long-range order over relatively long timescales, which may hamper rapid formation and recovery. Moreover, the prevalence of competitive binding groups (i.e. any non-charged molecule, salts) may disrupt bond formation and material assembly. Thus, it is important to define supramolecular interactions that have more specific associations to fabricate robust materials for biomedical interactions.

Toward this, direct associating systems are based on specific molecular recognition of a guest by its corresponding host molecule upon mixing (**Figure 3.1**). Such direct interactions do not require long-range order and therefore occur rapidly, with timescales governed by the association constant (k_a), enabling rapid initial material formation and self-healing upon rupture. Numerous molecular structures have been identified and designed to form guest-host pairs. These include the relatively weak association of crown ethers, cryptands, and related molecules;[23,24] though, such associations are generally more suited for ionic sequestration and not molecular recognition. Alternatively, an array of transient peptide and/or protein interactions have been devised,[25-29] which often display greater affinity and specificity, but at the cost of increasing complexity and laborious synthesis. Finally, the guest-host macrocycles combine rapid, high affinity molecular recognition with ease and scalability of synthesis.

Of the guest macrocycles, cyclodextrin (CD) is the most prevalent due to its relatively high water solubility, low toxicity, and extensive history of use. The first reference to CD was that of Villiers, in 1891, who isolated a crystalline substance

following bacterial digestion of cellulose.[30] While research continued on the formation and characterization of these crystalline dextrans, nearly half a century passed before their cyclic structure was proposed (D-glucose units arranged in a toroidal fashion through α-1,4 glycosidic bonds) and isolation of homogenous fractions of α, β, and γ cyclodextrin (which contain 6, 7, or 8 repeat units, respectively) was accomplished.[14] Importantly, improvements toward these synthesis and purification processes have proceeded to industrial scale, as have many strategies for their synthetic modification, resulting in a relatively cheap and abundant material source.[14,31] Enabled by the scalability of synthesis, CD molecules are used in a variety of industrial, commercial, and pharmaceutical applications and have been categorized by the Food and Drug Administration as "generally recognized as safe" (GRAS).[32-34] Moreover, the cavity sizes of CDs allow them to include a range of guest hydrophobic molecules in its interior. Of these potential guest molecules, adamantane (Ad) is widely regarded as having one of the greatest affinities ($K_{eq} \approx 10^5$ M^{-1}) due to its complementary size for βCD and high hydrophobicity.[35] Alternatively, responsive guest-host interactions have emerged as a means of regulating these intramolecular interactions. These include azobenzene and ferrocene, which are known to interact with numerous species of CD and are responsive to light[36] and redox conditions,[37,38] respectively. This behavior renders them particularly useful toward the development of responsive delivery vehicles,[39] actuating materials,[40,41] and dynamically assembling systems.[42-44]

More recently, alternate cavitands have emerged and demonstrated relevance toward biomedical applications. This second generation of cavitands includes cucurbit[n]urils (CBs), pillar[n]arenes, and calix[n]arenes. While CBs were first prepared in 1905,[45] investigation of their structure was not performed until 1981,[46] and numerous CBs (typically 5-10 repeat units) have since been explored. Recent examination has revealed mild *in vitro* toxicity of these groups, though only at doses far exceeding those

typical *in vivo*, supporting their continued pharmaceutical use.[47] Binding affinities for CBs are often greater than that of other cavitands and can reach values as high as $K_{eq} \approx 10^{15}$ M^{-1}.[48] This may be attributed, in part, to the binding of guest molecules through a combination of hydrophobic and cation-dipole interactions.[48-50] Moreover, the unique geometry of CB[8]s allows for multivalent binding of guest molecules (such as naphthalene and methyl viologen), which enables reinforcement of binding affinity by cooperation between π-π stacking or charge-transfer interactions for guest-host complex formation.[51] Recently, the use of the cup-shaped calix[n]arenes and pillar-shaped pillar[n]arenes toward biomedical applications has begun.[12] Their translation to this field has been previously hampered both by lower guest-host affinity and water solubility when compared to their CD and CB counterparts; though, recent work has sought to improve the affinity and water solubility of these macrocycles such as through repeated and efficient modification with solubilizing functional groups,[52] resulting in macrocycles with improved utility in aqueous environments.

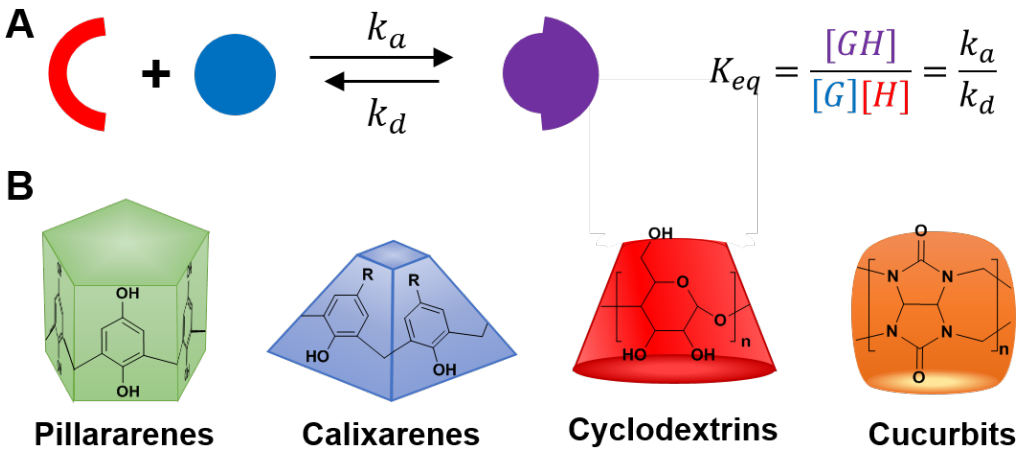

Figure 3.1. Molecular guest-host assembly. (A) Generalized schematic of host (red) interaction with its corresponding guest (blue) to form a guest-host complex (purple), with bonding equilibrium governed by the association (k_a) and dissociation (k_d) constants. (**B**) Schematic representation of cavitand host species, represented by pillar[5]arene, calix[4]arene, cyclodextrin, and cucurbit[n]uril.

3.2.2. POLYMERIC ASSEMBLY

Guest-host molecular recognition is particularly useful for the formation of supramolecular structures (i.e. guest-host hydrogels). Toward hydrogel formation, pioneering work by Harada demonstrated that poly(ethylene oxide) (PEO) could be threaded within multiple αCD moieties, yielding a rotaxane structure.[53] Pursuit of such systems further illustrated the formation of pseudopolyrotaxanes and a sol-gel transition upon simple mixing of PEO and αCD through crystallization of CD domains (**Figure 3.2A**).[54] These and similarly formed pseudopolyrotaxanes, such as through pendant polymer modification with PEO or similar polymers (**Figure 3.2B**), have since become a basis for supramolecular assembled hydrogels which have been separately reviewed.[55] Such systems may be limited in therapeutic use, due to long recovery times after injection,[56] which may hinder injection site retention, and the inaccessibility of CD in the network to interact with surrounding molecules.

Alternatively, modification of polymers with guest and host groups (either as end-groups or pendant modification) has become the primary method for fabrication of supramolecular networks from guest-host interactions. For example, the end-modification of mono- and bifunctional polymers has been examined (**Figure 3.2C**), where potential applications may include the self-sorting of linear supramolecular polymers or assembly of block copolymers with utility toward such materials as responsive micelle assembly.[57-59] In extension of this methodology, multiarm PEO has been modified with either βCD or cholesterol (the guest molecule) and van de Manakker and colleagues demonstrated formation of supramolecular hydrogels by mixing these precursors with controllable rheological erosion, and cargo release profiles. [60,61] Similarly, Charlot et al. extensively explored the rheological behavior of binary associating systems by conjugating βCD and Ad to chitosan, hyaluronic acid (HA), and other polymers as pendant groups (**Figure 3.2D**). While low modification resulted in

weak supramolecular networks (typical G' < 100Pa), their results demonstrated the importance of polymer concentration, charge, and competitive binding on network assembly.[62] Moreover, theoretical and experimental approaches have been combined to illustrate the importance of multivalent and inter-polymer interaction to generate high avidity and network stability.[63,64] Toward harnessing this understanding, our group has demonstrated that higher degrees of modification of HA with these same guest-host groups enables formation of more robust supramolecular hydrogels (G' = 10 kPa possible) through generation of larger net avidity between polymers which may be enhanced by multifold polymer junctions.[65]

CB macrocycles have also been explored to produce robust supramolecular hydrogels. This work has been pioneered by the Scherman group, where polymers were modified with pendant methyl viologen or napthoxy derivatives that form ternary complexes with soluble CB[8] with high affinity ($K_a \geq 10^{11}$ M^{-2}, **Figure 3.2E**). Such materials resulted in good network mechanical properties (typical G' > 500Pa) even at low polymer modification (5-10% of repeats).[66,67] For further information regarding polymer architecture and molecular organization in guest-host hydrogels and their influence on bulk hydrogel properties, the reader is referred to extensive reviews that cover these topics.[2,68]

Beyond the ability to assemble into networks, supramolecular guest-host interactions may be used to introduce structure at the nano- and micro-scales. Indeed, the organization of many natural structures is driven by supramolecular interactions, such as native extracellular matrix (e.g., fibrillar structure of collagen) and the DNA superstructure. Such aspects may be recapitulated by synthetic analogues.[69,70] Observations of such behavior have been noted in numerous self-assembling systems including peptide amphiphiles[71], DNA-based hydrogels[72], dendritic materials[8], and PEG-based supramolecular systems[73]. In recent years, there have been numerous reports

indicating that similar hierarchical structures are possible in guest-host hydrogels, though most include only observation of dried samples by electron microscopy. Recent reports have shown the formation of nanoparticles with well controlled size through synthesis of diblock copolymers containing βCD.[74] Moving this structure into two-dimensional assembly, semi-rigid four-arm macromolecules have been modified by methyl viologen and 2,6-dihydroxynaphthalene which assemble into two-dimensional films upon mixing with CB[8] in water. Both TEM and AFM confirmed a nanofibrillar structure, and SAXS estimated the spacing of these features to be well approximated by the theoretical pore size.[75] In an interesting example of three-dimensional structure, aggregation of N-isopropylacrylamide (NIPAAM) thermogels has been controlled by introducing CB[7] as polypseudorotaxane side chains. Such inclusion results in semi-rigid polymer segments that induce transition from a globular to porous morphology that could be observed by optical microscopy in a hydrated state.[76] Control of physical structure on these length scales holds great promise for the cell biology and biomaterials fields, as dynamic self-assembly of these structures may best recapitulate the natural processes that drive cell behavior. Though, systematic studies including the effects of polymer architecture, bond affinity, and other variables are still lacking.

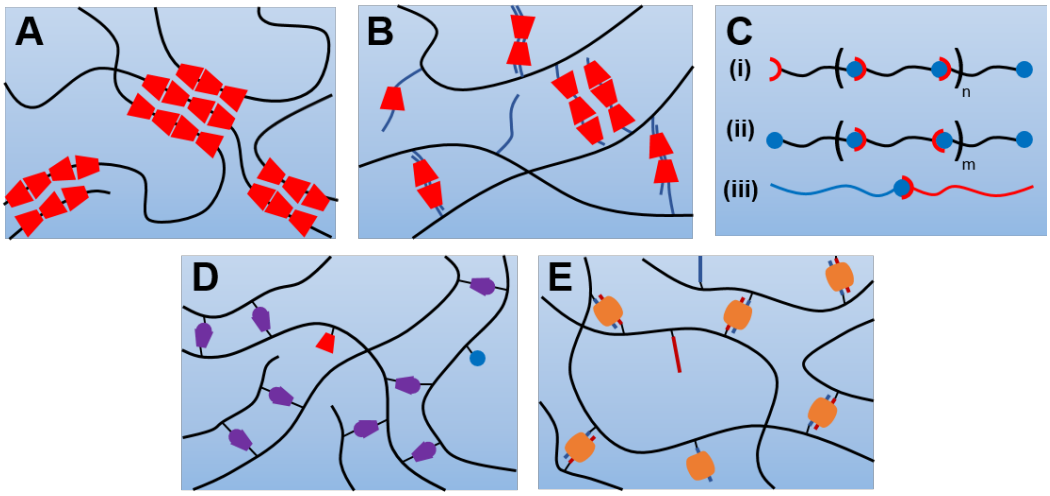

Figure 3.2. Schematic representation of guest-host polymeric assemblies. (**A**, **B**) CD-PEO pseudopolyrotaxanes; (**C**) supramolecular polymers from heterobifunctional (i), homobifunctional (ii), and monobifunctional (iii) gelators; (**D**) separate, pendant modification by βCD and adamantane; and (E) separate, pendant modification of polymers by methyl viologen or napthoxy derivatives with crosslinking by ternary complexes with soluble CB[8].

3.3. DIVERSE BIOMEDICAL APPLICATIONS

3.3.1. INJECTABLE HYDROGELS

Injectable materials have become important in the biomaterials community as they can be introduced in a minimally invasive manner through direct injection into a tissue or via catheters. Many methodologies exist for formation of injectable materials, including *in situ* gelling via initiated or autonomous polymerization, addition crosslinking, or thermogelation; however, there are numerous limitations to such systems based on gelation kinetics (i.e. too fast leads to clogging of delivery device, too slow leads to material dispersion upon injection). Alternatively, guest-host hydrogels may be formed prior to injection (**Figure 3.3A, i**) and extruded via shear-induced flow. Such shear-thinning properties are of interest for numerous supramolecular hydrogels,[77] due to their dynamic bonds that can be broken and then reformed. Many practical requirements should be considered when designing guest-host hydrogels as deliverable materials,

such as the injection process (i.e., ease of injection and capacity for retention), as well as the subsequent physical properties after injection (i.e., suitable moduli and degradation times).

For shear-thinning materials, the injection process is governed by the material response to shear stress; ideally, the material is pre-formed and then exhibits a decrease in viscosity (i.e., shear-thinning) during injection that permits flow. Indeed, this is the case for the majority of supramolecular materials, as the physical bonds that permit assembly are temporarily broken (**Figure 3.3A, ii**). The kinetics of bond formation, though, are of key interest to the shear response of hydrogels. Craig and coworkers extensively studied the relationship of bond kinetics and polymer relaxation timescales, demonstrating that disadvantageous shear-thickening behavior arises if polymer relaxation occurs more rapidly than reconnection of broken crosslinks.[78,79] As such, the decreased polymer relaxation may be accomplished through formation of multifold junctions in highly modified guest-host hydrogels to enforce shear-thinning behavior and ease of injection.[80] The physical chemistry underlying the flow process, as well as other fundamental behaviors of supramolecular networks have been recently reviewed.[9] Beyond regulating flow properties, the binding kinetics are also essential toward material formation following injection (**Figure 3.3A, iii**), as rapid bond reformation is essential for material retention. In recent work, we demonstrated that rapidly self-healing guest-host hydrogels are well retained (>98% of initial hydrogel volume) upon injection into myocardial tissue, whereas slowly crosslinking covalent controls were not retained as gelation was too slow.[81] This high material retention is essential, including toward successful implementation of injectable materials as tissue supplements, drug reservoirs, or cell delivery vehicles as discussed in subsequent sections.

Also critical to the success of injected biomaterials are the final properties *in vivo*, following injection. In many cases, material degradation may be desired to eliminate the

need for implant removal or permanent implantation. Guest-host assembled materials are of great utility toward this, as they undergo natural disassembly due to their dynamic bonds (**Figure 3.3A, iv**). Thus, their rate of degradation can be controlled through features such as material concentration, guest-host affinity, and number of guest-host bonds.[61,80] Additionally, the degradation rate of such materials may be altered by inclusion of conventional degradation mechanisms, including hydrolysis or enzymatic degradation. Toward such control of degradation, Tian et al utilized a hydrolytically degradable poly(organophosphazine) backbone grafted with PEO of differing molecular weights. In the presence of soluble αCD, hydrogels were formed which exhibited controlled release of bovine serum albumin (BSA) over a period of 2-12 days, with concurrent and prolonged hydrogel degradation.[82] More recently, bioactive degradation mechanisms have been demonstrated; in one embodiment, micelles and hydrogels were formed through inclusion of glutathione in the micelle core to enable bioreduction of the polymeric structures which controlled release of doxorubicin.[83] Additionally, pendant Ad modification of HA has included a peptide linker susceptible to cleavage by matrix metalloproteinases (MMPs) that are naturally produced in remodeling of the extracellular matrix. When combined with pendant modified βCD-HA, hydrogels were formed which exhibited enhanced degradation in the presence of mammalian MMP-2.[84] These means of degradation are of interest to the biomedical community to ensure clearance of the eroded materials (e.g. failed renal clearance of high molecular weight PEO may limit applicability of αCD-PEO hydrogels without inclusion of such hydrolysis mechanisms) and because bioresponsive degradation perpetuates such applications as on-demand drug release and tissue-material integration.

As an alternative to enhanced degradation, prolonged material presence may be desirable. Many supramolecularly assembled materials degrade in the course of days, which may be too rapid for numerous applications in cell delivery or tissue repair. One

approach to achieve improved degradation lifetimes is the use of higher affinity interactions, such as CB[8] with an electron transfer pair, which has enabled sustained release of biomolecules (BSA and lysozyme) for up to 160 days *in vitro.*[85] Interaction of CB[6] and polyamine modified HA has also been used, but implantation was achieved not by shear-thinning injection but instead by sequential subcutaneous injection of the two components, with supramolecular assembly *in vivo*. Inclusion of fluorescently labeled CB[6] in the hydrogel demonstrated presence as long as 11 days, whereas the free fluorophore was released within 24 hours as examined by *in vivo* fluorescence imaging.[86] These approaches demonstrate the capacity for high affinity guest-host pairs to provide prolonged delivery of biomolecules by diffusion or through modular modification with the host molecule, though such high affinity guest-host interactions may limit shear-thinning properties, hindering their use as injectable materials.[87]

Alternatively, the use of secondary stabilization chemistries, subsequent to supramolecular bonding, has been achieved to enhance mechanical stability without affecting injectability. Such processes have been accomplished in protein-based supramolecular assembly using photopolymerization or thermogelation as secondary gelation mechanisms.[28,88] To allow for *in vivo* crosslinking and long-term mechanical stability, we have recently introduced secondary crosslinking *in vivo* through autonomous Michael addition, enabling covalent crosslinking on clinically relevant timescales. Application in a rodent model of myocardial infarct (MI) demonstrated a capacity for mechanical stabilization of the injured tissue, tending to improve geometrical and functional outcomes relative to untreated MI or guest-host material controls without secondary crosslinking.[81] Though, care should be taken in these approaches, as rapid covalent crosslinking may result in delivery failure.

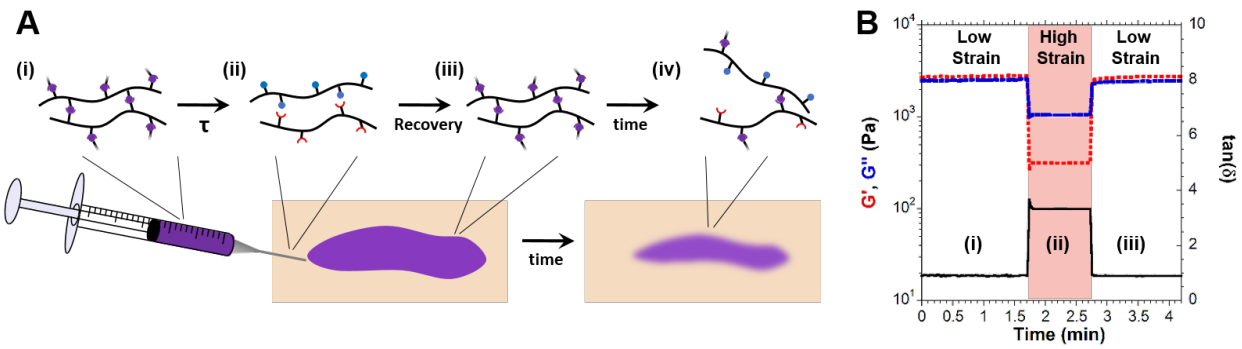

Figure 3.3. Guest-host hydrogel injection. (A) Hydrogels are pre-formed within the syringe through guest-host bonds (i) which are broken by shear stress (τ) within the needle (ii). Following extrusion, bonds rapidly re-form (iii) to enable retention within the tissue. Subsequent disassembly of the hydrogel *in vivo* occurs through spontaneous dissociation of the dynamic bonds and resultant surface erosion of the polymer (iv). (**B**) Representative oscillatory time sweep demonstrating initial hydrogel mechanics (i), yielding to enable flow under high strain (ii), and rapid recovery (iii) such as that proposed for injection. Adapted from Charlot et al. [63]

3.3.2. THERAPEUTIC DELIVERY

In addition to formation of injectable materials by guest-host mediated self-assembly, these unique interactions have significant applications in drug delivery strategies. The most widely used materials in this field have been the CD macrocycles, as they have been used in many pharmacological drug formulations including Sporanox©, Yaz©, and Abilify© among others.[89] CDs form inclusion complexes with various drugs, which improves the drug bioavailabilty by increasing drug solubility and protecting them from degradation, which has been reviewed extensively elsewhere.[13,89,90] Guest-host interactions have also been used recently to develop materials as drug delivery systems, providing novel biofunctionality through non-covalent conjugation of bioactive pendant groups, as well as the development of bulk materials to provide the controlled release of growth factors, genetic material, and small molecule therapeutics.

While improving the physiochemical properties of drugs has prevailed in the translational application of guest-host complexes, more advanced nanoparticle systems

are also being developed. These systems leverage the formation of guest-host complexes as a conjugation strategy to provide stealth or targeting, or to allow nanoparticles to carry hydrophobic payloads (**Figure 3.4A**). Work from the Davis group provides an excellent example of exploiting guest-host complexes in delivery systems that have translated to clinical trials.[91] They developed CD functionalized polymer backbones that form polyplexes with siRNA payloads, with surfaces that may be decorated with Ad coupled macromolecules such as PEG or transferrin.[92-94] This type of conjugation allows for rapid and modular modification of particle systems with a variety of ligands. Similar non-covalent conjugation strategies have been employed using other guest-host pairs such as CB[6] with polyamines to provide targeted delivery of nanocapsules.[95,96] In addition to strategies for noncovalent surface modification, macrocycles have been incorporated into nanoparticles to act as molecular "docking" sites that can facilitate drug loading (**Figure 3.4B**). This carrier functionality has been exploited using amphiphilic CD nanocapsules to entrap tamoxifen, ionic βCD nanoparticles as doxorubicin carriers, and CB[6] particles to carry paclitaxel.[96-98] Furthermore, macrocycle interactions have provided an avenue for direct, noncovalent conjugation of biofunctional groups to drug molecules (**Figure 3.4C**). As examples, βCD functionalized with lactoferrin and saccharide ligands has been used to complex and target drugs to lactoferrin and mannose receptors, respectively.[99,100]

In addition to nanoparticle strategies, guest-host systems have been leveraged in bulk hydrogels to provide controlled release of therapeutic payloads. Many groups have employed guest-host assembly to drive the formation of hydrogels that can provide sustained release of biomolecule payloads such as proteins and growth factors (**Figure 3.4D**). These systems provide diffusive release kinetics that may be tuned through network properties such as porosity, mesh size, and degradation, which may in part be mediated by dynamic supramolecular interactions. For example, Liu et al used

polyrotaxane assembly between αCD and tri-block copolymers to form gels that display tunable sustained release of dextran molecules as a model for release.[101] Furthermore, the Scherman group developed systems based on CB[8] assembly that provide tunable release of bioactive proteins over sustained periods *in vitro*, as previously discussed.[85] Finally, work from the Hennink group as well as our own have shown tunable protein release from βCD-based hydrogels, where crosslink density was used to control release for up to 60 days.[65,102] These applications have recently been extended *in vivo*, where the guest-host hydrogel was used as an injectable material for diffusive local delivery of multiple biomolecules (interleukin-10 and anti-transforming growth factor β) to treat chronic kidney injury.[103] Similarly, hydrogels composed of αCD pseudopolyrotaxanes with PEO terminated block copolymers have been used as an injectable reservoir for delivery of erythropoietin (EPO) in a rodent model of MI. The therapy resulted in a tendency toward increased vascular density as well as a significant decline in apoptosis and increase in myocardial function (fractional shortening) as compared to saline, hydrogel alone, and soluble EPO injection. These examples demonstrate the multifaceted use of such material systems as an easily prepared injectable material to generate diffusively controlled drug delivery reservoirs i*n vivo*.

A last mechanism by which guest-host interactions can control release of molecules is through inclusion effects of therapeutics with macrocycles anchored to a polymer backbone (**Figure 3.4E**). Several groups have investigated covalently crosslinked hydrogels containing CD pendant groups to provide sustained release of small molecules.[104-109] In one example, the von Recum group developed polyurethane gels containing CD as device coatings for the controlled release of numerous antibiotics.[110] Work from our own group has also explored CD retentive effects for controlled release of small molecules including doxorubicin, doxycycline, and peptides containing tryptophan residues, from guest-host assembled networks, leveraging these

interactions to provide materials that are simultaneously injectable and exhibit sustained release properties.[109] These systems provide tunable small molecule release through the engineering of host content, as well as the guest affinity for the host included in the network.

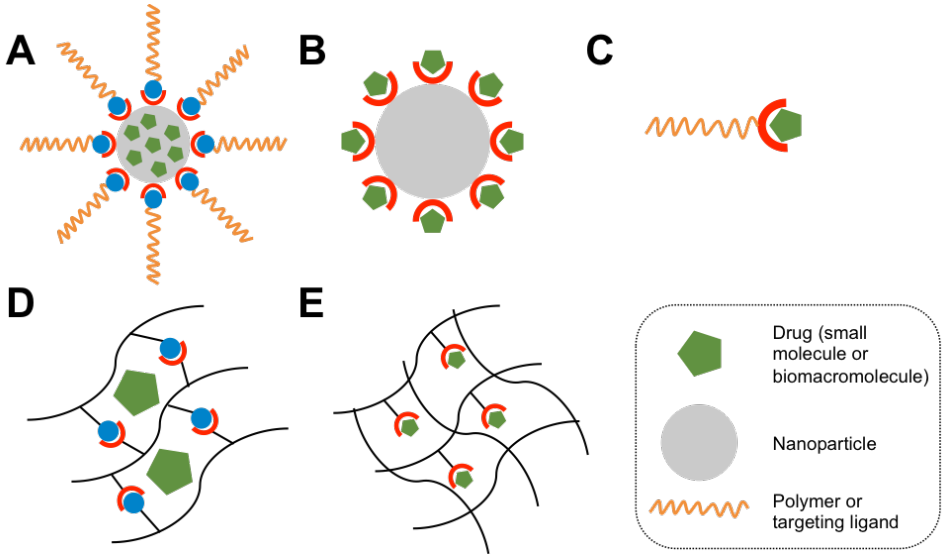

Figure 3.4. Guest-host interactions in drug delivery systems. Guest-host chemistry may be used for direct, non-covalent modification of drug molecules with targeting ligands (**A**), to provide non-covalent modification of nanoparticle drug carriers with targeting or stealth ligands (**B**), and to impart molecular carrier functionality to nanoparticles (**C**). Furthermore, in hydrogel systems, guest-host chemistry may be used to tune crosslinks in hydrogels for the diffusive release of biomacromolecular therapeutics (**D**) or to promote retention of small molecule therapeutics within the hydrogel (**E**).

3.3.3. CELL-MATERIAL INTERACTIONS

While the above applications have targeted material implantation and therapeutic delivery through guest-host mediated assembly, still others have sought to develop methods for the direct modification of cell-material interactions using guest-host chemistry. These approaches to modulate cell-material interactions have primarily taken two forms: modification of material surfaces and the pursuit of material-assisted cell delivery.

Surface modification strategies are useful to introduce various biophysical and biochemical signals to cells, and guest-host interactions provide an opportunity to

introduce dynamic signals that can alter cell behavior. Stupp and colleagues utilized the guest-host complexation of guest-bound adhesive peptide sequences to alginate-βCD surfaces to dynamically control biomolecule display.[111] Specifically, they utilized the fibronectin derived cell-adhesion sequence RGD bound to the guest molecule Ad or naphthalene, suspended in culture medium, to impart cell adhesion and spreading on the material surface. Importantly, spreading was observed to be dependent on the affinity of the guest for βCD and was reversible when napthyl-RGD was removed by competitive binding with the higher affinity non-cell adhesive sequence Ad-RGES. In concurrent work, the Cooper-White group used supramolecular interactions to display RGD in nanopatterned topographies produced by the segregation of Ad terminated polystyrene-co-PEO block copolymers (PS-PEO-Ad).[112] Such topographies are known to influence cell behaviors, including adhesion, spreading, and differentiation.[113-115] The ratio of PS-PEO/PS-PEO-Ad used to control the concentration of βCD-RGD bound within the nanodomains influenced cell adhesion and area. Interestingly, the facile conjugation process enabled the concurrent addition of RGD and the laminin derived sequence IKVAV in set molar ratios, demonstrating similar adhesion across all ratios with spreading and stress fiber organization dependent on RGD concentration alone.

These methods of dynamic surface modification have demonstrated promise toward influencing cell adhesion and spreading; however, little work has been performed to directly demonstrate influence over cell differentiation. There is a growing interest in the field to understand the effects of substrate properties on differentiation, as indicated by the recent use of covalently or ionically crosslinked hydrogels with tunable viscous behaviors (i.e., creep and viscoelasticity) to study differentiation.[116-118] Toward understanding differentiation in response to mechanically dynamic substrates, αCD-PEO polyrotaxane coated surfaces have recently been explored. Here, the mobility of αCD was modulated by methacrylation—thus varying its affinity for PEO. Subsequent coating

of this polyrotaxane surface by fibronectin produced a cell-adhesive surface which demonstrated enhanced osteogenic differentiation in response to molecular mobility. Though, results are complicated by a lack of standardization in fibronectin density between groups.[119]

Cell delivery for therapeutic applications is often problematic, as cells have limited retention at injection sites; however, hydrogels can be used to enhance cell retention, particularly with rapidly re-assembling hydrogels.[88,120] Toward such a delivery approach, Kimoon Kim and colleagues have developed an *in situ* forming supramolecular hydrogel (**Figure 3.5**) based on the interaction of hyaluronic acid modified by CB[6] and alkylammonium ions 1,6-diaminohexane (DAH) or spermine (SPM). Initial studies demonstrated the rapid formation of a hydrogel upon mixing of CB[6]-HA with either DAH-HA or SPM-HA, though SPM-HA hydrogels exhibited significant toxicity toward fibroblasts in culture. In contrast, DAH-HA hydrogels exhibited good cytocompatibility and fibroblast proliferation was observed when hydrogels included the cell adhesive RGD sequence which was modularly included by guest-host interaction through preparation and addition of c(RGDyK)-CB[6].[86] Building upon this work, they utilized the materials as a platform for the delivery of engineered mesenchymal stem cells (eMSCs) for suppression of tumor growth.[121] The authors engineered MSCs to produce interleukin-12 (IL-12) through adenoviral transfection and demonstrated increased IL-12 production by hydrogel inclusion of retinoic acid (RA, hydrolytically bound to HA) and CB[6] conjugated dexamethasone (Dexa-CB[6], guest-host bound). Assessment of enhanced green fluorescent protein (EGFP) expression in a subcutaneous injection model demonstrated cell retention and continued protein expression beyond 60 days, greater than three-fold longer than control hydrogels. Delivery of IL-12 producing eMSCs in a subcutaneous murine melanoma model was successful in retarding tumor growth and enhancing survival outcomes. Importantly, this

effect was enriched by inclusion of Dexa-CB[6] and RA, demonstrating the utility of supramolecular drug inclusion.

While these studies by the Kim group have utilized sequential injection of the hydrogel precursors and in situ hydrogel formation, such approaches may be enhanced by *a priori* hydrogel formation in the presence of cells and subsequent shear-thinning delivery. Indeed, numerous shear-thinning hydrogel systems have increased delivery efficiency both by increasing cell viability and retention at the target site. Toward these efforts, the use of shear-thinning hydrogels based on CD-HA and Ad-HA, previously discussed, have been used to encapsulate and deliver endothelial progenitor cells (EPCs) to myocardial infarct tissue in rodents. Results demonstrated enhanced engraftment of the EPCs with hydrogel delivery (via constitutive GFP expression) at 1 week post-injection when compared to injection of suspended EPC controls. The cell-hydrogel therapy likewise resulted in enhanced vasculogenesis and contractile function when compared to controls of saline, EPC suspension, and hydrogel alone injections.[122] While results from such studies are promising, there is still much work to be done to optimize injection conditions of guest-host systems to make certain that viable cells are being delivered. However, it is known that guest-host type hydrogels exhibit characteristic shear-thinning and shear-banding, similar to other supramolecular hydrogels where such studies have been performed. For example, in alternative supramolecular systems such as in β-hairpin peptide hydrogels, shear-thinning behavior resulted in plug-flow through cylindrical channels (mimicking injection through a needle or catheter), which reduced exposure of encapsulated cells to shear stresses and increased viability.[123] Continuation of this work in loosely crosslinked alginate hydrogels has highlighted the importance of extensional flow, such as near entrance to the syringe needle, as a primary cause of acute cell death.The[124] Extension of these studies toward

direct assembling guest-host hydrogels is essential toward understanding cell viability with respect to clinical applications of cell delivery.

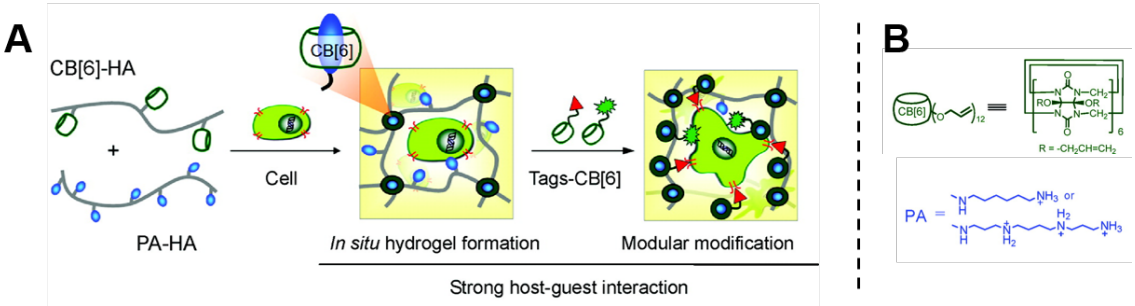

Figure 3.5. Schematic representation of *in situ* supramolecular hydrogel formation. Schematic of cell encapsulation (**A**), through mixing of cucurbit[6]uril-conjugated hyaluronic acid (CB[6]-HA) and polyamine-conjugated HA (PA-HA) and subsequent modular modification with various CB[6] bound tags. The chemical structures (**B**) of CB[6] and PAs of diaminohexane (DAH) and spermine (SPM). Adapted from Sun et al. [83]

3.4. CONCLUSIONS

Supramolecular guest-host chemistry has made great strides over the past decades since formalization of synthetic methods for their production and subsequent polymer modifications. Particularly in the field of bioengineering, these unique chemistries have shown great potential toward numerous applications. Arguably, the most advanced of these is therapeutic delivery, where the use of cavitands (cyclodextrin in particular) to enhance solubility and bioavailability of pharmaceutical drugs has become common practice. However, the capacity to harness these interactions for drug delivery systems (i.e. nanotherapeutics, drug-eluting coatings, and bioresponsive materials) currently remains primarily limited to basic research. Similar to alternative methods of now conventional delivery, such as liposomal formulation of chemotherapeutics, these methods hold promise as a means to revolutionize the pharmaceutical industry; though, their development to industrial scale and market approval remains a challenge.

At a more basic level, the use of guest-host materials as injectable therapeutics is of great interest to the medical community. Such material systems perpetuate numerous applications, including the local delivery of biomolecular therapeutics via diffusion and the supramolecularly controlled delivery of small molecules or suitably modified biomolecules. The use of such materials may also be of interest in tissue bulking applications (e.g., dermal fillers, regenerative scaffolds) and therapeutic cell delivery. However, the investigation of these important material systems and applications is mainly limited to *in vitro* investigation, with exceedingly few examples demonstrating *in vivo* efficacy. Further investigation of the *in vivo* material properties is needed to develop an understanding of material degradation, mechanics, and therapeutic elution. Similarly, the biological response to guest-host materials, including macrophage recruitment and long-term fibrotic encapsulation remains almost wholly unexamined. Further understanding of these systems in a functional, biological setting is a needed priority in the field.

Finally, with respect to basic biological understanding—guest-host assembly offers a unique platform for investigation of cell behavior in response to substrates that mimic aspects of the dynamic ECM. This is embodied in the capacity to dynamically alter cell culture substrates, including to mimic features such as adhesion ligand mobility and substrate viscoelasticity in an attempt to represent more biomimetic cellular environments. Toward the applications discussed herein, understanding of the underlying chemical processes and polymer physics are of utmost importance, as they ultimately control the bulk material properties to enable dynamic, tunable, and responsive materials and bioconjugated systems.

3.5. REFERENCES

1. Service RF. How far can we push chemical self-assembly. Science. 2005;309(5731):95-.
2. Yang L, Tan X, Wang Z, Zhang X. Supramolecular Polymers: Historical Development, Preparation, Characterization, and Functions. Chemical Reviews. 2015;115(15):7196-239.
3. Pedersen CJ. The discovery of crown ethers (Noble Lecture). Angewandte Chemie International Edition in English. 1988;27(8):1021-7.
4. Cram DJ. The design of molecular hosts, guests, and their complexes (Nobel lecture). Angewandte Chemie International Edition in English. 1988;27(8):1009-20.
5. Lehn JM. Supramolecular chemistry—scope and perspectives molecules, supermolecules, and molecular devices (Nobel Lecture). Angewandte Chemie International Edition in English. 1988;27(1):89-112.
6. Hoeben FJ, Jonkheijm P, Meijer E, Schenning AP. About supramolecular assemblies of π-conjugated systems. Chemical Reviews. 2005;105(4):1491-546.
7. Fyfe MC, Stoddart JF. Synthetic supramolecular chemistry. Accounts of Chemical Research. 1997;30(10):393-401.
8. Percec V, Dulcey AE, Balagurusamy VS, Miura Y, Smidrkal J, Peterca M, et al. Self-assembly of amphiphilic dendritic dipeptides into helical pores. Nature. 2004;430(7001):764-8.
9. Seiffert S, Sprakel J. Physical chemistry of supramolecular polymer networks. Chemical Society Reviews. 2012;41(2):909-30.
10. Kakuta T, Takashima Y, Nakahata M, Otsubo M, Yamaguchi H, Harada A. Preorganized Hydrogel: Self‐Healing Properties of Supramolecular Hydrogels

Formed by Polymerization of Host–Guest-Monomers that Contain Cyclodextrins and Hydrophobic Guest Groups. Adv Mater. 2013;25(20):2849-53.

11. Zhou J, Ritter H. Cyclodextrin functionalized polymers as drug delivery systems. Polym Chem-Uk. 2010;1(10):1552-9.

12. Ma X, Zhao Y. Biomedical Applications of Supramolecular Systems Based on Host–Guest Interactions. Chemical Reviews. 2014;115(15):7794-839.

13. Brewster ME, Loftsson T. Cyclodextrins as pharmaceutical solubilizers. Adv Drug Deliver Rev. 2007;59(7):645-66.

14. Szejtli J. Introduction and general overview of cyclodextrin chemistry. Chemical Reviews. 1998;98(5):1743-53.

15. Lagona J, Mukhopadhyay P, Chakrabarti S, Isaacs L. The cucurbit[n]uril family. Angewandte Chemie International Edition. 2005;44(31):4844-70.

16. Appel EA, del Barrio J, Loh XJ, Scherman OA. Supramolecular polymeric hydrogels. Chemical Society Reviews. 2012;41(18):6195-214.

17. Rüdiger V, Eliseev A, Simova S, Schneider H-J, Blandamer MJ, Cullis PM, et al. Conformational, calorimetric and NMR spectroscopic studies on inclusion complexes of cyclodextrins with substituted phenyl and adamantane derivatives. Journal of the Chemical Society, Perkin Transactions 2: Physical Organic Chemistry. 1996(10):2119-23.

18. Harries D, Rau DC, Parsegian VA. Solutes probe hydration in specific association of cyclodextrin and adamantane. J Am Chem Soc. 2005;127(7):2184-90.

19. Kwon GS. Diblock copolymer nanoparticles for drug delivery. Critical Reviews™ in Therapeutic Drug Carrier Systems. 1998;15(5).

20. Deming TJ. Methodologies for preparation of synthetic block copolypeptides: materials with future promise in drug delivery. Adv Drug Deliver Rev. 2002;54(8):1145-55.

21. Hudalla GA, Murphy WL. Biomaterials that regulate growth factor activity via bioinspired interactions. Adv Funct Mater. 2011;21(10):1754-68.

22. Purcell BP, Lobb D, Charati MB, Dorsey SM, Wade RJ, Zellars KN, et al. Injectable and bioresponsive hydrogels for on-demand matrix metalloproteinase inhibition. Nature Materials. 2014;13:653-61.

23. Huang F, Nagvekar DS, Slebodnick C, Gibson HW. A supramolecular triarm star polymer from a homotritopic tris (crown ether) host and a complementary monotopic paraquat-terminated polystyrene guest by a supramolecular coupling method. J Am Chem Soc. 2005;127(2):484-5.

24. Yan X, Xu D, Chi X, Chen J, Dong S, Ding X, et al. A Multiresponsive, Shape‐Persistent, and Elastic Supramolecular Polymer Network Gel Constructed by Orthogonal Self‐Assembly. Adv Mater. 2012;24(3):362-9.

25. Foo C, Lee JS, Mulyasasmita W, Parisi-Amon A, Heilshorn SC. Two-component protein-engineered physical hydrogels for cell encapsulation. P Natl Acad Sci USA. 2009;106(52):22067-72.

26. Zhang X, Chu X, Wang L, Wang H, Liang G, Zhang J, et al. Rational Design of a Tetrameric Protein to Enhance Interactions between Self‐Assembled Fibers Gives Molecular Hydrogels. Angewandte Chemie. 2012;124(18):4464-8.

27. Lu HD, Charati MB, Kim IL, Burdick JA. Injectable shear-thinning hydrogels engineered with a self-assembling Dock-and-Lock mechanism. Biomaterials. 2012;33(7):2145-53.

28. Lu HD, Soranno, D.E., Rodell, C.B., Kim, I. L., Burdick, J.A. Secondary Photocrosslinking of Injectable Shear-Thinning Dock-and-Lock Hydrogels. Advanced healthcare materials. 2013;2(7):1028-36.

29. Grove TZ, Forster J, Pimienta G, Dufresne E, Regan L. A modular approach to the design of protein-based smart gels. Biopolymers. 2012;97(7):508-17.

30. Villiers A. Sur la transformation de la fécule en dextrine par le ferment butyrique. Compt Rend Fr Acad Sci. 1891;112:435-8.

31. Biwer A, Antranikian G, Heinzle E. Enzymatic production of cyclodextrins. Appl Microbiol Biot. 2002;59(6):609-17.

32. GRAS Notice No. GRN 000155: alpha-cyclodextrin. In: Administration USFaD, editor. 2004.

33. GRAS Notice No. GRN 000074: beta-cyclodextrin. In: Administration USFaD, editor. 2001.

34. GRAS Notice No. GRN 000046: gamma-cyclodextrin. In: Administration USFaD, editor. 2000.

35. Rekharsky MV, Inoue Y. Complexation thermodynamics of cyclodextrins. Chem Rev. 1998;98(5):1875-918.

36. Bortolus P, Monti S. cis. dblharw. trans Photoisomerization of azobenzene-cyclodextrin inclusion complexes. Journal of Physical Chemistry. 1987;91(19):5046-50.

37. Matsue T, Evans DH, Osa T, Kobayashi N. Electron-transfer reactions associated with host-guest complexation. Oxidation of ferrocenecarboxylic acid in the presence of beta-cyclodextrin. J Am Chem Soc. 1985;107(12):3411-7.

38. Kaifer AE. Interplay between molecular recognition and redox chemistry. Accounts of Chemical Research. 1999;32(1):62-71.

39. Mura S, Nicolas J, Couvreur P. Stimuli-responsive nanocarriers for drug delivery. Nature Materials. 2013;12(11):991-1003.

40. Takashima Y, Hatanaka S, Otsubo M, Nakahata M, Kakuta T, Hashidzume A, et al. Expansion–contraction of photoresponsive artificial muscle regulated by host–guest interactions. Nat Commun. 2012;3:1270.

41. Nakahata M, Takashima Y, Hashidzume A, Harada A. Redox-Generated Mechanical Motion of a Supramolecular Polymeric Actuator Based on Host–Guest Interactions. Angewandte Chemie International Edition. 2013;52(22):5731-5.

42. Wang Y, Ma N, Wang Z, Zhang X. Photocontrolled Reversible Supramolecular Assemblies of an Azobenzene-Containing Surfactant with α-Cyclodextrin. Angewandte Chemie International Edition. 2007;46(16):2823-6.

43. Tamesue S, Takashima Y, Yamaguchi H, Shinkai S, Harada A. Photoswitchable supramolecular hydrogels formed by cyclodextrins and azobenzene polymers. Angewandte Chemie. 2010;122(41):7623-6.

44. Zhou L, Li J, Luo Q, Zhu J, Zou H, Gao Y, et al. Dual stimuli-responsive supramolecular pseudo-polyrotaxane hydrogels. Soft Matter. 2013;9(18):4635-41.

45. Behrend R, Meyer E, Rusche F. I. Ueber Condensationsproducte aus Glycoluril und Formaldehyd. Justus Liebigs Annalen der Chemie. 1905;339(1):1-37.

46. Freeman WA, Mock WL, Shih NY. Cucurbituril. J Am Chem Soc. 1981;103(24):7367-8.

47. Oun R, Floriano RS, Isaacs L, Rowan EG, Wheate NJ. The ex vivo neurotoxic, myotoxic and cardiotoxic activity of cucurbituril-based macrocyclic drug delivery vehicles. Toxicology research. 2014;3(6):447-55.

48. Liu S, Ruspic C, Mukhopadhyay P, Chakrabarti S, Zavalij PY, Isaacs L. The cucurbit[n]uril family: prime components for self-sorting systems. J Am Chem Soc. 2005;127(45):15959-67.

49. Mock WL, Shih NY. Structure and selectivity in host-guest complexes of cucurbituril. J Org Chem. 1986;51(23):4440-6.

50. Moghaddam S, Yang C, Rekharsky M, Ko YH, Kim K, Inoue Y, et al. New Ultrahigh Affinity Host− Guest Complexes of Cucurbit [7] uril with Bicyclo [2.2. 2] octane and Adamantane Guests: Thermodynamic Analysis and Evaluation of M2 Affinity Calculations. J Am Chem Soc. 2011;133(10):3570-81.

51. Ko YH, Kim E, Hwang I, Kim K. Supramolecular assemblies built with host-stabilized charge-transfer interactions. Chem Commun. 2007(13):1305-15.

52. Ryu E-H, Zhao Y. Efficient synthesis of water-soluble calixarenes using click chemistry. Organic Letters. 2005;7(6):1035-7.

53. Harada A, Li J, Kamachi M. The molecular necklace: a rotaxane containing many threaded α-cyclodextrins. Nature. 1992;356(6367):325-7.

54. Li J, Harada A, Kamachi M. Sol–gel transition during inclusion complex formation between α-cyclodextrin and high molecular weight poly (ethylene glycol) s in aqueous solution. Polym J. 1994;26(9):1019-26.

55. Liu KL, Zhang Z, Li J. Supramolecular hydrogels based on cyclodextrin–polymer polypseudorotaxanes: materials design and hydrogel properties. Soft Matter. 2011;7(24):11290-7.

56. Li J, Ni XP, Leong KW. Injectable drug-delivery systems based on supramolecular hydrogels formed by poly(ethylene oxide) and alpha-cyclodextrin. J Biomed Mater Res A. 2003;65A(2):196-202.

57. Liu Y, Yu Y, Gao J, Wang Z, Zhang X. Water‐Soluble Supramolecular Polymerization Driven by Multiple Host‐Stabilized Charge‐Transfer Interactions. Angewandte Chemie. 2010;122(37):6726-9.

58. Zeng F, Han Y, Chen C-F. Self-sorting behavior of a four-component host–guest system and its incorporation into a linear supramolecular alternating copolymer. Chem Commun. 2015;51(17):3593-5.

59. Rauwald U, Scherman OA. Supramolecular block copolymers with cucurbit [8] uril in water. Angewandte Chemie International Edition. 2008;47(21):3950-3.

60. van de Manakker F, Vermonden T, el Morabit N, van Nostrum CF, Hennink WE. Rheological behavior of self-assembling PEG-β-cyclodextrin/PEG-cholesterol hydrogels. Langmuir. 2008;24(21):12559-67.

61. van de Manakker F, Braeckmans K, el Morabit N, De Smedt SC, van Nostrum CF, Hennink WE. Protein-Release Behavior of Self-Assembled PEG-beta-Cyclodextrin/PEG-Cholesterol Hydrogels. Adv Funct Mater. 2009;19(18):2992-3001.

62. Charlot A, Auzely-Velty R, Rinaudo M. Specific interactions in model charged polysaccharide systems. J Phys Chem B. 2003;107(32):8248-54.

63. Charlot A, Auzely-Velty R. Synthesis of novel supramolecular assemblies based on hyaluronic acid derivatives bearing bivalent beta-cyclodextrin and adamantane moieties. Macromolecules. 2007;40(4):1147-58.

64. Semenov A, Charlot A, Auzely-Velty R, Rinaudo M. Rheological properties of binary associating polymers. Rheologica Acta. 2007;46(5):541-68.

65. Rodell CB, Kaminski AL, Burdick JA. Rational Design of Network Properties in Guest–Host Assembled and Shear-Thinning Hyaluronic Acid Hydrogels. Biomacromolecules. 2013;14(11):4125-34.

66. Appel EA, Biedermann F, Rauwald U, Jones ST, Zayed JM, Scherman OA. Supramolecular Cross-Linked Networks via Host-Guest Complexation with Cucurbit 8 uril. J Am Chem Soc. 2010;132(40):14251-60.

67. Appel EA, Loh XJ, Jones ST, Biedermann F, Dreiss CA, Scherman OA. Ultrahigh-Water-Content Supramolecular Hydrogels Exhibiting Multistimuli Responsiveness. J Am Chem Soc. 2012;134(28):11767-73.

68. Xu J-F, Chen L, Zhang X. How to Make Weak Noncovalent Interactions Stronger. Chemistry - A European Journal. 2015;21(34):11938-46.

69. Zayed JM, Nouvel N, Rauwald U, Scherman OA. Chemical complexity—supramolecular self-assembly of synthetic and biological building blocks in water. Chemical Society Reviews. 2010;39(8):2806-16.

70. Mendes AC, Baran ET, Reis RL, Azevedo HS. Self‐assembly in nature: using the principles of nature to create complex nanobiomaterials. Wiley Interdisciplinary Reviews: Nanomedicine and Nanobiotechnology. 2013;5(6):582-612.

71. Hartgerink JD, Beniash E, Stupp SI. Self-assembly and mineralization of peptide-amphiphile nanofibers. Science. 2001;294(5547):1684-8.

72. Aldaye FA, Senapedis WT, Silver PA, Way JC. A structurally tunable DNA-based extracellular matrix. J Am Chem Soc. 2010;132(42):14727-9.

73. Dankers PYW, Hermans TM, Baughman TW, Kamikawa Y, Kieltyka RE, Bastings MMC, et al. Hierarchical Formation of Supramolecular Transient Networks in Water: A Modular Injectable Delivery System. Adv Mater. 2012;24(20):2703-9.

74. Zhang M, Xiong Q, Shen W, Zhang Q. Facile synthesis of well-defined cyclodextrin-pendant polymer via ATRP for nanostructure fabrication. RSC Advances. 2014;4(58):30566-72.

75. Zhang X, Nie C-B, Zhou T-Y, Qi Q-Y, Fu J, Wang X-Z, et al. The construction of single-layer two-dimensional supramolecular organic frameworks in water through the self-assembly of rigid vertexes and flexible edges. Polym Chem-Uk. 2015;6(11):1923-7.

76. Chen H, Ma H, Chieng YY, Hou S, Li X, Tan Y. Aggregation and thermal gelation of N-isopropylacrylamide based cucurbit [7] uril side-chain polypseudorotaxanes with low pseudorotaxane content. RSC Advances. 2015;5(27):20684-90.

77. Guvendiren M, Lu HD, Burdick JA. Shear-thinning hydrogels for biomedical applications. Soft Matter. 2012;8(2):260-72.

78. Xu D, Hawk JL, Loveless DM, Jeon SL, Craig SL. Mechanism of shear thickening in reversibly cross-linked supramolecular polymer networks. Macromolecules. 2010;43(7):3556-65.

79. Xu DH, Liu CY, Craig SL. Divergent Shear Thinning and Shear Thickening Behavior of Supramolecular Polymer Networks in Semidilute Entangled Polymer Solutions. Macromolecules. 2011;44(7):2343-53.

80. Rodell CB, Kaminski AL, Burdick JA. Rational Design of Network Properties in Guest-Host Assembled and Shear-Thinning Hyaluronic Acid Hydrogels. Biomacromolecules. 2013;14(11):4125-34.

81. Rodell CB, MacArthur JW, Dorsey SM, Wade RJ, Wang LL, Woo YJ, et al. Shear-Thinning Supramolecular Hydrogels with Secondary Autonomous Covalent Crosslinking to Modulate Viscoelastic Properties In Vivo. Adv Funct Mater. 2015;25(4):636-44.

82. Tian Z, Chen C, Allcock HR. Injectable and biodegradable supramolecular hydrogels by inclusion complexation between poly (organophosphazenes) and α-cyclodextrin. Macromolecules. 2013;46(7):2715-24.

83. Sun L, Liu W, Dong C-M. Bioreducible micelles and hydrogels with tunable properties from multi-armed biodegradable copolymers. Chem Commun. 2011;47(40):11282-4.

84. Rodell CB, Wade RJ, Purcell BP, Dusaj NN, Burdick JA. Selective Proteolytic Degradation of Guest–Host Assembled, Injectable Hyaluronic Acid Hydrogels. Acs Biomater Sci Eng. 2015;1(4):277-86.

85. Appel EA, Loh XJ, Jones ST, Dreiss CA, Scherman OA. Sustained release of proteins from high water content supramolecular polymer hydrogels. Biomaterials. 2012;33(18):4646-52.

86. Park KM, Yang JA, Jung H, Yeom J, Park JS, Park K-H, et al. In Situ Supramolecular Assembly and Modular Modification of Hyaluronic Acid Hydrogels for 3D Cellular Engineering. Acs Nano. 2012;6(4):2960-8.

87. Rybtchinski B. Adaptive supramolecular nanomaterials based on strong noncovalent interactions. Acs Nano. 2011;5(9):6791-818.

88. Cai L, Dewi RE, Heilshorn SC. Injectable Hydrogels with In Situ Double Network Formation Enhance Retention of Transplanted Stem Cells. Adv Funct Mater. 2015;25(9):1344-51.

89. Loftsson T, Duchene D. Cyclodextrins and their pharmaceutical applications. Int J Pharmaceut. 2007;329(1):1-11.

90. Uekama K, Hirayama F, Irie T. Cyclodextrin drug carrier systems. Chemical reviews. 1998;98(5):2045-76.

91. Davis ME. The first targeted delivery of siRNA in humans via a self-assembling, cyclodextrin polymer-based nanoparticle: from concept to clinic. Mol Pharmaceut. 2009;6(3):659-68.

92. Gonzalez H, Hwang SJ, Davis M. New class of polymers for the delivery of macromolecular therapeutics. Bioconjugate chemistry. 1999;10(6):1068-74.

93. Bartlett DW, Davis ME. Physicochemical and biological characterization of targeted, nucleic acid-containing nanoparticles. Bioconjugate chemistry. 2007;18(2):456-68.

94. Bellocq NC, Pun SH, Jensen GS, Davis ME. Transferrin-containing, cyclodextrin polymer-based particles for tumor-targeted gene delivery. Bioconjugate chemistry. 2003;14(6):1122-32.

95. Theodossiou TA, Gonçalves AR, Yannakopoulou K, Skarpen E, Berg K. Photochemical Internalization of Tamoxifens Transported by a “Trojan‐Horse” Nanoconjugate into Breast‐Cancer Cell Lines. Angew Chem Int Ed. 2015;54(16):4885-9.

96. Park KM, Suh K, Jung H, Lee D-W, Ahn Y, Kim J, et al. Cucurbituril-based nanoparticles: a new efficient vehicle for targeted intracellular delivery of hydrophobic drugs. Chem Commun. 2009(1):71-3.

97. Memisoglu-Bilensoy E, Vural I, Bochot A, Renoir JM, Duchene D, Hıncal AA. Tamoxifen citrate loaded amphiphilic β-cyclodextrin nanoparticles: In vitro characterization and cytotoxicity. J Control Release. 2005;104(3):489-96.

98. Gil ES, Li J, Xiao H, Lowe TL. Quaternary Ammonium β-Cyclodextrin Nanoparticles for Enhancing Doxorubicin Permeability across the In Vitro Blood−Brain Barrier. Biomacromolecules. 2009;10(3):505-16.

99. Benito JM, Gómez-García M, Ortiz Mellet C, Baussanne I, Defaye J, García Fernández JM. Optimizing saccharide-directed molecular delivery to biological receptors: design, synthesis, and biological evaluation of glycodendrimer-cyclodextrin conjugates. J Am Chem Soc. 2004;126(33):10355-63.

100. Ye Y, Sun Y, Zhao H, Lan M, Gao F, Song C, et al. A novel lactoferrin-modified β-cyclodextrin nanocarrier for brain-targeting drug delivery. Int J Pharmaceut. 2013;458(1):110-7.

101. Li J, Li X, Ni X, Wang X, Li H, Leong KW. Self-assembled supramolecular hydrogels formed by biodegradable PEO–PHB–PEO triblock copolymers and α-cyclodextrin for controlled drug delivery. Biomaterials. 2006;27(22):4132-40.

102. van de Manakker F, van der Pot M, Vermonden T, van Nostrum CF, Hennink WE. Self-assembling hydrogels based on β-cyclodextrin/cholesterol inclusion complexes. Macromolecules. 2008;41(5):1766-73.

103. Rodell CB, Rai R, Faubel S, Burdick JA, Soranno DE. Local immunotherapy via delivery of interleukin-10 and transforming growth factor β antagonist for treatment of chronic kidney disease. J Control Release. 2015;206(0):131-9.

104. Thatiparti TR, von Recum HA. Cyclodextrin Complexation for Affinity-Based Antibiotic Delivery. Macromol Biosci. 2010;10(1):82-90.

105. Xu J, Li X, Sun F. Cyclodextrin-containing hydrogels for contact lenses as a platform for drug incorporation and release. Acta Biomater. 2010;6(2):486-93.

106. Mateen R, Hoare T. Injectable, in situ gelling, cyclodextrin–dextran hydrogels for the partitioning-driven release of hydrophobic drugs. J Mater Chem B. 2014;2(32):5157-67.

107. Lima AC, Puga AM, Mano J, Concheiro A, Alvarez-Lorenzo C. Free and copolymerized γ-cyclodextrins regulate the performance of dexamethasone-loaded dextran microspheres for bone regeneration. Journal of Materials Chemistry B. 2014;2(30):4943-56.

108. Peng K, Tomatsu I, Korobko AV, Kros A. Cyclodextrin–dextran based in situ hydrogel formation: a carrier for hydrophobic drugs. Soft Matter. 2009;6(1):85-7.

109. Mealy J, Rodell C, Burdick JA. Sustained Small Molecule Delivery from Injectable Hyaluronic Acid Hydrogels through Host-Guest Mediated Retention. Journal of Materials Chemistry B. 2015.

110. Thatiparti TR, Shoffstall AJ, von Recum HA. Cyclodextrin-based device coatings for affinity-based release of antibiotics. Biomaterials. 2010;31(8):2335-47.

111. Boekhoven J, Perez CMR, Sur S, Worthy A, Stupp SI. Dynamic Display of Bioactivity through Host-Guest Chemistry. Angewandte Chemie-International Edition. 2013;52(46):12077-80.

112. Li HQ, Frith J, Cooper-White JJ. Modulation of Stem Cell Adhesion and Morphology via Facile Control over Surface Presentation of Cell Adhesion Molecules. Biomacromolecules. 2014;15(1):43-52.

113. Arnold M, Cavalcanti-Adam EA, Glass R, Blümmel J, Eck W, Kantlehner M, et al. Activation of integrin function by nanopatterned adhesive interfaces. Chemphyschem. 2004;5(3):383-8.

114. Cavalcanti-Adam EA, Volberg T, Micoulet A, Kessler H, Geiger B, Spatz JP. Cell spreading and focal adhesion dynamics are regulated by spacing of integrin ligands. Biophysical Journal. 2007;92(8):2964-74.

115. Frith JE, Mills RJ, Cooper-White JJ. Lateral spacing of adhesion peptides influences human mesenchymal stem cell behaviour. Journal of Cell Science. 2012;125(2):317-27.

116. Cameron AR, Frith JE, Cooper-White JJ. The influence of substrate creep on mesenchymal stem cell behaviour and phenotype. Biomaterials. 2011;32(26):5979-93.

117. Cameron AR, Frith JE, Gomez GA, Yap AS, Cooper-White JJ. The effect of time-dependent deformation of viscoelastic hydrogels on myogenic induction and Rac1 activity in mesenchymal stem cells. Biomaterials. 2014;35(6):1857-68.

118. Chaudhuri O, Gu L, Darnell M, Klumpers D, Bencherif SA, Weaver JC, et al. Substrate stress relaxation regulates cell spreading. Nat Commun. 2015;6.

119. Seo JH, Kakinoki S, Yamaoka T, Yui N. Directing Stem Cell Differentiation by Changing the Molecular Mobility of Supramolecular Surfaces. Advanced healthcare materials. 2015;4(2):215-22.

120. Parisi-Amon A, Mulyasasmita W, Chung C, Heilshorn SC. Protein-Engineered Injectable Hydrogel to Improve Retention of Transplanted Adipose-Derived Stem Cells. Advanced healthcare materials. 2013;2(3):428-32.

121. Yeom J, Kim SJ, Jung H, Namkoong H, Yang J, Hwang BW, et al. Supramolecular Hydrogels for Long-Term Bioengineered Stem Cell Therapy. Advanced healthcare materials. 2015;4(2):237-44.

122. Gaffey AC, Chen MH, Venkataraman CM, Trubelja A, Rodell CB, Dinh PV, et al. Injectable shear-thinning hydrogels used to deliver endothelial progenitor cells, enhance cell engraftment, and improve ischemic myocardium. The Journal of Thoracic and Cardiovascular Surgery.

123. Yan C, Mackay ME, Czymmek K, Nagarkar RP, Schneider JP, Pochan DJ. Injectable Solid Peptide Hydrogel as a Cell Carrier: Effects of Shear Flow on Hydrogels and Cell Payload. Langmuir. 2012;28(14):6076-87.

124. Aguado BA, Mulyasasmita W, Su J, Lampe KJ, Heilshorn SC. Improving Viability of Stem Cells During Syringe Needle Flow Through the Design of Hydrogel Cell Carriers. Tissue Engineering Part A. 2012;18(7-8):806-15.

CHAPTER 4

SUSTAINED SMALL MOLECULE DELIVERY FROM SUPRAMOLECULAR HYALURONIC ACID HYDROGELS THROUGH GUEST-HOST MEDIATED RETENTION

Adapted from:

Mealy JE, Rodell CB, Burdick JA. Sustained small molecule delivery from injectable hyaluronic acid hydrogels through host–guest mediated retention. Journal of Materials Chemistry B. 2015;3(40):8010-9.

4.1. INTRODUCTION

Towards the development of translational, multifaceted strategies for treating disease, self-assembled hydrogels provide unique properties to deliver therapeutics (e.g., cells, drugs) to tissues. Self-assembly, driven through non-covalent interactions, may impart shear-thinning and self-healing properties to hydrogels, which allows direct injection into tissues. A number of non-covalent interactions have been investigated to form self-assembled hydrogels, including hydrophobic interactions or guest-host assembly of macrocycles such as cucurbiturils and cyclodextrins (CDs).[1-3]

CDs are cyclic macromolecules formed from 6, 7, or 8 α-D-glucopyranoside units, termed α-, β-, and γ-CD respectively. As a strategy for self-assembly, these molecular interactions have been employed to form hydrogels between polymers modified with β-CD and adamantane (Ad), α-CD and PEG, and β-CD and azobenzene, among other polymer systems.[3-5] These self-assembled hydrogels have been used towards a number of biomedical therapies, including mechanical interventions, cell

delivery, and sustained therapeutic release.[6-9] CD guest-host chemistry has previously been used in the design of drug delivery systems. Notably, the Davis group has developed cationic CD polymers that ionically complex with nucleic acids to form nanoparticles, that may be functionalized with targeting ligands via Ad interactions to promote receptor-mediated endocytosis.[10] Regarding sustained release, self-assembled hydrogels provide easily injectable depots of therapeutics; however, their investigation as drug delivery systems has largely been focused on macromolecules where release is governed through network properties. Despite recent advances in supramolecular systems, few supramolecular hydrogels have been investigated for small molecule release, due to difficulties associated with using these traditional mechanisms (e.g. matrix erosion, control of mesh size) to sustain the release of small molecules.

Small molecule therapeutics are potent drugs that can be used in such strategies as chemotherapy or the inhibition of pathologic matrix metalloproteinase (MMP) activity, where there is a need for systems that permit localized and sustained therapeutic delivery.[11] Due to the highly hydrated nature of hydrogels and their large mesh size, most small molecules will diffuse out rapidly in a matter of hours, which is often too fast to provide sustained therapeutic effects. To address this challenge, strategies using composite systems of hydrogels and hydrophobic micro/nanoparticles or covalent conjugation of drugs to polymer backbones have been developed to provide sustained small molecule release.[12] While these strategies are effective, they require added complexity in hierarchical formulation or offer regulatory translational limitations by modifying drug molecules. A third strategy that may be used to sustain small molecule release is to engineer non-covalent affinity between small molecules and polymers to increase retention time. Hydrogels using affinity mediated sustained release have recently been developed leveraging interactions between therapeutic peptides or

hydrophobic molecules and polypeptide-based hydrogels, as well as between macrocycle hosts and guest ligands.[7,13,14]

CDs have remarkable affinity for a wide variety of small molecule guests, which has led to the use of CDs as excipients in a number of small molecule pharmaceuticals.[15,16] In addition, these guest-host interactions have been leveraged to increase molecule retention within covalently crosslinked hydrogels.[14,17-20] In one example, antibiotic release was sustained for ~10 days from covalently crosslinked polyurethane hydrogels of β-CD and multivalent isocyanates that were used to coat metal screws and polymer meshes.[14,21] β-CD also forms inclusion complexes with a wide variety of other molecules, including chemotherapeutics such as doxorubicin, MMP inhibitors such as doxycycline, and even aromatic amino acids such as tryptophan.[22-26] However, β-CD inclusion complexes have not yet been leveraged to provide sustained small molecule release from hydrogels formed via supramolecular self-assembly.

Recently, our group developed a two component supramolecular hydrogel formed from hyaluronic acid (HA) modified with Ad (Ad-HA) and HA modified with β-CD (CD-HA).[3] HA is a natural component of the extracellular matrix, which interacts with cell surface receptors and can even provide stem cell recruitment.[27,28] We hypothesized that alterations in CD content and payload affinity for CD would alter the release of molecules from hydrogels (**Figure 4.1**). Such a system combines the unique shear-thinning and self-healing properties previously reported in these hydrogels with the unique guest-host inclusion capability of β-CD for a number of small molecule drugs.

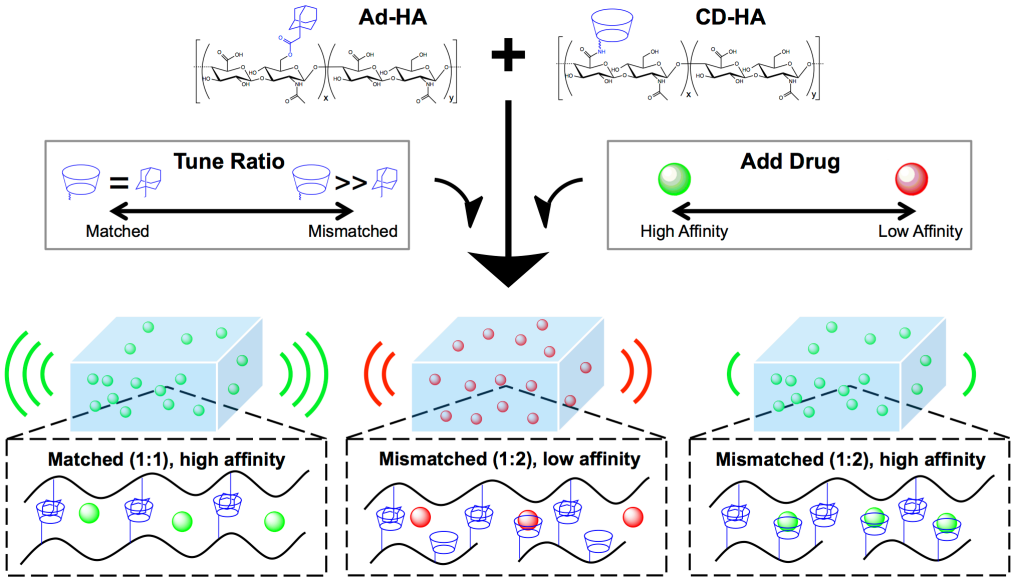

Figure 4.1. Scheme for tuning release of small molecules from drug loaded supramolecular hydrogels. Ad-HA and CD-HA macromers were synthesized and evaluated for functionalization (x/[x+y]) using ^{1}H-NMR. Macromers were dissolved in solutions containing varying drugs (green = high affinity for CD, red = low affinity for CD) and combined in varying ratios (Ad:CD) to produce bulk hydrogels. Release kinetics were tuned by varying the CD content available for drug binding or by altering the affinity of the loaded drug for CD.

4.2. METHODS

4.2.1. MATERIALS

Sodium hyaluronic acid (HA, 90kDa) was purchased from Lifecore (Chaska, MN). β-cyclodextrin (CD), 1-adamantane acetic acid, and hexanediamine (HDA) were purchased from TCI America (Portland, OR). Fluorenylmethyloxycarbonyl (FMOC) protected amino acids and (1H-Benzotriazol-1-yloxy)(dimethylamino)-N,N-dimethylmethaniminium hexafluorophosphate (HBTU) were purchased from Novabiochem (Billerica, MA). All other materials were purchased from Sigma-Aldrich (St Louis, MO).

4.2.2. MACROMER SYNTHESIS

Ad-HA was synthesized according to previously reported protocols.[3] Briefly, HA was first converted to a tetrabutylammonium salt (HA-TBA) through the use of an ion exchange resin (Dowex 50Wx4). HA was dissolved in DI water at 3 wt% and mixed with the resin for 4 h to allow for ion exchange. The resulting solution was filtered, neutralized with tetrabutylammonium hydroxide, frozen, and lyophilized to produce the HA-TBA salt. To synthesize Ad-HA, HA-TBA, 4-methylaminepyridine, di-tertbutyl dicarbonate and Ad were then dissolved using dimethyl sulfoxide (DMSO) and allowed to react for 20 h at 45 °C under nitrogen. The resulting Ad-HA product was then purified by dialysis against DI water for 3 days, precipitated in acetone, and then further dialyzed against DI water for a total of 2 weeks. The aqueous polymer solution was then frozen, lyophilized, and analyzed for purity and percent modification using ^{1}H-NMR (DMX 360, Bruker, Billerica, MA). All Ad-HA used in this study had ~25 % of HA repeat units modified with Ad groups (**Figure 4.2**).

To facilitate conjugation to HA, β-CD was aminated using an HDA linker. First, β-CD was tosylated through the reaction of *p*-toluenesulfonyl chloride and β-CD in aqueous solution. Sodium hydroxide (3 mol NaOH/ mol CD) was added dropwise to the solution and stirred for 30 min at room temperature. Next, ammonium chloride was added to adjust the pH to ~8.5 and precipitate the β-CD tosylate. β-CD tosylate was repeatedly washed in water and acetone and then dried under vacuum to use in the amination reaction. A 2-neck flask was charged with β-CD tosylate, HDA, and DMF. The flask was connected to a condenser, purged by nitrogen, and reacted for 16 h at 80 °C. CD-HDA was purified by repeated washes with acetone and diethyl ether to yield aminated β-CD (CD-HDA). To form CD-HA, HA-TBA, CD-HDA, and (benzotriazol-1-ylozy)tris(dimethylamino)phosphonium hexafluorophosphate were dissolved in DMSO in a round bottom flask. The reaction was allowed to proceed for 3 h at room temperature.

CD-HA was then purified by dialysis against water for 2 weeks, frozen, lyophilized, and characterized using ^{1}H-NMR. CD-HA used in this study was modified at ~35 % of HA repeat units for calorimetry experiments and ~25 % for all other experiments (**Figure 4.2**).

Methacrylated HA (MeHA) was synthesized according to previously reported protocols.[29] Briefly, sodium HA was dissolved in DI water and methacrylic anhydride was added incrementally to the solution, while maintaining the pH between 7.5 - 8.5 for 5 h. The solution was then dialyzed extensively against DI water, frozen, lyophilized, and characterized using ^{1}H-NMR. MeHA used in this study was modified at ~30 % of HA repeat units (**Figure 4.2**).

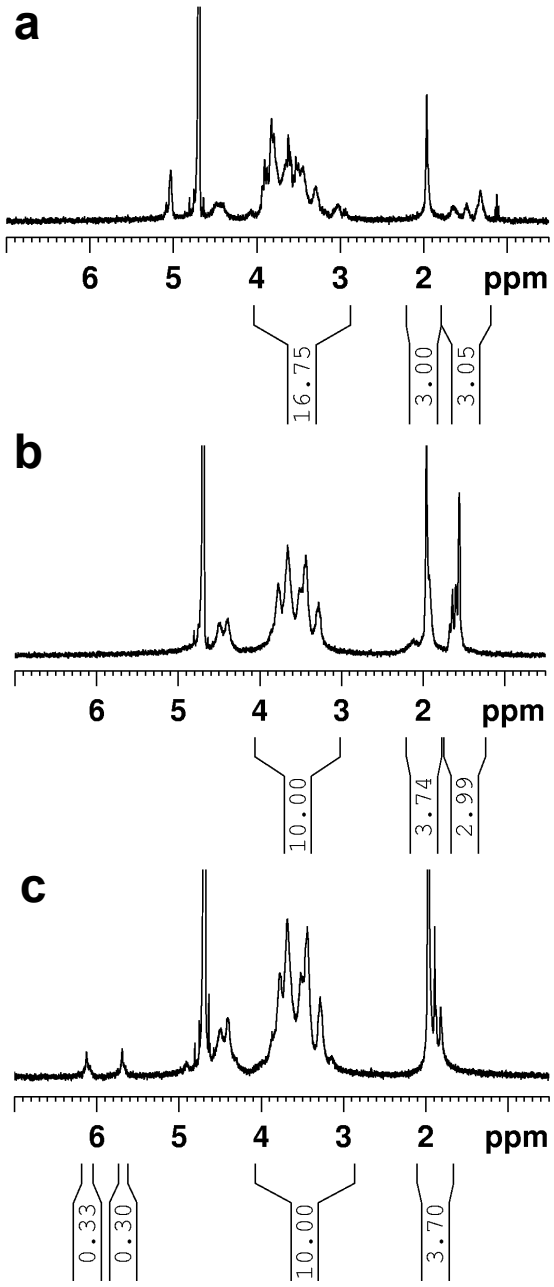

Figure 4.2. NMR spectra for various modifications of HA. ^{1}H-NMR for CD-HA (a), Ad-HA (b), and MeHA (c).

4.2.3. PEPTIDE SYNTHESIS

Peptides were synthesized using standard solid phase synthesis on a solid phase peptide synthesizer (PS3, Protein Technologies Inc., Tuscon, AZ). Two fluorescein modified peptides, GKWEWKWE-FITC (3W) and GKGEGKGE-FITC (NoW)

were synthesized as model drugs that have a high or low affinity for β-CD, respectively. Peptides were synthesized on a glycinol 2-chlorotrityl resin and with FMOC protected amino acids. Peptides were cleaved in a mixture of trifluoroacetic acid, triisopropylsilane, and water (95:2.5:2.5) and then purified through precipitation in cold diethylether. Solid peptides were dissolved in DI water, frozen, and lyophilized. Peptide purity and sequence were confirmed using MALDI-TOF spectroscopy (Multiflex, Bruker, Billerica, MA). Masses for both 3W (expected 1549.6, m/z 1571.8, corresponding to a complex with Na ion) and NoW (expected 1162.1, m/z 1162.6) confirmed successful peptide synthesis.

4.2.4. HYDROGEL PREPARATION

Hydrogels were prepared by first dissolving CD-HA and Ad-HA in phosphate buffered saline (PBS) or PBS containing drug overnight at room temperature. The CD-HA and Ad-HA solutions were mixed to induce gelation. For notation, hydrogels are referred to as x:y (z wt%) hydrogels, with x:y referring to the Ad:CD stoichiometric ratio within a given hydrogel, and z wt% referring to the total macromer weight percent of the hydrogel. All guest-host hydrogels were made using 25 % modified CD-HA and 25 % modified Ad-HA.

MeHA hydrogels were formed through a photoinitiated radical polymerization of a macromer solution. MeHA at 7.8 wt% macromer concentration was dissolved in PBS containing fluorescent peptides and 0.05 wt% I2959 photoinitiator. MeHA macromer solution was then stored under nitrogen and polymerized using UV light at 10 mW/cm^2 for 5 min to induce gelation.

4.2.5. ISOTHERMAL TITRATION CALORIMETRY

Isothermal titration calorimetry (ITC) was performed using a low volume isothermal titration calorimeter (Microcal iTC200, Worcestershire, UK). Briefly, aqueous polymer solutions at 1 mg/mL and 0.468 mg/mL for CD-HA and HA, respectively, were titrated in 2 µL aliquots to a thermal cell filled with 200 µL of tryptophan at 40 µM. Differential power was recorded between the sample cell and a reference cell containing MiliQ water at a constant temperature of 25 °C. Baseline titrations of polymer solution into MilliQ water were subtracted in order to remove heats of dilution associated with polymer solution injection. The resulting isotherms were analyzed with Origin 7 software according to a one-binding site fit to determine association constants. In order to reduce errors associated with fitting multiple parameters (K, ΔH, n), stoichiometry was pre-defined according to CD modification determined through ^{1}H-NMR.

4.2.6. RHEOLOGY

Hydrogel mechanics were assessed using a stress-controlled rheometer (AR2000, TA Instruments, New Castle, DE). Oscillatory time sweeps were conducted at 0.1, 1, and 10 Hz at 1% strain. Additionally, oscillatory frequency sweeps were performed between 0.01 Hz and 100 Hz at 1 % strain. Finally, to simulate injection, hydrogels underwent a cycle of strain between 1 % (low strain) and 500 % (high strain) at 1 Hz. Storage and loss moduli were analyzed for both drug loaded and unloaded hydrogels.

4.2.7. FLUORESCENCE RECOVERY AFTER PHOTOBLEACHING

Fluorescence recovery after photobleaching (FRAP) experiments were conducted on a confocal microscope (TCS SP5, Leica, Wetzlar, Germany). In each experiment, 20 µL hydrogels were placed on glass slides and covered with a glass cover

slip. The 488 nm line of an argon laser was set to 50 % power and all images were taken using the 10x objective with the pinhole fully opened. Pre-bleach images were recorded over 2 seconds using 0.1 % transmission. A 30 μm diameter region was then bleached for 4 seconds using 100 % transmission. Post-bleach images were then recorded with the laser returned to 0.1 % transmission for 230 s of recovery. Data was analyzed using a custom MATLAB script that fit recovery profiles using nonlinear least squares regression to the Soumpasis equation:

$$F(t) = k \bullet e^{-\frac{\tau_D}{2t}}\left[I_0\left(\frac{\tau_D}{2t}\right) + I_1\left(\frac{\tau_D}{2t}\right)\right] \quad (1)$$

where $F(t)$ is the normalized fluorescence recovery profile, k is the mobile fraction, τ_D represents the characteristic diffusion time (s), t represents time (s), and I_0 and I_1 are zero and first order modified Bessel functions of the first kind.[30] Effective diffusivities were then calculated according to:

$$D_{eff} = \frac{w^2}{\tau_D} \quad (2)$$

where D_{eff} is the effective diffusivity ($\mu m^2\ s^{-1}$) and w represents the bleach spot radius (μm). This protocol was adapted from previous work conducting similar analyses.[31]

4.2.8. MOLECULE RELEASE PROFILES

Release assays were conducted in custom made acrylic erosion cells. Erosion cells were fabricated with a 4.3 mm diameter hydrogel chamber overlaid with a 1.6 cm diameter supernatant chamber, each chamber having depths of 7 mm and 10 mm, respectively. 30 μL of the hydrogel was deposited in the chamber, the chamber was centrifuged to provide an even hydrogel surface, and the hydrogel was covered with 1

mL of PBS. Once loaded, erosion cells were stored in an incubator at 37 °C. Supernatant was collected at regular intervals and replaced with fresh PBS. Molecule release was determined with a plate reader (Infinite M200, Tecan, Männedorf, Switzerland). FITC labeled peptides were analyzed using 495/525 nm excitation emission, doxycycline was analyzed using 350 nm absorbance, and doxorubicin was analyzed using 480/590 nm excitation/emission. At the end of each assay, any remaining hydrogel was collected along with supernatant and disassociated with addition of 5 mg/mL Ad solution in DMSO to obtain final fluorescence/absorbance readings. Fluorescence and absorbance values were then compared to standard curves to determine total molecule release.

4.2.9. STATISTICAL ANALYSIS

Affinity measurements are presented as an average of affinity constants determined from n = 3 isotherms per trial. Mechanical measurements are presented as an average and standard deviation for n = 3 samples. FRAP measurements were conducted for n = 4 recovery profiles, and presented as average effective diffusivities and standard deviations. Release profiles are presented as average cumulative percent release and standard deviation of cumulative release for n = 4 samples. Statistical analyses on ITC and rheology measurements were conducted using two-tailed student t tests. One-way ANOVA with post-hoc Tukey's Honestly Significant Difference testing was conducted on diffusivity measurements using R.

4.3. RESULTS AND DISCUSSION

4.3.1. SMALL MOLECULE BINDING TO HA

HA was successfully functionalized with CD to produce CD-HA, with ~35 % of HA repeat units modified. It was first investigated whether CD modification of HA could increase the polymer affinity for small molecules, using ITC. As a representative small molecule, L-tryptophan was used to investigate this interaction, due to its aromatic structure, hydrophobic nature, and previous investigation of affinity with CD.[15,24,26] Additionally, as a natural amino acid, L-tryptophan presents an interesting binding target, as it allows for peptide design with natural compounds that may promote polymer affinity.

Isotherms produced by CD-HA and unmodified HA titrations were vastly different (**Figure 4.3 a,b**). CD-HA produced a distinct exothermic reaction upon mixing with tryptophan in the sample cell, while unmodified HA remained at near baseline levels for all injections. Isotherms were quantitatively analyzed in Origin 7 software by a one-binding site model fit to determine the apparent association constant (K_A) between the polymer and tryptophan. The binding site stoichiometry value (n) was set to 0.35 to account for CD modification as determined by ^{1}H-NMR and to reduce error associated with fitting multiple parameters. Fits for isotherms of CD-HA and tryptophan produced an average K_A of $1.6\times10^4 \pm 2.9\times10^3$ M^{-1}. While this value is slightly higher than previously reported values for this interaction, the increase may be attributed to changes in CD chemistry upon conjugation to HA, as it has been shown that these changes can alter binding affinities to tryptophan.[26] Accurate values for K_A were not attainable in unmodified HA isotherms due to high error associated with parameters obtained from fits, which is attributed to randomly scattered integrated heat values resulting from near baseline heat changes for all injections. Taken together, these data suggest that modification of HA with CD provides a multiple orders of magnitude increase in affinity

for tryptophan. Since the cyclic domains such as the indole moiety found in tryptophan are found in many pharmacologic small molecules, this increase in affinity suggests that HA modification would allow increased affinity for many small molecules.[32]

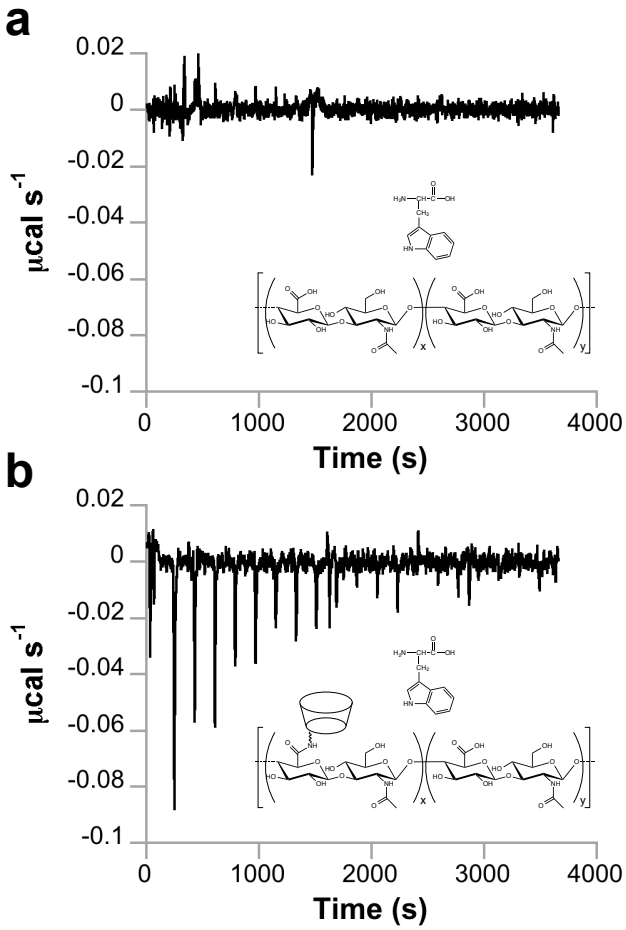

Figure 4.3. Isothermal titration calorimetry for HA binding to tryptophan. Solutions of HA (either unmodified or modified with CD) dissolved in MilliQ water were titrated into 40 µM tryptophan in MilliQ water. Baseline isotherms of modified or unmodified HA into water were subtracted to account for heats of dissolution. Representative isotherms and chemical structures of binding components are shown for (a) unmodified HA binding to tryptophan or (b) CD-HA binding to tryptophan.

4.3.2. EFFECT OF DRUG LOADING ON HYDROGEL MECHANICS

HA was also successfully modified with Ad groups to form Ad-HA. Gelation occurred instantaneously upon mixing of CD-HA and Ad-HA macromer solutions,

through guest-host interactions of Ad and CD groups. Since incorporated small molecules also complex with CD, it is important to understand the competitive effect of drug loading on hydrogel mechanics. As a model drug, a peptide modified with tryptophan and FITC (termed 3W, due to 3 tryptophan residues per peptide) was loaded (1 mg/mL) into 1:1 (5 wt%) hydrogels. This notation of the form 'x:y (z wt%)' refers to the molar ratio of Ad:CD in the hydrogel (x:y) and the total polymer weight percent in the hydrogel (z). This formulation was selected for mechanical testing since it would have the greatest chance to reduce hydrogel mechanics with drug loading, as the Ad:CD ratio is 1:1. The loading concentration for 3W of 1 mg/mL is at the peptide solubility limit and is ~5 % of the total CD content in the hydrogel. Furthermore, this concentration is orders of magnitude higher than loading concentrations used in subsequent release assays. Please note that the peptide was not designed for any bioactivity, but rather for use as a model molecule to investigate the influence of hydrogel design on diffusivity and release.

To examine the effect of molecule incorporation on hydrogel mechanical properties, frequency response profiles for G', G", and tan(δ) were obtained. Hydrogels displayed frequency responsive behaviors that are characteristic of self-assembling, two-component systems (**Figure 4.4a**). Both molecule-loaded and unloaded hydrogels exhibited similar frequency response profiles for these parameters, showing qualitative similarity in mechanics. Time sweeps were conducted to assess differences between these two groups in shear and loss moduli at 0.1 Hz, 1 Hz, and 10 Hz. Both formulations displayed frequency responsive increases in storage moduli (**Figure 4.4b**) and loss moduli (**Figure 4.4c**) and there were no significant differences in either storage or loss moduli ($p > 0.05$) between the formulations. One explanation for the lack of difference in bulk mechanics with and without encapsulated small molecules is the relative difference in affinity of tryptophan for CD as compared to AD. The association constant for the Ad-CD complex has been reported to be as high as 10^5 M^{-1}, orders of magnitude higher

than previous reports for tryptophan-CD, suggesting that there would be minimal competition between the two.[15,26] Considering that a wide variety of small molecules complex with CD on the same order of magnitude as tryptophan, it is unlikely that loading of therapeutics would compete with the formation of the Ad-CD complex and cause a decrease in hydrogel mechanics.[15]

Finally, loaded hydrogels were subjected to a cyclic strain protocol, whereby hydrogels were placed under cycles of high and low oscillatory strain to simulate conditions during injection and recovery after injection. This technique has been used previously to examine network disassembly and reassembly in self-assembling systems from a mechanical perspective.[33-36] Hydrogels showed a rapid decrease in storage modulus under high strain, indicating a reduction in elastic properties and a more fluid-like behavior, as well as a rapid recovery of the storage modulus under low strain, suggesting a return to a more elastic, gel-like state (**Figure 4.4d**). Hydrogels loaded with the peptide rapidly assembled after injection, indicating that there would be minimal extravasation during administration (**Figure 4.5**). These characteristics are important in the development of translational therapies, so that both hydrogel and drugs may be precisely localized. This aspect can be challenging with alternative injectable hydrogels that covalently crosslink at the injection site, as hydrogels may clog the delivery device if gelation occurs too quickly or may diffuse from the injection site prior to gelation if gelation is too slow.[6]

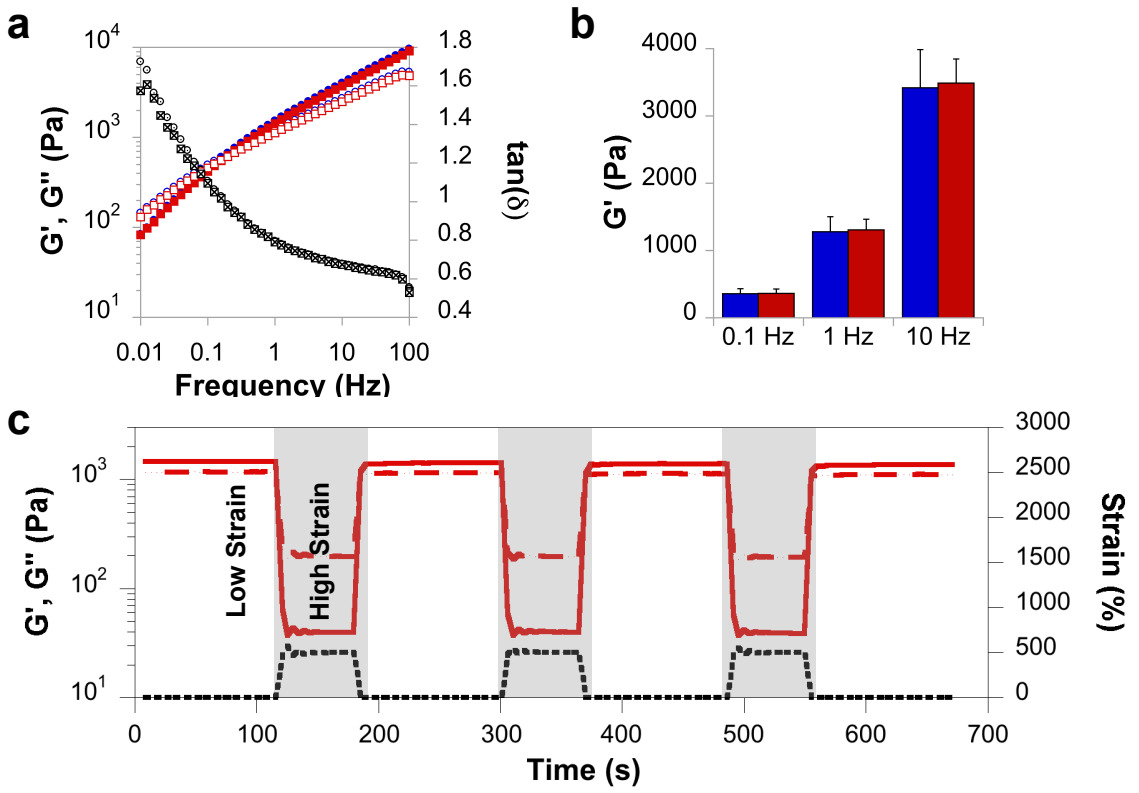

Figure 4.4. Comparison of mechanical properties in unloaded and drug loaded (3W peptide, 1mg/mL) hydrogels (1:1 (5 wt%)). (a) Representative frequency sweeps showing G' (unloaded=blue solid circles, loaded=red solid squares), G" (unloaded=blue open circles, loaded=red open squares), and tan(δ) (unloaded=black open circles, loaded=black crossed squares). (b) Average G' values for time sweeps for unloaded (blue) and loaded (red) hydrogels for 0.1Hz, 1Hz, and 10Hz frequencies. (c) Representative cyclic strain experiment showing G' (red solid line), G" (red dashed line), and strain (black dotted line) for loaded hydrogels undergoing cycles of low and high strains.

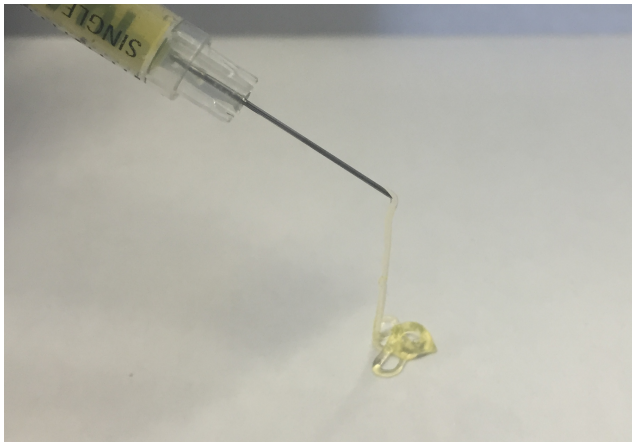

Figure 4.5. Hydrogel injection. Injection of a 1:2 (7.8 wt%) hydrogel loaded with 100 μM 3W peptide through a 27G needle.

4.3.3. EFFECT OF MOLECULE AND HYDROGEL PARAMETERS ON DRUG MOBILITY

Fluorescence recovery after photobleaching experiments were used to assess encapsulated molecule mobility within hydrogels as a function of hydrogel parameters and molecule interaction with CD. Using this technique, small regions of hydrogels loaded with mobile fluorescent payloads were bleached with a high intensity laser. The recovery of fluorescence due to diffusion of unbleached molecules into the region was then monitored and quantified to determine the diffusivity of the fluorescent payload within the hydrogel. Two fluorescently labeled peptides were used in these experiments: a high affinity peptide for CD (3W), as well as a lower affinity peptide, in which the tryptophan residues were replaced with glycine (NoW, GKGEGKGE-FITC). These peptides were used as model drugs to represent payloads of varying molecular affinities, and were loaded into hydrogels at 100 μM.

To assess the influence of hydrogel formulation on molecule mobility, CD content within hydrogels was altered by increasing the overall CD-HA concentration (1:1 (5 wt%), 1:2 (7.8 wt%), and 1:3 (10.5 wt%)). As CD concentration increased, the effective diffusivity of the 3W peptide significantly decreased within the hydrogel (**Figure 4.6a**). These data suggest that the increase in CD-HA content does reduce peptide mobility within the hydrogel. To address the potential confounding effects that an increase in total macromer concentration may have on mobility, an additional formulation at a 1:2 Ad:CD ratio was compared to the 1:1 Ad:CD ratio, with both hydrogels at 5 wt%. The 1:2 Ad:CD formulation showed significantly lower effective diffusivities than the 1:1, despite maintaining a similar total macromer concentration of 5 wt% (**Figure 4.6b**). This comparison suggests that the CD-HA component itself is a significant contributor to molecule diffusivity, which is supported by the binding affinity results quantified by ITC analysis.

To further investigate this affinity mediated reduction in mobility, we explored the effect of removing the tryptophan residue from the 3W peptide by using the NoW peptide. A 1:2 (7.8 wt%) hydrogel was loaded with 100 μM NoW peptide and compared to a similarly formulated hydrogel with 100 μM 3W peptide. It was observed that the NoW peptide had significantly higher diffusivity in the same hydrogel when compared to the 3W for the given 100 μM concentration (**Figure 4.6c**). These results can be observed visually in **Figure 4.6d**. Both peptides were bleached with similar efficiencies (1 s), but show differences in recovery profiles (3 s and 8 s) until both reach almost full recovery (30 s). The influence of peptide chemistry on mobility further implies the importance of CD affinity in controlling peptide mobility in these hydrogels.

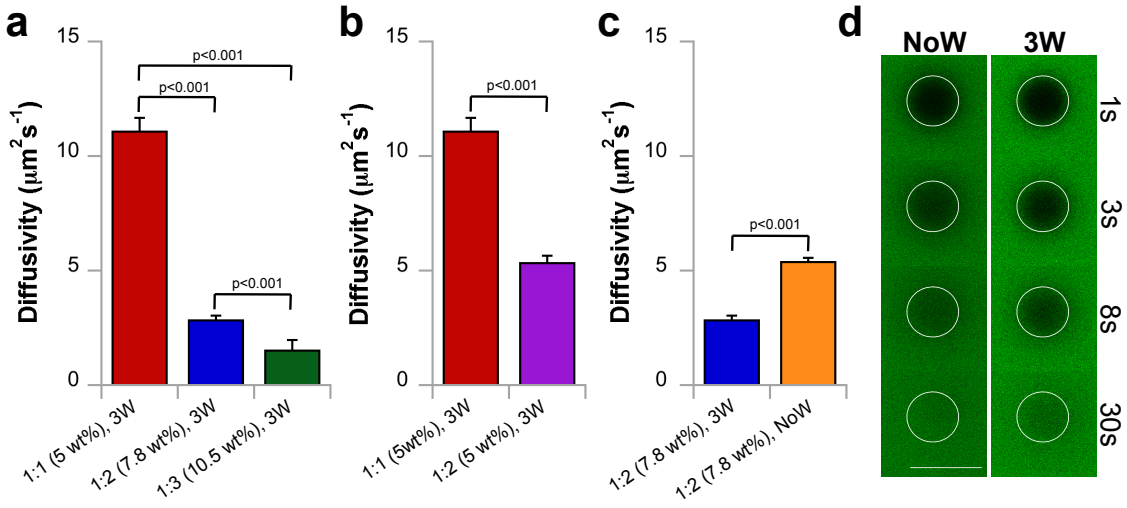

Figure 4.6. Fluorescence recovery after photobleaching experiments. Hydrogels loaded with fluorescent peptides were assessed with FRAP analysis to determine payload mobility within the hydrogel. Diffusivity of fluorescent peptide payloads in hydrogels was assessed with changes in (a) CD-HA wt%, (b) Ad:CD ratio at a total polymer concentration of 5 wt%, and (c) payload chemistry (3W versus NoW). (d) Representative FRAP images for changes in payload chemistry, scale bar = 50 mm.

4.3.4. EFFECT OF MOLECULE AND HYDROGEL PARAMETERS ON BULK RELEASE PROFILES

Towards investigating the small molecule sustained release properties of these hydrogels, we next investigated the effect that both hydrogel and payload parameters have on bulk release profiles. As in the FRAP experiments, groups were selected to compare the effects of increasing CD-HA concentration, increasing the Ad:CD ratio for a given total weight percent, and changing the relative affinity of a fluorescently labeled payload. In order to provide a contrast to this affinity-based interaction, release from a covalently crosslinked hydrogel with no CD content was examined. MeHA hydrogels containing no CD content were formed through the photoinitated polymerization of 30 % modified MeHA at 7.8 wt% and containing 100 μM of the 3W peptide. Peptide release into PBS was examined over 8 days. This profile (**Figure 4.7**) showed ~90 % release in the first 24 h and exemplifies the issues with sustaining small molecule release from traditional swollen hydrogels.

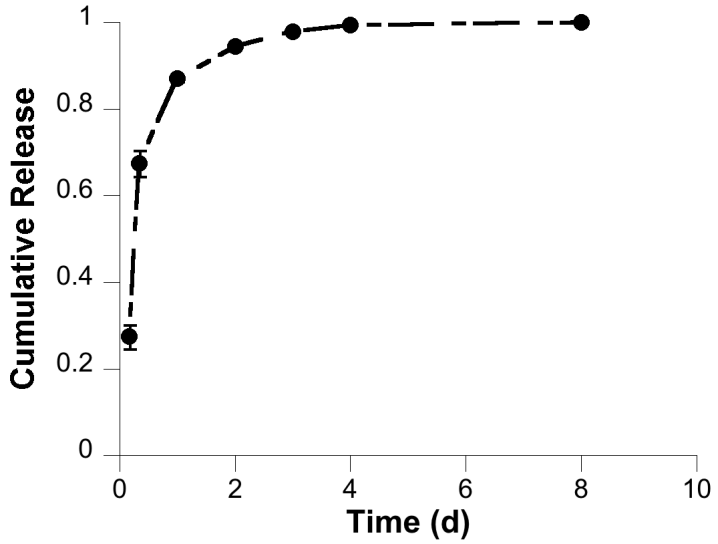

Figure 4.7. Cumulative 3W release. 3W release from covalently crosslinked hydrogel containing no cyclodextrin (MeHA).

Towards investigating the cyclodextrin retentive effect in our hydrogels, several formulations were explored. All supramolecular hydrogels discussed here were loaded with 100 μM of peptide. This represents approximately a 1:100 ratio of peptide to CD available for binding (i.e., CD that has not been paired with Ad) in a 1:2 (7.8 wt%) system. This ratio is consistent with values investigated in previous modeling studies investigating affinity mechanisms in drug release.[37] The effect of increasing CD-HA macromer concentration was assessed in these hydrogels by conducting release experiments on a 1:1 (5 wt%), 1:2 (7.8 wt%), and 1:3 (10.5 wt%) hydrogels. Results of these systems are shown in **Figure 4.8a**. Analogous to trends observed in molecule diffusivity from FRAP studies, increasing the CD-HA content of these hydrogels produced slower bulk release kinetics. In the first 24 h, ~70 %, ~35 % and ~20 % of the initial payload was released for the 1:1 Ad:CD, 1:2 Ad:CD, and 1:3 Ad:CD systems, respectively. These results are markedly improved over the MeHA system, and show the increased ability of mismatched systems to sustain the release of small molecule payloads. Furthermore, even matched systems, where there is an equal molar ratio of Ad and CD, present some sustained release capabilities. This is likely due to spatial limitations in the network that prohibit complete consumption of CD by Ad guests, leaving the remaining CD available to bind to drugs. It should also be noted that only marginal improvements in sustained release were observed when shifting from 1:2 to 1:3 Ad:CD hydrogels. Likely this is due to an upper limit on retentive effects that can be achieved through CD-peptide guest-host interactions for this particular payload and concentration. These materials also displayed moderate erosion during the three-week assay, and are comparable to our previous reports on the degradation of this material (**Figure 4.9**). [3]

A comparison of release profiles between a 1:1 (5 wt%) to a 1:2 (5 wt%) hydrogel (**Figure 4.8b**) further indicates that the sustained properties are a result of CD content

within the hydrogel. A mismatched system of the same macromer concentration produced slower sustained release profiles, which can be attributed to the increased amount of unbound CD available to bind and retain the peptide. Finally, the effect of varying peptide affinity on bulk release was investigated. Hydrogels were formulated at 1:2 (7.8 wt%) and 100 μM concentration of either 3W or NoW peptide. Release over 21 days was markedly slower for 3W when compared to the NoW peptide (**Figure 4.8c**). However, the NoW peptide still shows some degree of sustained release from these hydrogels, since CD binds with a number of small hydrophobic moieties such as the fluorescein dye on NoW. Release data of these peptides with varying structure further reinforces the importance of CD affinity in these systems.

Overall, these release studies have elucidated a number of properties about these hydrogels and the release of small molecules. First, our self-assembled hydrogels provided sustained release of two different peptides for up to 3 weeks. This shows remarkable improvement over the capacity of traditional systems (i.e., hydrogels without a drug affinity component) to sustain the release of molecules of this size (**Figure 4.7**). These systems have tunable profiles that can be changed through a number of parameters. Engineering molecule affinity is one mechanism that can provide specific control of release profiles on a drug-to-drug basis. This is useful particularly in the delivery of peptide therapeutics, as these can be readily engineered with groups such as tryptophan that will promote the appropriate release profile. Finally, and most importantly, by varying the amount of CD-HA macromer in these hydrogels, the extent of molecule retention and subsequent release can be easily controlled. These multiple controllable parameters allow for potential tunability over a wide range of molecules as payloads.

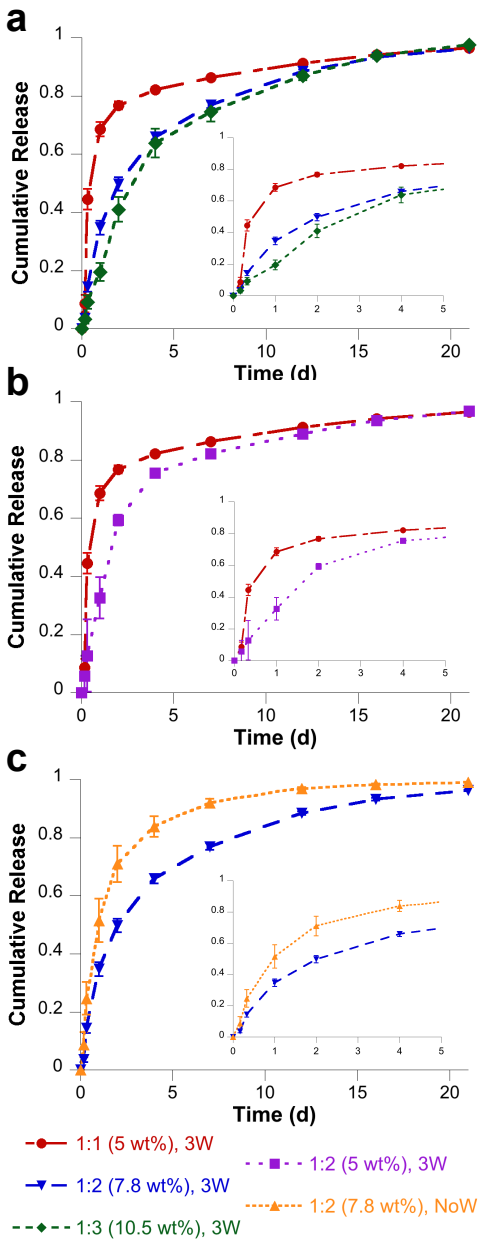

Figure 4.8. Release profiles of entrapped peptides. Hydrogels containing fluorescent peptides were injected in custom designed erosion cells and peptides released into PBS were quantified. Cumulative release profiles were determined in gels with changes in (a) CD-HA wt%, (b) Ad:CD ratio at total polymer concentration of 5 wt%, and (c) payload chemistry (3W versus NoW). Insets show an expanded view of time points collected during the first 5 days.

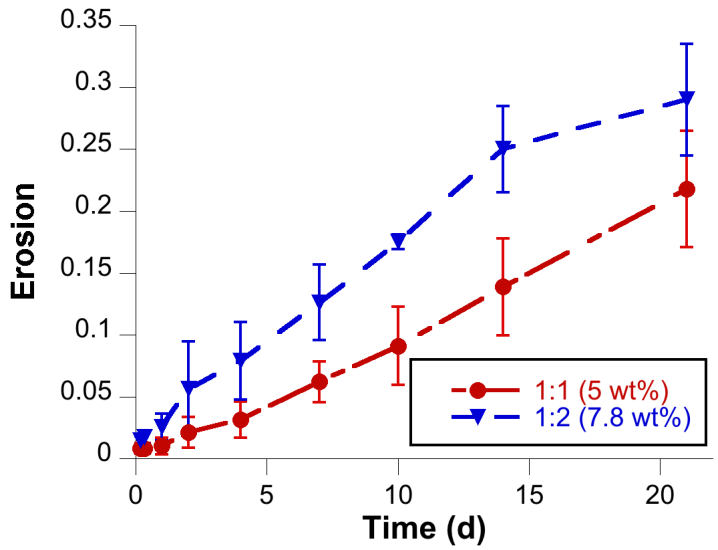

Figure 4.9. Hydrogel degradation. Hydrogel erosion for matched and mismatched CD-HA/Ad-HA systems.

4.3.5. SUSTAINED RELEASE OF DOXYCYCLINE AND DOXORUBICIN

To show the application of these systems towards small molecule pharmacologics, two clinically used small molecule therapeutics (i.e., DOX, DXY) were investigated. These drugs were selected as DOX is a chemotherapeutic that acts through intercalating with DNA and DXY has been investigated as an MMP inhibitor, both classes of drugs that benefit from localized delivery and both been shown previously to form complexes with CDs and their derivatives.[22,25,38-40] Both the 1:1 (5 wt%) and a 1:2 (7.8 wt%) hydrogel formulations were investigated for release, with drug loading at 1 mg/mL. DOX release was sustained over the first 14 days of the study (**Figure 4.10a**). As observed with fluorescently labeled peptide substrates, increasing CD-HA content in DOX loaded hydrogels produced a similar reduction in release kinetics, particularly noticeable during the first week. DXY loaded hydrogels also showed similar trends to the DOX loaded systems (**Figure 4.10b**). The sustained release effect of increased CD-HA content was more pronounced in DXY release profiles, and this may be attributed to differences in CD affinity between DXY and DOX, which have been

reported at 503 M^{-1} and 297 M^{-1}, respectively.[22,41] Profiles for the 1:2 Ad:CD formulation for both drugs also indicate incomplete release of the encapsulated payload, with an increased fraction of drug retained in the hydrogel at the study endpoints. These data show the versatility of the presented hydrogel system in delivering a number of small molecules in a readily translatable manner. As injectable systems, hydrogels providing sustained release of either of these two molecules could find biomedical applications, such as in cancer therapies.[39,42] Although the work here did not illustrate bioactivity of released drugs, we do not expect any comprised activity since we have not chemically modified the drugs and others have shown activity of molecules in delivery systems leveraging non-covalent inclusion complexes.[43,44]

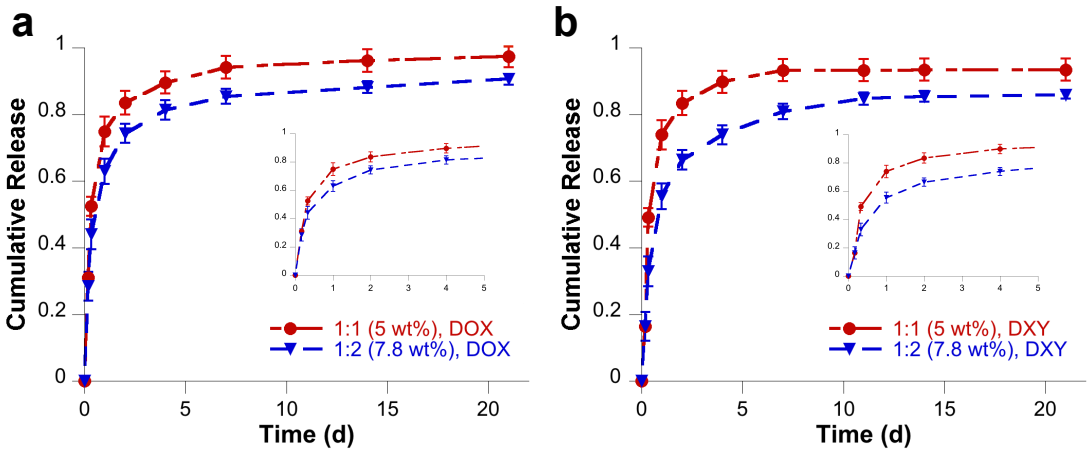

Figure 4.10. Release of doxorubicin (DOX) and doxycycline (DXY) from injectable hydrogels. Cumulative release of (a) DOX or (b) DXY for 1:1 (5 wt%) (red) or 1:2 (7.8 wt%) (blue) formulations over 3 weeks. Insets show an expanded view of time points collected during the first 5 days.

4.4. CONCLUSIONS

Here, we have developed a physically assembled hydrogel system for the tunable and sustained release of small molecules using CD guest-host interactions. Modification of HA with CD increased affinity for model small molecules by multiple

orders of magnitude, and this affinity was leveraged to tune the release of peptide model drugs, as well as doxorubicin and doxycycline, from assembled hydrogels. Furthermore, hydrogel drug-loading had minimal effects on mechanics and allowed the hydrogels to retain their injectable and rapid self-assembly properties. Ultimately, the work presented in this paper shows a small molecule, controlled release system that is rapidly formulated, easily tuned, and avoids the potential challenges associated with other injectable delivery systems.

4.5. REFERENCES

1. Foo CTSWP, Lee JS, Mulyasasmita W, Parisi-Amon A, Heilshorn SC. Two-component protein-engineered physical hydrogels for cell encapsulation. P Natl Acad Sci USA. 2009;106(52):22067-72.
2. Appel EA, Biedermann F, Rauwald U, Jones ST, Zayed JM, Scherman OA. Supramolecular cross-linked networks via host-guest complexation with cucurbit[8]uril. J Am Chem Soc. 2010;132(40):14251-60.
3. Rodell CB, Kaminski AL, Burdick JA. Rational design of network properties in guest-host assembled and shear-thinning hyaluronic acid hydrogels. Biomacromolecules. 2013;14(11):4125-34.
4. Li J, Li X, Ni X, Wang X, Li H, Leong KW. Self-assembled supramolecular hydrogels formed by biodegradable PEO-PHB-PEO triblock copolymers and alpha-cyclodextrin for controlled drug delivery. Biomaterials. 2006;27(22):4132-40.
5. Yamaguchi H, Kobayashi Y, Kobayashi R, Takashima Y, Hashidzume A, Harada A. Photoswitchable gel assembly based on molecular recognition. Nat Commun. 2012;3:603.

6. Rodell CB, MacArthur JW, Dorsey SM, Wade RJ, Wang LL, Woo YJ, et al. Shear-Thinning Supramolecular Hydrogels with Secondary Autonomous Covalent Crosslinking to Modulate Viscoelastic Properties In Vivo. Adv Funct Mater. 2014.
7. Mulyasasmita W, Cai L, Hori Y, Heilshorn SC. Avidity-controlled delivery of angiogenic peptides from injectable molecular-recognition hydrogels. Tissue engineering Part A. 2014;20(15-16):2102-14.
8. Mulyasasmita W, Cai L, Dewi RE, Jha A, Ullmann SD, Luong RH, et al. Avidity-controlled hydrogels for injectable co-delivery of induced pluripotent stem cell-derived endothelial cells and growth factors. J Control Release. 2014;191:71-81.
9. Appel EA, Loh XJ, Jones ST, Dreiss CA, Scherman OA. Sustained release of proteins from high water content supramolecular polymer hydrogels. Biomaterials. 2012;33(18):4646-52.
10. Bellocq NC, Pun SH, Jensen GS, Davis ME. Transferrin-containing, cyclodextrin polymer-based particles for tumor-targeted gene delivery. Bioconjugate chemistry. 2003;14(6):1122-32.
11. Turk B. Targeting proteases: successes, failures and future prospects. Nat Rev Drug Discov. 2006;5(9):785-99.
12. Hoare TR, Kohane DS. Hydrogels in drug delivery: Progress and challenges. Polymer. 2008;49(8):1993-2007.
13. Zhang S, Anderson MA, Ao Y, Khakh BS, Fan J, Deming TJ, et al. Tunable diblock copolypeptide hydrogel depots for local delivery of hydrophobic molecules in healthy and injured central nervous system. Biomaterials. 2014;35(6):1989-2000.
14. Thatiparti TR, von Recum HA. Cyclodextrin complexation for affinity-based antibiotic delivery. Macromol Biosci. 2010;10(1):82-90.

15. Rekharsky MV, Inoue Y. Complexation Thermodynamics of Cyclodextrins. Chem Rev. 1998;98(5):1875-918.

16. Loftsson T, Brewster ME. Pharmaceutical applications of cyclodextrins: basic science and product development. J Pharm Pharmacol. 2010;62(11):1607-21.

17. Peng K, Tomatsu I, Korobko AV, Kros A. Cyclodextrin–dextran based in situ hydrogel formation: a carrier for hydrophobic drugs. Soft Matter. 2009;6(1):85-7.

18. Xu J, Li X, Sun F. Cyclodextrin-containing hydrogels for contact lenses as a platform for drug incorporation and release. Acta Biomater. 2010;6(2):486-93.

19. Lima AC, Puga AM, Mano J, Concheiro A, Alvarez-Lorenzo C. Free and copolymerized γ-cyclodextrins regulate the performance of dexamethasone-loaded dextran microspheres for bone regeneration. Journal of Materials Chemistry B. 2014;2(30):4943-56.

20. Mateen R, Hoare T. Injectable, in situ gelling, cyclodextrin–dextran hydrogels for the partitioning-driven release of hydrophobic drugs. Journal of Materials Chemistry B. 2014;2(32):5157-67.

21. Thatiparti TR, Shoffstall AJ, von Recum HA. Cyclodextrin-based device coatings for affinity-based release of antibiotics. Biomaterials. 2010;31(8):2335-47.

22. Husain N, Ndou TT, Muñoz De La Peña A, Warner IM. Complexation of doxorubicin with β-and γ-cyclodextrins. Appl Spectrosc. 1992;46(4):652-8.

23. Vargas-Estrada D, Gracia-Mora J, Sumano H. Pharmacokinetic study of an injectable long-acting parenteral formulation of doxycycline hyclate in calves. Res Vet Sci. 2008;84(3):477-82.

24. Matsuyama K, El-Gizawy S, Perrin J. Thermodynamics of binding of aromatic amino acids to α-, β-and γ-cyclodextrins. Drug development and industrial pharmacy. 1987;13(15):2687-91.

25. Gil ES, Li J, Xiao H, Lowe TL. Quaternary Ammonium β-Cyclodextrin Nanoparticles for Enhancing Doxorubicin Permeability across the In Vitro Blood−Brain Barrier. Biomacromolecules. 2009;10(3):505-16.

26. Liu Y, Han B-H, Li B, Zhang Y-M, Zhao P, Chen Y-T, et al. Molecular Recognition Study on Supramolecular System. 14.1 Synthesis of Modified Cyclodextrins and Their Inclusion Complexation Thermodynamics with l-Tryptophan and Some Naphthalene Derivatives. The Journal of Organic Chemistry. 1998;63(5):1444-54.

27. Avigdor A, Goichberg P, Shivtiel S, Dar A, Peled A, Samira S, et al. CD44 and hyaluronic acid cooperate with SDF-1 in the trafficking of human CD34+ stem/progenitor cells to bone marrow. Blood. 2004;103(8):2981-9.

28. Burdick JA, Prestwich GD. Hyaluronic acid hydrogels for biomedical applications. Adv Mater. 2011;23(12):H41-56.

29. Khetan S, Guvendiren M, Legant WR, Cohen DM, Chen CS, Burdick JA. Degradation-mediated cellular traction directs stem cell fate in covalently crosslinked three-dimensional hydrogels. Nat Mater. 2013;12(5):458-65.

30. Soumpasis DM. Theoretical analysis of fluorescence photobleaching recovery experiments. Biophys J. 1983;41(1):95-7.

31. Brandl F, Kastner F, Gschwind RM, Blunk T, Tessmar J, Gopferich A. Hydrogel-based drug delivery systems: comparison of drug diffusivity and release kinetics. J Control Release. 2010;142(2):221-8.

32. Kaushik NK, Kaushik N, Attri P, Kumar N, Kim CH, Verma AK, et al. Biomedical importance of indoles. Molecules. 2013;18(6):6620-62.

33. Lu HD, Charati MB, Kim IL, Burdick JA. Injectable shear-thinning hydrogels engineered with a self-assembling Dock-and-Lock mechanism. Biomaterials. 2012;33(7):2145-53.

34. Olsen BD, Kornfield JA, Tirrell DA. Yielding behavior in injectable hydrogels from telechelic proteins. Macromolecules. 2010;43(21):9094-9.

35. Appel EA, Loh XJ, Jones ST, Biedermann F, Dreiss CA, Scherman OA. Ultrahigh-water-content supramolecular hydrogels exhibiting multistimuli responsiveness. J Am Chem Soc. 2012;134(28):11767-73.

36. Wei Z, Yang JH, Zhou J, Xu F, Zrínyi M, Dussault PH, et al. Self-healing gels based on constitutional dynamic chemistry and their potential applications. Chemical Society Reviews. 2014;43(23):8114-31.

37. Vulic K, Pakulska MM, Sonthalia R, Ramachandran A, Shoichet MS. Mathematical model accurately predicts protein release from an affinity-based delivery system. J Control Release. 2015;197:69-77.

38. He Z-x, Wang Z-h, Zhang H-h, Pan X, Su W-r, Liang D, et al. Doxycycline and hydroxypropyl-β-cyclodextrin complex in poloxamer thermal sensitive hydrogel for ophthalmic delivery. Acta Pharmaceutica Sinica B. 2011;1(4):254-60.

39. Golub LM, Lee HM, Ryan ME, Giannobile WV, Payne J, Sorsa T. Tetracyclines inhibit connective tissue breakdown by multiple non-antimicrobial mechanisms. Adv Dent Res. 1998;12(2):12-26.

40. Tacar O, Sriamornsak P, Dass CR. Doxorubicin: an update on anticancer molecular action, toxicity and novel drug delivery systems. Journal of Pharmacy and Pharmacology. 2013;65(2):157-70.

41. Suárez DF, Consuegra J, Trajano VC, Gontijo SM, Guimarães PP, Cortés ME, et al. Structural and thermodynamic characterization of doxycycline/β-cyclodextrin supramolecular complex and its bacterial membrane interactions. Colloids and Surfaces B: Biointerfaces. 2014;118:194-201.

42. Fingleton B. Matrix metalloproteinases as valid clinical target. Current pharmaceutical design. 2007;13(3):333-46.

43. Hamada H, Ishihara K, Masuoka N, Mikuni K, Nakajima N. Enhancement of water-solubility and bioactivity of paclitaxel using modified cyclodextrins. Journal of bioscience and bioengineering. 2006;102(4):369-71.

44. Ma D, Hettiarachchi G, Nguyen D, Zhang B, Wittenberg JB, Zavalij PY, et al. Acyclic cucurbit [n] uril molecular containers enhance the solubility and bioactivity of poorly soluble pharmaceuticals. Nature Chemistry. 2012;4(6):503-10.

CHAPTER 5

GUEST-HOST HYDROGELS FOR THE DELIVERY OF SMALL MOLECULE MMP INHIBITORS TO ATTENUATE LEFT VENTRICULAR REMODELING AFTER MYOCARDIAL INFARCTION

5.1. INTRODUCTION

Myocardial infarction (MI) is an occlusion of a coronary artery that results in an ischemic region within the myocardium.[1] The heart then undergoes a series of events that can result in a loss of mechanical function and progression to long-term heart failure and mortality.[2] Specifically, in the days to months after the initial infarction event, the heart undergoes structural changes, collectively known as left ventricular (LV) remodeling.[3,4] Initiated by the loss of contractile cells and inflammation, the left ventricle ultimately dilates, the myocardial wall thins, and the infarct region expands and transitions to scar tissue.[5-7] Currently, treatments for MI focus on initial tissue reperfusion and decreasing the work-load of the heart; however, few treatments actually address the underlying processes that drive the progression of LV remodeling.[1]

A major biological process that contributes to LV remodeling is the maladaptive upregulation of matrix metalloproteinases (MMPs) - proteases that are responsible for degradation of the extracellular matrix (ECM).[5,8,9] The role of MMPs in MI has been widely investigated over the past two decades and transgenic deletion of MMPs or systemic inhibition via pharmacologics have shown that MMPs play a key role in regulating LV remodeling, and ultimately, cardiac dysfunction.[4,10-15] MMP upregulation is a result of early inflammation and altered activity of fibroblasts and other endogenous cells; while the purpose of this inflammatory response is to promote invasion of

macrophages to clear cellular debris and to induce new vasculature in the myocardium, the collateral damage on tissue mechanical properties significantly promotes adverse LV remodeling.[5,6,9] MMP changes are largely localized to the infarcted tissue and are specific to a small subset of MMPs.[14,16]

Endogenously, MMP activity is regulated through the activity of the four tissue inhibitors of matrix metalloproteinases (TIMPs). TIMPs undergo a significant down-regulation in MI, concomitant with the aforementioned increase in MMP activity.[14] Furthermore, deletion of TIMP-3 in animal models increases LV remodeling and loss of cardiac function after an MI.[17-19] As a means to replicate the function of TIMPs, numerous small molecule MMP inhibitors have been developed that have broad-spectrum or targeted inhibition on a subset of MMPs. These molecules have faced challenges clinically, frequently producing off-target effects such as musculoskeletal syndrome (MSS) in patients enrolled in trials with systemic delivery of MMP inhibitors for indications such as cancer and arthritis.[20-22] Due to these concerns, a clinical trial evaluating the inhibitor PG116800 for treatment of MI, PREMIER, ultimately reduced the dosing of the inhibitor from initially administered levels.[20] While this new dose did not produce MSS, the drug failed to influence LV geometry and function, likely due to inadequate concentrations to achieve therapeutic efficacy.

Biomaterials provide an opportunity to localize MMP inhibitors to the tissue of interest to avoid off-target issues, while maintaining high enough doses for efficacy. For MI, hydrogels (water-swollen crosslinked polymer networks) are particularly appealing, due to their diverse properties and potential for injection into cardiac tissue, including through percutaneous routes. Indeed, numerous hydrogels have already been injected into the myocardium after MI to impart mechanical stability to the remodeling tissue.[23-27] Additionally, hydrogels have been widely explored for local drug delivery, where the therapeutic is entrapped during gelation and then released based on diffusion and

degradation mechanisms.[28,29] We previously used this approach to deliver exogenous TIMP-3 after MI and observed improvements with respect to remodeling and cardiac function, without spill-over to the circulation.[23,30]

Beyond the delivery of TIMPs, there is great interest in the local delivery of small molecule MMP inhibitors, including those that showed promise but were not explored further due to concerns with systemic delivery. One of these molecules is SD7300, an MMP inhibitor developed by Pfizer, that has shown potential in preclinical studies to provide improvements in cardiac outcomes after MI, but there are concerns with off-target effects such as MSS.[31] However, there are particular challenges to the delivery of small molecules from hydrogels, as their size leads to rapid diffusion from the network.[28] To address this, we describe here the development of an injectable hydrogel that sustains the release of SD7300, through interactions between the hydrogel and the drug. Further, we investigate delivery and efficacy in an ischemia/reperfusion model of MI in swine, including delayed percutaneous delivery.

5.2. METHODS

5.2.1. MACROMER SYNTHESIS

All materials were purchased from Sigma-Aldrich unless otherwise indicated. Hyaluronic acid (HA) (74kDa, Lifecore) was first converted to a tetrabutylammonium salt (HA-TBA) through the use of an ion exchange resin (Dowex 50Wx4), where HA in deionized (DI) water was mixed with the resin for 4 h and the product was filtered, neutralized with tetrabutylammonium hydroxide (TBA), frozen, and lyophilized to produce the HA-TBA salt. Subsequent synthesis of adamantane modified HA (Ad-HA) and cyclodextrin modified HA (CD-HA) was conducted according to previously described protocols.[32] HA-TBA, 4-methylaminepyridine, di-tertbutyl dicarbonate and adamantane

were dissolved in dimethyl sulfoxide (DMSO) and allowed to react for 20 h at 45 °C under nitrogen to produce Ad-HA, which was purified by dialysis against DI water for 3 days, precipitated in acetone, and then further dialyzed against DI water for a total of 2 weeks. The aqueous polymer solution was then frozen, lyophilized, and analyzed for purity and modification using ^{1}H-NMR (DMX 360, Bruker, Billerica, MA). All Ad-HA used in this study had ~25 % of HA repeat units modified with adamantane.

To facilitate conjugation to HA, β-CD was aminated using a hexamethane diamine (HDA) linker, as described previously to yield aminated β-CD (CD-HDA).[32] To form CD-HA, HA-TBA, CD-HDA, and (benzotriazol-1-ylozy)tris(dimethylamino)phosphonium hexafluorophosphate were dissolved in DMSO in a round bottom flask. The reaction was allowed to proceed for 18 h at room temperature. CD-HA was then purified by dialysis against water for 2 weeks, frozen, lyophilized, and characterized using ^{1}H-NMR. CD-HA used in this study was modified at ~35 % of HA.

5.2.2. HYDROGEL FORMATION AND CHARACTERIZATION

Hydrogels were prepared by first dissolving CD-HA and Ad-HA in phosphate buffered saline (PBS) or PBS containing the small molecule for encapsulation (i.e., SD7300, IR800) and the mixing for immediate gelation. Hydrogels of varying formulations were generated, containing the relative molar ratios of cyclodextrin to adamantane of 1:1, 2:1, and 3:1 at 6 wt% total macromer concentration. Hydrogels were characterized using a stress-controlled rheometer (AR2000, TA Instruments) fitted with a 20 mm diameter cone (0.995° angle) and a 27 μm gap. Oscillatory time sweeps were conducted at 0.1, 1, and 10 Hz at 1% strain. Additionally, oscillatory frequency sweeps were performed between 0.01 Hz and 100 Hz at 1 % strain. Continuous flow experiments were conducted at shear rates ranging from 1 s^{-1} to 10 s^{-1}. Injection force

testing was conducted using an Instron compressive testing apparatus with a 1 mL syringe and 21G needle, with extrusion rates conducted at 12, 30, and 60 mm/min..

5.2.3. DRUG RELEASE AND ACTIVITY

Release assays were conducted in custom made acrylic erosion cells. Erosion cells were fabricated with a 4.3 mm diameter hydrogel chamber overlaid with a 1.6 cm diameter supernatant chamber, each chamber having depths of 7 mm and 10 mm, respectively. 30 µL of the hydrogel was deposited in the chamber, the chamber was centrifuged to provide an even hydrogel surface, and the hydrogel was covered with 1 mL of PBS. Once loaded, erosion cells were stored in an incubator at 37 °C. Supernatant was collected at regular intervals and replaced with fresh PBS. At the end of the study, any remaining hydrogel was collected along with supernatant and disassociated with addition of 5 mg/mL Ad solution in DMSO.

Molecule release was determined with a plate reader (Infinite M200, Tecan). SD7300 content was measured at 270/304 nm excitation/emission and IR 800 was analyzed at 774/800 nm excitation/emission. Fluorescence and absorbance values were then compared to standard curves to determine total molecule release. The MMP-2 inhibitory activity of hydrogel releasates was determined using a fluorogenic MMP-2 activity assay. Briefly, rhMMP-2 was activated with 4-aminophenylmerucric acetate for 1h at 37 °C. In a 96 well plate, 50 uL of MMP-2 solution was added to 40 uL of hydrogel releaseate and incubated for 1 h to allow for binding of SD-7300 to the active site of MMP-2. Finally, 10 uL of fluorogenic MMP substrate was added to each well, yielding final concentrations of 0.25 ng/µL MMP-2 and 20 µM fluorogenic substrate. Immediately after addition of the fluorogenic substrate, samples were read for a 5 min kinetic cycle with a plate reader at 320/405 nm. The slope of the initial linear portion of this curve was used as a metric for enzyme activity, and baseline values (i.e., fluorogenic substrate with

no MMP-2) were subtracted from data points, and values were subsequently normalized to samples containing no MMP-inhibitor.

5.2.4. PORCINE MI MODEL

Mature pigs (n=19) (Yorkshire, male, 15-20 kg) were administered amiodarone (200 mg PO) and aspirin (81 mg PO) for 3 days pre-operatively and a broad spectrum antibiotic (Draxxin, 2.5 mg/kg, IM) at least once pre-operatively. On the day of surgery, pigs were sedated (ketamine/acepromazine/atropine: 22/1.1/0.04 mg/kg IM, respectively), intubated, and then maintained on 1.5-2% isoflurane delivered in an oxygen/nitrous mixture (3:1 L/min, respectively). Buprenorphine (0.05 mg/kg IM) was administered as pre-surgery analgesia. An intravenous infusion (via ear vein cannula) of Benadryl (25 mg) in conjunction with a continuous lidocaine infusion (4 mg/kg/hr) and lactated ringers solution (10 mL/kg/hr) was initiated. This anesthesia/premedication protocol prevented refractory arrhythmias during the IR protocol.

The region encompassing the right femoral artery was prepared in a sterile fashion, the main branch of the femoral artery surgically exposed, and a catheter introducer (6F Input Introducer Sheath, Medtronic) positioned and stabilized in the artery. A bolus of heparin was administered (4000 units, IV) prior to placement of the guide catheter followed by an additional bolus every hour (1000 units, IV). Under fluoroscopic guidance (GE OEC 9600, UT), a coronary angiography catheter/launcher (5F Launcher guiding catheter .058" HSI, Medtronic) was placed in the left coronary ostia, and an angioplasty balloon catheter containing an injection lumen (3mm x 10mm Sprinter OTW balloon catheter, Medtronic) was positioned in the lower portion of the left anterior descending artery (LAD; as defined as 1cm below the First Diagonal). The LAD was occluded by balloon inflation (12 ATM balloon inflation pressure, Everest 30 Disposable inflation device, Medtronic) and maintained for 90 minutes.

Prior to the initiation of the procedure, the pigs were randomly assigned, in a blinded fashion to the following groups: IR induction only (IR-only; n=8), IR-gel only (IR-gel; n=4), or IR-gel containing SD7300 (IR-gel/7300; n=7). The balloon was then deflated and the catheter system disengaged and removed. The femoral artery was ligated and the incision closed. A transdermal fentanyl patch was placed for 3 days for post-operative analgesia.

5.2.5. HYDROGEL INJECTIONS INTO PIGS

To perform the MI injections, the pigs randomized to this protocol were returned to the cardiac surgical laboratory 3-5 days after MI, and anesthesia performed as described previously [ref]. A 1.5 cm incision was made at the right anterior sternal-costal cartilage junction, just superior to the xiphoid process. A pediatric Finochietto retractor was placed and the anterior aspect of the LV containing the MI region exposed. The pericardium was incised, and the MI region constituting a ~3X3 cm area was visualized and the basal and apical borders of the MI identified.

A preloaded syringe containing the hydrogel was connected to a 2", 24 gauge needle (BD), and 9 injections of 100 uL volume each were placed in a equidistant diamond shape pattern within the MI region at a depth of 5 mm, forming clear solid gel pockets below the epicardial surface of the MI. At the conclusion of the injections, the incisions were closed without irrigation, and the total procedural time was 30±5 min. Only transient, non-sustained arrhythmias were encountered during the actual injections, and no other intra/post-operative complications were encountered.

To visualize hydrogel distribution, cardiac tissue (n=1) was explanted immediately after injections and imaged on a 9.4T MRI scanner (Siemens). A T2-weighted turbo spin echo with the following parameters was used to acquire segments for 3D reconstruction: matrix size 320x256x65, voxel size = 0.3125x0.3125x1.0 mm^3,

repetition time = 1128 ms, echo time = 71 ms, 4 signal averages. Hydrogel pockets were visualized using 3D reconstructions of myocardial segments in ITK-SNAP[2].

To track small molecule release *in vivo*, IR800 dye (Licore) was used as a representative small molecule and loaded into guest-host hydrogels at a concentration of 1 mg/mL hydrogel and injected into MI regions as described above. Sacrifice (n=1) occurred 2 days after injection, at which point the myocardium was sectioned into 0.25 cm thick, short-axis sections and imaged using an IVIS transdermal imaging system and presented as overlay images with bright field images of the myocardial section.

5.2.6. FUNCTIONAL ANALYSIS

Baseline echocardiography prior to IR induction, as well as 14 and 28 days post-IR were performed. To accomplish this, animals were sedated (diazepam, 200mg-PO, Barr Laboratories, Pomona, NY) and echocardiography performed (GE Vivid E9 Dimension Ultrasound System: M5S 1.5-4.6 MHz active matrix array sector transducer probe) in order to measure LV volumes, left atrial (LA) area, posterior LV free wall thickness, and ejection fraction. In addition, mitral valve inflow velocities and tissue Doppler were used to compute an estimate of pulmonary capillary wedge pressure. Digital loops of the two-dimensional echocardiography for the LV long and mid-papillary short axis (acquired at 40 Hz) were digitally acquired for analysis (EchoPac, Vingmed, General Electric).

5.2.7. TISSUE ANALYSIS

28 days post-IR and after echocardiography, pigs were anesthetized (5% isoflurane) and the LV region containing the MI and remote tissue (LV posterior wall encompassing the posterior descending artery) were harvested. LV sections were then subjected to histochemical staining for MI size. Briefly, 0.25 cm thick sections of the

myocardium were immersed in triphenyl tetrazolium chloride (TTC) solution for 20 min. Sections were imaged and quantified using ImageJ. Tissue was also stained for collagen content using a picosirius red staining kit. Sections from the MI region were taken for subsequent RNA isolation (RNALater, Qiagen). An additional group of pigs (n=6) of identical age and weight were included in this terminal study protocol in order to obtain referent normal LV myocardium for comparative analysis.

RNA was extracted from the LV samples (RNeasy Fibrous Tissue Mini Kit, Qiagen) and the quality and quantity of the extracted RNA determined (Experion Automated Electrophoresis System; Bio-Rad Laboratories, Hercules, CA). The RNA was reverse transcribed (iScript cDNA Synthesis Kit; Bio-Rad, Hercules, CA), and pig specific primer/probe arrays for apoptosis and inflammation (RT^2 Profiler PCR Custom Array, PASS-0122 and CAPS11182, respectively, Qiagen) were completed. The reaction was performed (RT^2 SYBR Green@qPCR Mastermix, Qiagen) and quantified by real time (CFX96 real-time PCR detection system, Bio-Rad, Hercules, CA). The real time PCR fluorescence signal was converted to cycle times (Ct) normalized to GAPDH (ΔCt method). All PCR assays were performed in duplicate.

5.2.8. STATISTICAL ANALYSIS

Injection force (n=3), SD-7300 release (n=4), and MMP activity (n=4) are presented as mean and standard deviations. For functional studies, pigs were separated into three treatment groups, MI (n=8), MI/Gel (n=4), and MI/Gel/SD7300 (n=7). Functional data is reported as mean and standard error of the mean. Significance was determined using a two-way ANOVA followed by pair-wise comparisons using the least significant difference post hoc study. For change from baseline data, a t-test was performed using a null hypothesis of a zero mean value. For MI size, PCR, and collagen staining data, a one-way ANOVA was performed and pairwise comparisons were

performed by an adjusted t-test. All analyses were performed with SPSS software (version 24.0, SPSS Inc) and a p-value of < 0.05 was considered statistically significant.

5.3. RESULTS AND DISCUSSION

This study showcases a biomaterials approach to localize the delivery of a small molecule MMP inhibitor. The development of MMP inhibitors for a variety of conditions has been hampered by the induction of musculoskeletal syndrome as a result of off-target action when the inhibitor is delivered systemically. [20,21] Thus, while molecules such as SD7300 have been shown to be efficacious in their treatment of disease, their utility has been limited in cases of MI, due to limited appropriate delivery mechanisms. Here, an injectable hydrogel was developed that could be injected into a tissue to locally release an MMP inhibitor.

5.3.1. MATERIAL DEVELOPMENT AND CHARACTERIZATION

Towards the hydrogel design, we build on our previous work in developing shear-thinning hyaluronic acid (HA) hydrogels, that assemble from non-covalent guest-host crosslinks between β-cyclodextrin and adamantane, allowing them to be injectable into tissues (**Figure 5.1a,b**).[25,26,32] In addition to adamantane, β-cyclodextrin has been shown to have affinity for a wide range of small molecules, and is frequently used in the pharmaceutical industry to solubilize and stabilize small molecules.[33,34] Thus, we engineered an appropriate interaction for SD7300 sustained release where the molecule binds to β-cyclodextrin for retention and controlled release (**Figure 5.1c**).

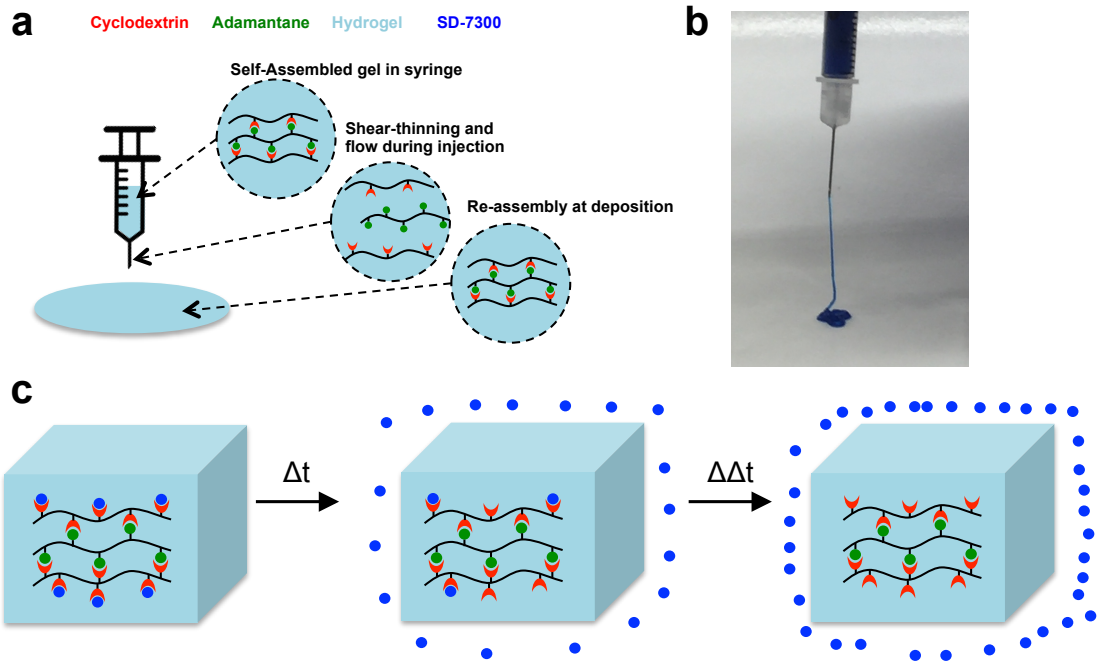

Figure 5.1. Schematic for hydrogel injection and SD-7300 release from guest-host hydrogels. (a) Guest-host hydrogels are formed through self-assembly between cyclodextrin (red) and adamantane (green) and loaded into syringes as a single component. Upon application of shear via the syringe plunger, guest-host bonds dissociate and material flows in a fluid-like state. Upon deposition, guest-host bonds reassemble and the material behaves as a solid hydrogel. (b) Image of injection of guest-host hydrogel onto a dry surface. (c) Cyclodextrin and SD-7300 (blue) interact through reversible interactions at the hydrophobic core of cyclodextrin. Hydrogel formulations containing excess cyclodextrin moieties relative to adamantane provide binding sites for SD-7300. Affinity for the hydrogel backbone controls retention and sustained release from the hydrogel over time.

Cyclodextrin modified HA (CD-HA) was synthesized by aminating β-cyclodextrin and subsequently coupling this to HA via amidation so that 35% of repeat units on HA were modified with CD (**Figure 5.2a**). Adamantane modified HA (Ad-HA) was synthesized via esterification of HA with 1-ademantane acetic acid so that 25% of repeat units on HA were modified with adamantane (**Figure 5.2b**). Hydrogels were rapidly formed through the simple mixing of solutions of purified CD-HA and Ad-HA dissolved in PBS. We have previously shown that these materials possess unique mechanical properties that allow for shear-thinning and self-assembly.[32] Furthermore, these hydrogels possess tunable mechanics based on the relative modification of HA

macromers and injection into the myocardium can indeed provide functional benefits due to tissue bulking effects.[26] Finally, we have previously used this hydrogel system for cell and drug delivery. [24,33]

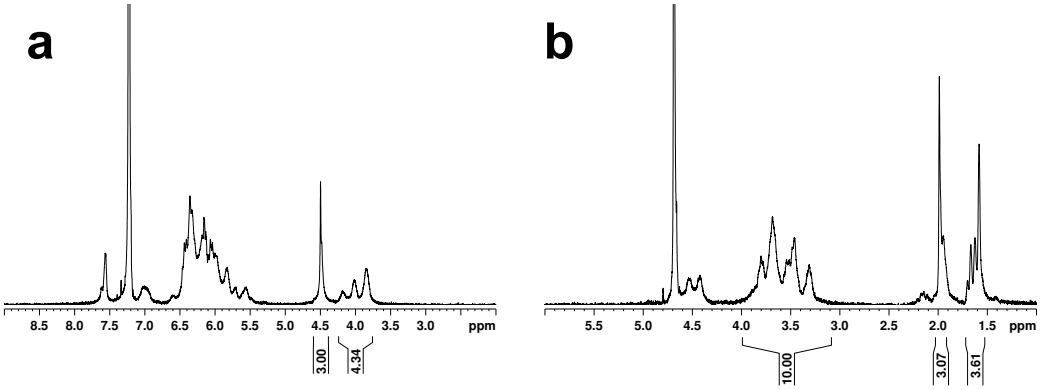

Figure 5.2. ^{1}H NMR spectra for modified hyaluronic acid. (a) NMR spectra for 35% functionalized CD-HA and (b) NMR spectra for 25% functionalized Ad-HA.

Towards the design of hydrogels for clinical application, various features are important, including injectability and controlled release. A variety of parameters can be modulated to alter such properties and here, we explored the tuning of the ratio of CD:Ad groups (1:1, 2:1, 3:1) in hydrogels with the same polymer concentration (6 wt%). We observed that all hydrogels were viscoelastic and that hydrogels with the 1:1 ratio maintained the highest level of mechanical properties (storage modulus) as determined by frequency sweeps (**Figure 5.3a**), while increasing this ratio led to a drop in mechanical properties. This is likely due to the mis-match in the guest-host groups, which alters the number of effective crosslinks within the network. To probe the shear-thinning behavior of the hydrogels, we conducted a shear rate sweep. Increasing the CD:Ad ratio led to a more rapid decrease in viscosity in response to shear, suggesting better shear-thinning behavior (**Figure 5.3b**). The greater mis-match in the guest-host groups likely facilitated easier failure of the network under shear forces, due to lower crosslinking.

Because a formulation with a balance of mechanical properties for stability and shear-thinning behavior for injectability is necessary, as well as an excess of cyclodextrin to bind to encapsulated drugs, we selected the 2:1 formulation to proceed with future studies. To directly evaluate injectability, we measured the injection force of the 2:1 formulation under several different flow rates from a 1 mL syringe through a 21G needle. We observed low injection forces across these injection rates (<50N)(**Figure 5.3 c**), which are comparable to clinically used hyaluronic acid dermal fillers.[35]

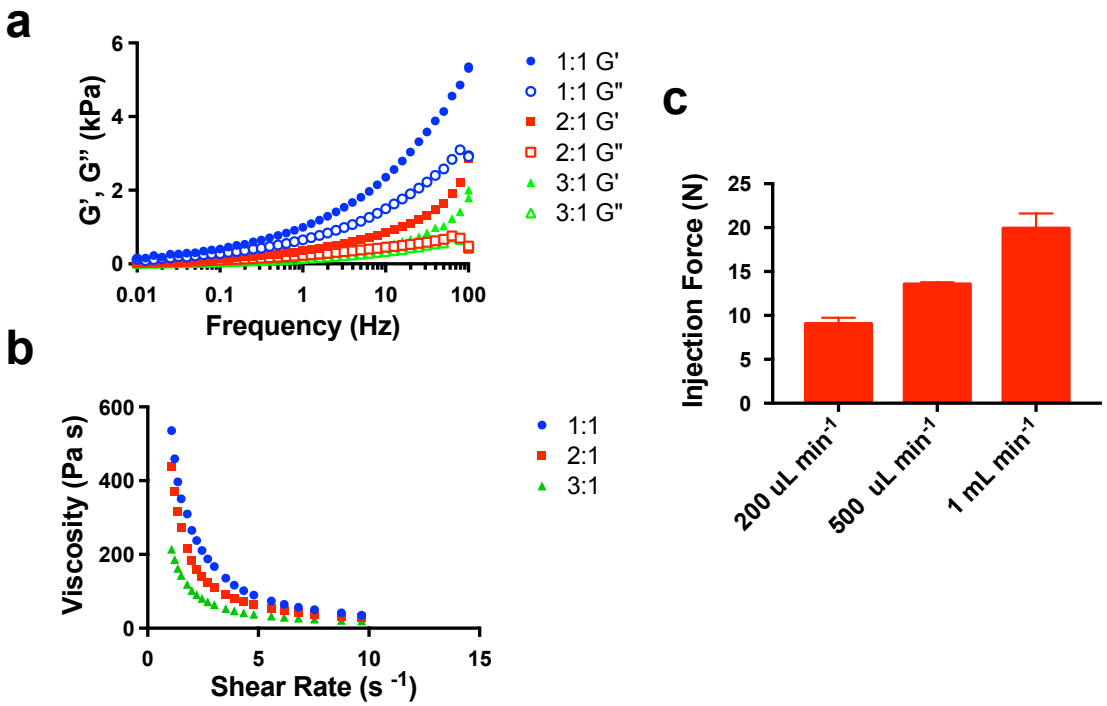

Figure 5.3. Mechanical testing of various guest-host hydrogel formulations. (a) Representative frequency sweeps (conducted at 1% strain between 0.01 Hz and 100 Hz using a cone and plate geometry) of guest-host hydrogel formulations containing 1:1, 2:1, and 3:1 molar ratios of cyclodextrin to adamantane. Increasing cyclodextrin to adamantane ratio corresponded to a decrease in mechanical properties for these formulations. (b) Continuous flow studies (conducted between 1 and 10 Hz) of representative samples of various guest-host hydrogel formulations. All materials displayed shear-thinning behavior, with more rapid shear-thinning occurring in formulations containing higher cyclodextrin to adamantane ratios. (c) Injection force data at various rates of injection for 2:1 guest-host gel formulation. Bars represent average and standard deviation of n = 3 separate runs.

5.3.2. DRUG RELEASE AND ACTIVITY

Hydrogels formed from the 2:1 formulation were loaded with SD7300 at a final concentration of 0.5mg/mL. The SD7300 release was sustained over 3 weeks with a decrease in the release rate over time (**Figure 5.4a**). This sustained release is a result of inclusion of the small-molecule binding cyclodextrin in the hydrogel formulation, which was presented in excess of adamantane. In addition to directly measuring SD7300 release, the bioactivity of released SD7300 was measured using an *in vitro* estimate of MMP-2 inhibitory activity (**Figure 5.4b**). At all time-points during release, we observed almost complete inhibition of MMP-2 activity, suggesting that this formulation is highly bioactive during the first month of use (**Figure 5.4c**).

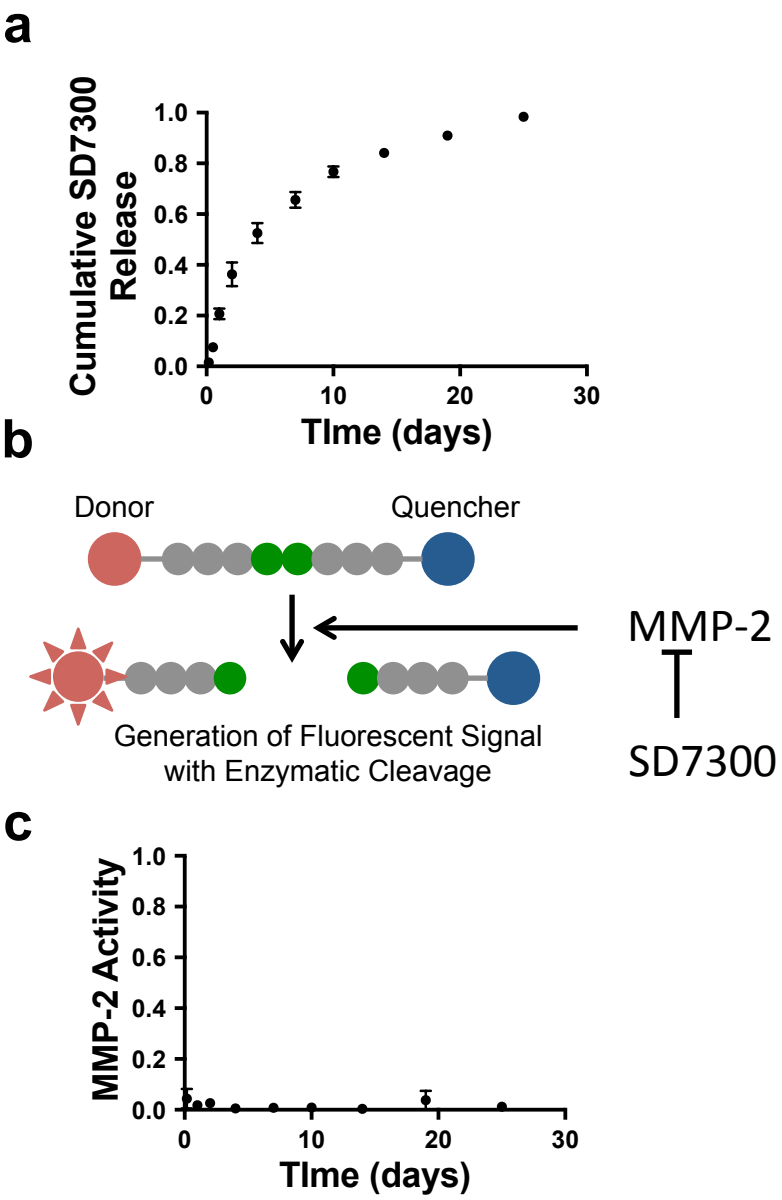

Figure 5.4. SD-7300 release from guest-host hydrogels and associated MMP-2 inhibitory activity. (a) SD7300 release profile from guest-host hydrogels showing sustained release for approximately three weeks. (b) Schematic of fluorogenic MMP-2 activity assay. A fluorogenic peptide, when cleaved in the presence of MMP-2, generates a fluorescent signal. The kinetics of this generation can be correlated with MMP activity, and are decreased through MMP inhibition by SD7300. (c) MMP-2 activity associated with release time points obtained during SD7300 release study. Activity was negligible for all time points during the release assay.

Inclusion of cyclodextrin as a binding component for small molecules was shown to be a successful approach for the sustained release of SD7300. Cyclodextrin is

frequently used in numerous pharmaceutical formulations and is an FDA GRAS molecule, lending translational merit to this approach for materials design. Because of the widespread use of cyclodextrin in pharmaceutical formulations, this approach could be broadly applicable for a number of small molecules requiring localized delivery in broad applications (e.g. chemotherapeutics). The profile of drug release and activity appropriately matches the acute phase of MI. Administration of MMP inhibition during this time frame has been shown to be successful in providing attenuation of LV remodeling, both in systemic and local administration of inhibitors.[23,30,36] By inhibiting matrix degradation during this early phase, the mechanical strength of the myocardium can be maintained, leading to improved ventricular geometry and function.

5.3.3. MI INDUCTION AND LOCAL HYDROGEL INJECTION

MI was induced in mature Yorkshire pigs using a catheter balloon occlusion of the left anterior descending artery for 90 minutes, then removal of the occlusion to allow for reperfusion. Animals were returned for injection ~4 days after induction of MI, and hydrogels were injected via a minimally invasive epicardial approach. Hydrogels were subsequently injected across 9 injections of 100uL in a 3x3 array pattern within the infarcted LAD region (**Figure 5.5a,b**). The injections left small pockets of transparent hydrogel spaced throughout the infarcted myocardium. Heart tissue was explanted after injection and imaged using MRI to evaluate the presence of hydrogel within the tissue. Sample short-axis and long axis views show the presence of hydrogel within the infarcted myocardial wall (**Figure 5.5c,d**). After 3D reconstruction, we observed that these injection sites contain distinct depots of material within the tissue, suggesting retention of the material through injection with this method (**Figure 5.5e**).

Additionally, we evaluated our material for the ability to localize a small molecule to the myocardium. We loaded hydrogels with IR800 as a model small molecule tracker

that could be detected using near-IR fluorescence imaging and tracked its release over time (**Figure 5.6a**). Injections were performed post-infarction, and heart tissue was explanted and sectioned into 0.25 cm thick sections 48 hours after hydrogel injection and imaged using an IVIS transdermal imaging system. We observed localization of fluorescent signal to infarcted myocardium, indicating successful localization of payload to the areas of injection in the heart (**Figure 5.6 b**).

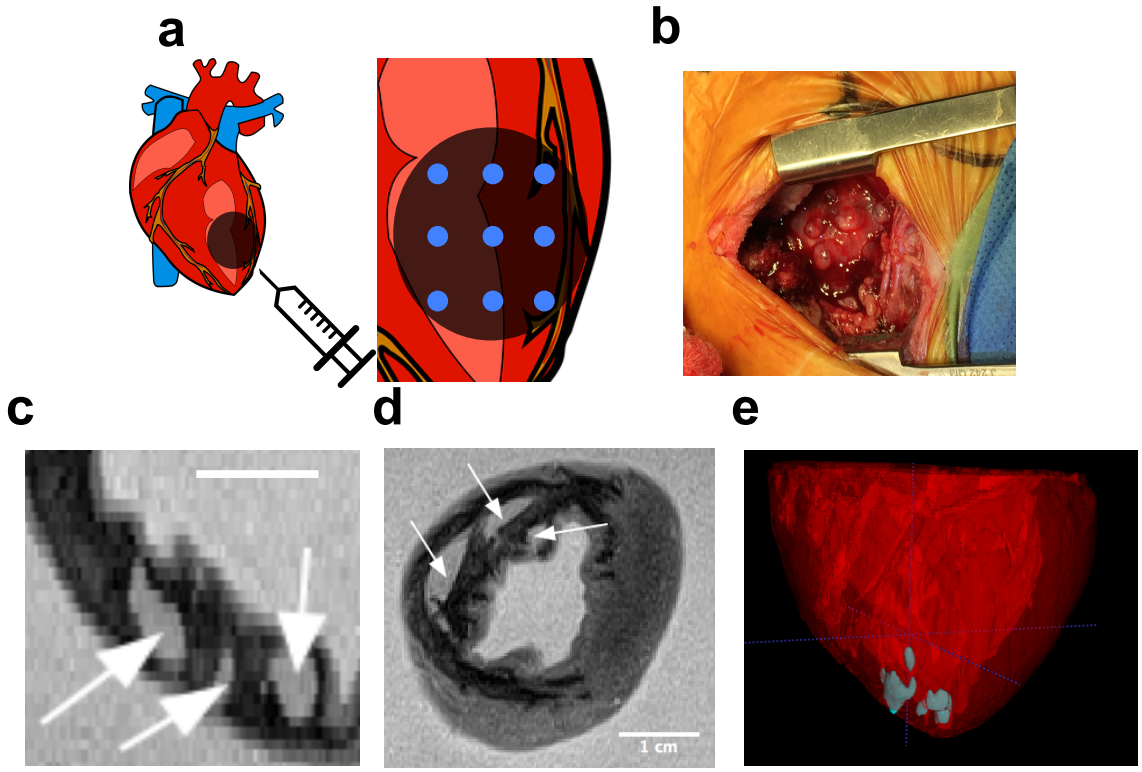

Figure 5.5. Injection of 2:1 guest-host hydrogel formulation into porcine myocardium. Guest-host hydrogel was injected in a 3x3 array in the infarct region of the myocardial wall using an epicardal injection, accessed via a mini-thoracotamy. (b) Image of heart after hydrogel injections. (c) MRI long axis view of hydrogel injection sites in explanted porcine myocardium immediately after injection. (d) MRI short axis view of hydrogel injection sites in explanted porcine myocardium after injection. (e) 3D reconstruction of hydrogel injection sites in explanted porcine myocardium.

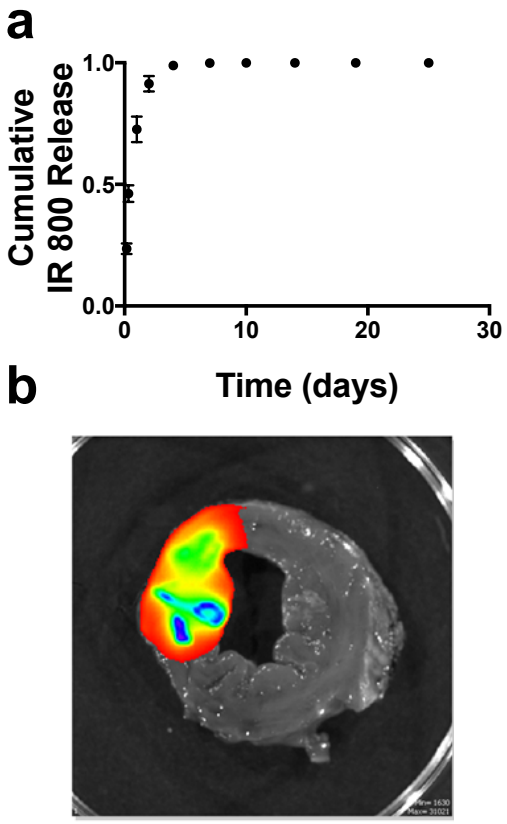

Figure 5.6. Release of near IR dye *in vitro* and *in vivo.* (a) *In vitro* release profiles of IR 800 from 2:1 guest-host hydrogels. IR 800 released over approximately 1 week from guest-host hydrogels. (b) Near IR fluorescent imaging of porcine myocardial sections showing IR 800 intensity 48 h after injection. IR 800 was localized to the infarcted region of the myocardium, suggesting minimal off target delivery of small molecules.

Small molecule MMP inhibitors have had limited success clinically in large part due to their inability to be administered systemically without off target effects.[20-22] Generally, it is hypothesized that the broad musculoskeletal syndrome that has come to be associated with systemic administration of these drugs is a result of the disruption of normal matrix turnover in healthy sites of the body. While steps have been made to address this by targeting specific subsets of MMPs through altering molecule design, this has largely been inefficient in providing a means to attenuate these off-target effects.[37] Using near-IR imaging and near-IR payloads, we have shown the ability for our materials to localize small molecules to injection sites in the infarcted myocardium. This

allows for direct mitigation of off-target toxicity through localization of SD7300 to only the diseased areas of the heart.

5.3.4. LV GEOMETRY AND CARDIAC FUNCTION

After confirmation of successful material and small molecule retention within the infarcted myocardium, we explored the ability of SD7300 loaded hydrogels to promote functional improvement after delivery. We evaluated three treatment groups, MI with saline injections (n=8), MI with delayed hydrogel injections (n=4), and MI with delayed SD7300 loaded hydrogel injections (n=7). Animals were evaluated using echocardiography at 14 and 28 days after infarction to determine ventricular geometry and filling metrics (**Figure 5.7**).

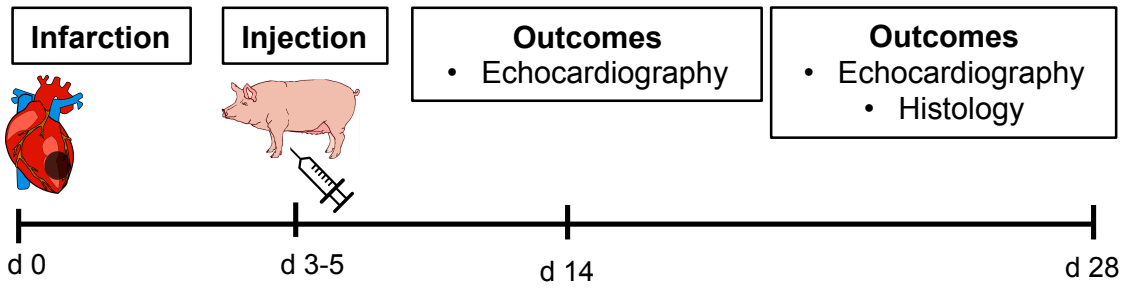

Figure 5.7. Schematic representation of animal model for functional studies. Infarction was generated at day 0 using an ischemia-reperfusion injury, followed by a return for material injection at day 3-5. Echocardiography was taken at d 14 and d 28, as well as histologic and gene array analysis at d 28.

Treatment with MI/Gel/SD7300 shows significant decrease in left atrial (LA) area, pulmonary capillary wedge pressure (PCWP), E/A ratio, and a significant increase in E' at both 14 d and 28 d time points as compared to saline controls, while gel only treatment showed no statistical significance, but a trend for improvement in these metrics over saline alone (**Figure 5.8a-d**). These data suggest that that gel./SD7300

combination treatment provided increased benefit over gel alone treatment and was important for improving diastolic function in the heart.

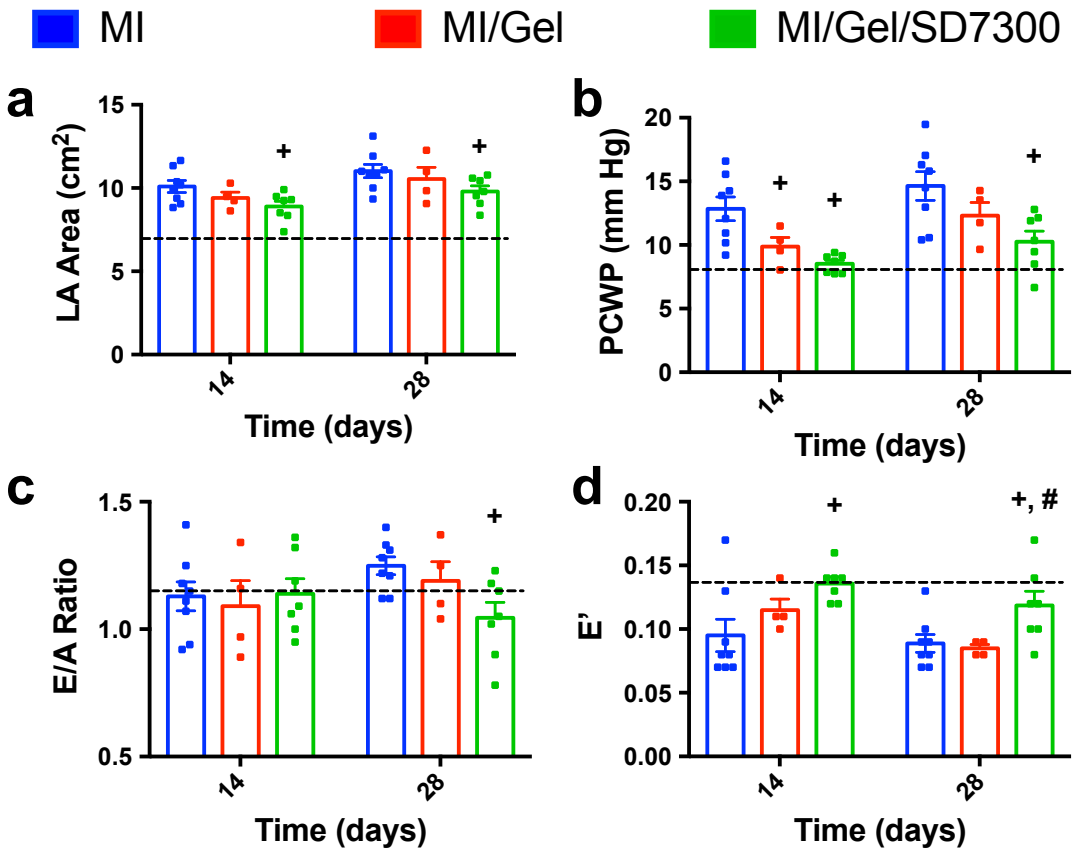

Figure 5.8. Indices of filling for longitudinal functional study of SD-7300 loaded hydrogels. (a) Left atrial (LA) area, (b) pulmonary capillary wedge pressure (PCWP), (c) E/A ratio, a ratio of peak blood flow during early diastole to peak blood flow in late diastole and a metric of left ventricular function, and (d) E' of animal groups treated with MI only (blue, n= 8), MI/Gel (red, n =4) and MI/Gel/SD7300 (green, n= 7) at baseline and 14 and 28 days after MI. At day 14, animals treated with MI/Gel/SD7300 had significantly lower LA Areas, lower PCWP, and higher E' than animals receiving MI alone. At day 28, animals treated with MI/Gel/SD7300 had significantly lower LA Areas, lower PCWP, lower E/A ratios, and higher E' than animals receiving MI alone. Dashed line represents the average of baseline values for all animals used in the study. Statistics were determined using two-way ANOVA, with + representing $p<0.05$ in comparison to MI group and # representing $p<0.05$ in comparison to MI/Gel group.

Analysis of ventricular geometry shows significant increase in ejection fraction at 14 d and 28 d time points for the MI/Gel/SD7300 treatment as compared to the saline treatment, with a non-significant trend for improvement over the gel alone treatment

(**Figure 5.9a**). Similarly, MI/Gel/SD7300 treatment showed significantly lower LV end diastolic and systolic volumes at both 14 and 28 days, with a non-significant trend for a decrease over the gel alone therapy (**Figure 5.9b,c**). Finally, while no significant trends were observed in LV pulmonary wedge thickness at end diastole, MI/Gel/SD7300 provided significantly higher LV septal thicknesses at end diastole as compared to saline controls (**Figure 5.9d,e**). These trends are also reflected in an analysis of these parameters' percent change from baseline values (**Figure 5.10**). Taken together, these data suggest that Gel/SD7300 combination treatment provided increased benefit over gel alone treatment in improving cardiac function and attenuating LV dilation.

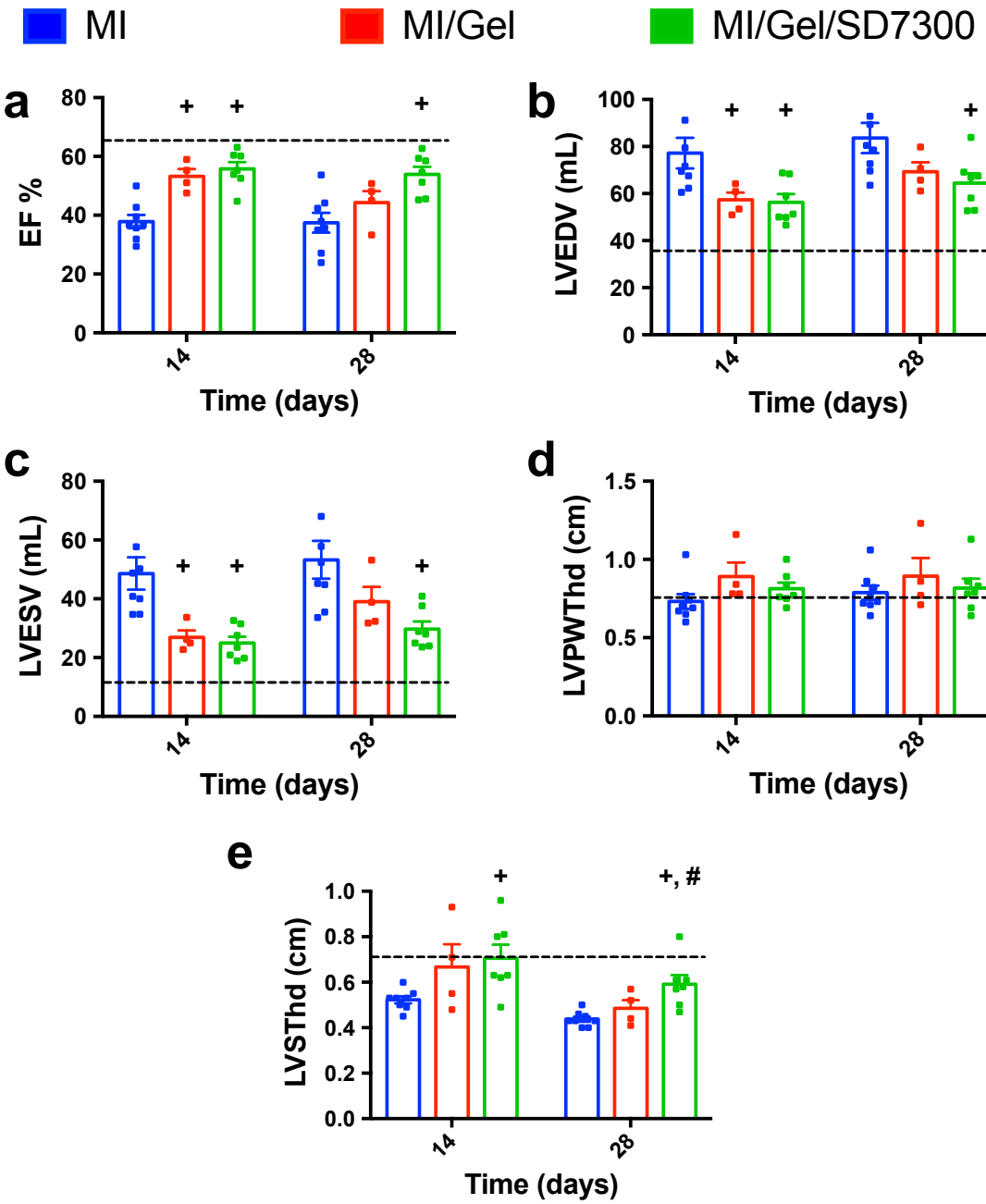

Figure 5.9. LV Geometry and Function. (a) Ejection fraction (EF), (b) LV end diastolic volume (EDV), (c) LV end systolic volume (ESV), (d) LV pulmonary wall thickness (LVPWThd) at end diastole, and (e) LV septal thickness at end diastole (LVSThD) for animals treated with MI (blue, n=8), MI/Gel (red, n=4), and MI/Gel/SD7300 (green, n=7) at baseline and 14 and 28 days after MI. Animals in the MI/Gel/SD7300 group had significantly higher EF, lower LVEDV, lower LVESV, and higher LVSThd at 14 and 28 days as compared to the MI group. Dashed line represents the average of baseline values for all animals used in the study. Statistics were determined using one-way ANOVA, with + representing $p<0.05$ in comparison to MI group and # representing $p<0.05$ in comparison to MI/Gel group.

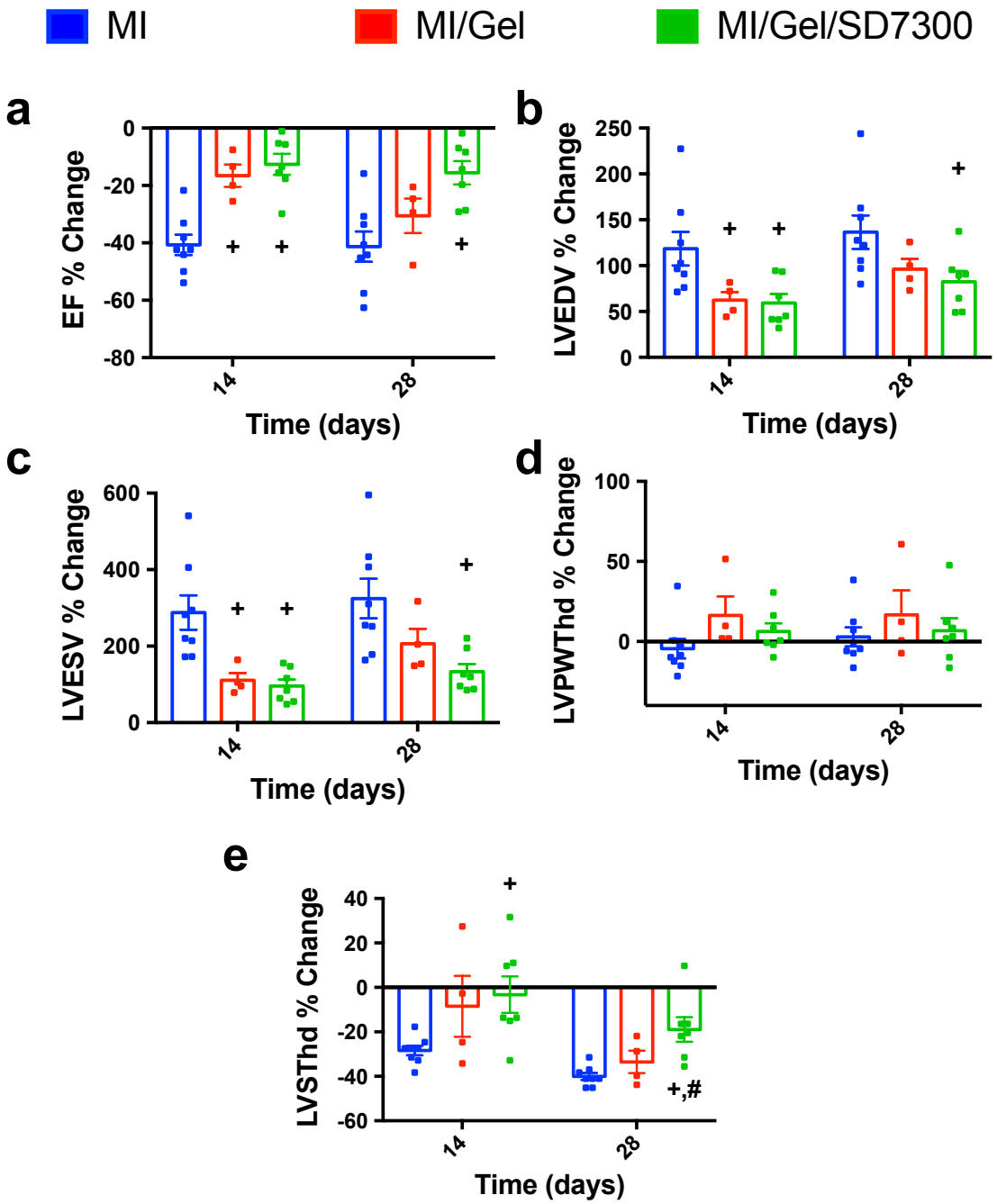

Figure 5.10. Percent change in LV Geometry and Function. Percent change in (a) ejection fraction (EF), (b) LV end diastolic volume (EDV), (c) LV end systolic volume (ESV), (d) LV pulmonary wall thickness (LVPWThd) at end diastole, and (e) LV septal thickness at end diastole (LVSThD) for animals treated with MI (blue, n=8), MI/Gel (red, n=4), and MI/Gel/SD7300 (green, n=7) at baseline and 14 and 28 days after MI. Animals in the MI/Gel/SD7300 group had significantly lower decreases in EF, lower increases in LVEDV, lower increases in LVESV, and higher increases LVSThd at 14 and 28 days as compared to the MI group. Statistics were determined using one-way ANOVA, with + representing $p<0.05$ in comparison to MI group and # representing $p<0.05$ in comparison to MI/Gel group.

Both the generation of infarction and the timing of biomaterial delivery are important factors when considering the design of MI animal models. It is important to consider the generation of clinically relevant infarcts when evaluating new potential therapies. In this study, we utilized a balloon catheter approach to provide an ischemia/reperfusion injury to the myocardium, as opposed to traditional methods of ligation. Importantly, as the majority of patients undergoing an infarction will receive intervention to provide reperfusion of the infarcted tissue, this model recreates the scenario of reperfused, ischemic tissue in the myocardium. Furthermore, Yoshizumi et al provided evidence suggesting that the timing of biomaterial delivery after an infarct plays a critical role in determining the efficacy of improvement in tissue and functional outcomes.[38] It is also important to consider timing from a translational standpoint, as biomaterials-based interventions would likely not be administered for at least 24 hours or longer after diagnostic and logistical considerations. A significant impact of this work lies in the fact that these materials have been evaluated in an ischemia-reperfusion model of MI with delayed biomaterial injections. Functional data indicates that these materials are effective mechanically and bioactively at delayed time points, suggesting their utility in clinically relevant infarcts and time frames.

5.3.5. TISSUE ANALYSIS

At 28 days, hearts were harvested from animals and frozen for subsequent analysis. First, to assess infarct size and expansion, hearts were sectioned into 4 cm thick sections and stained with TTC to assess the metabolically active/inactive regions of the myocardium (i.e. healthy/infarcted tissue). Analysis of these sections showed that gel/SD7300 treatment provided a significant decrease in absolute MI areas, percentage MI of total LV area, and percentage MI of area at risk, as well as a generally non-significant trend for improvement with gel alone treatment (**Figure 5.11**). These data

suggest improved attenuation of infarct expansion by treatment with SD7300, although some effect was observed with injection of hydrogel alone.

To further probe mechanistic effects of localized inhibitor treatment, we conducted PCR arrays assessing cytokines and fibroblast gene profiles in the infarcted region of the myocardium (Table 5.1 and Table 5.2). Almost all genes investigated in this study were significantly different than healthy referent controls. This indicates the significant underlying biological changes that occur in fibroblast and cytokine expression after the induction of MI. Looking closer at gene expression related to ECM production, we observed non-significant decreases in Col1A1 and Col6A expression in the myocardium in animals treated with Gel/SD7300 as compared to gel alone and MI controls (**Figure 5.12a,b**). Furthermore, collagen presence in the myocardium was measured using picrosirus red staining, and we observed a significant decrease in collagen in animals treated with Gel/SD7300 as compared to gel alone and saline controls (**Figure 5.12c**). Taken together, these data suggest that Gel/SD7300 treatment provides direct influence on cellular phenotype and gene expression in the myocardium, ultimately contributing to a decreased fibrotic response.

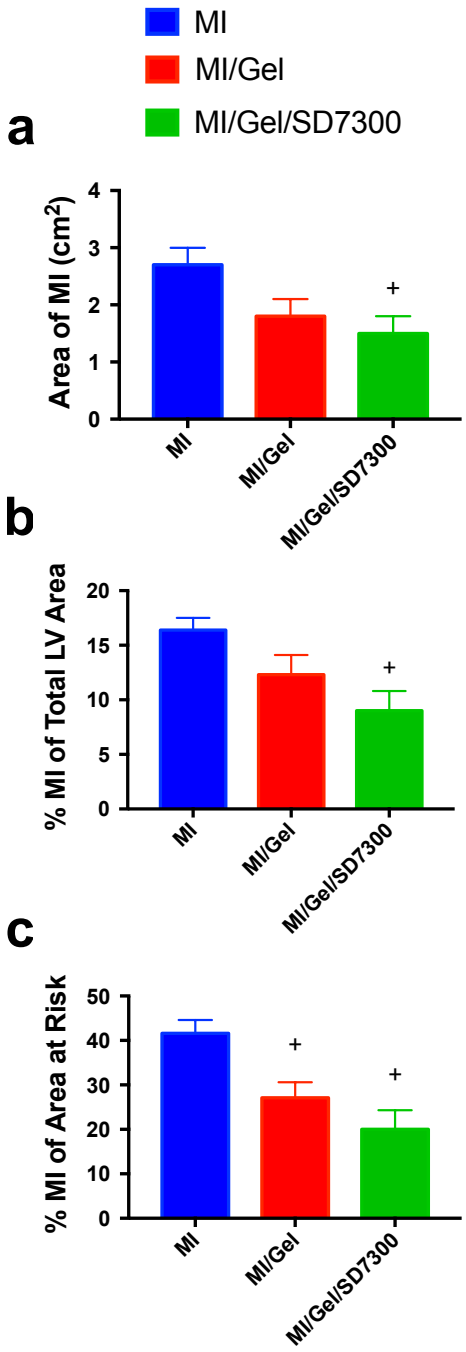

Figure 5.11. TTC staining of sectioned myocardium. (a) Infarct area, (b) percentage infarct of total LV area, and (c) percentage infarct of area at risk for animals treated with MI (blue, n=8), MI/Gel (red, n=4), and MI/Gel/SD7300 (green, n=7) at 28 days. Animals treated with MI/Gel/SD7300 had significantly lower infarct size, and percentage infarct of LV and area at risk. Statistics were determined using one-way ANOVA, with + representing $p<0.05$ in comparison to MI group and # representing $p<0.05$ in comparison to MI/Gel group.

Table 5.1 Cytokine PCR Array Results. A one-way ANOVA test was used to determine statistical significance against a referent control (RC) ($p<0.05$, *) or against MI only ($p<0.05$, +)

Gene	RC Detected n	MI Only	n	MI/Gel	n	MI/Gel/ SD7300	n
ACTA2	5	4.67±1.12 *	4	4.42±0.72 *	4	3.93±1.23 *	6
CCL2	5	2.55±1.07	6	3.24±0.95 *	4	3.42±1.10 *	6
CCL3L1	3	3.50±0.81 *	6	5.76±1.69 *	4	5.30±0.12 *	3
CD44	5	2.80±0.77 *	6	2.74±0.65 *	4	2.65±0.86 *	6
CSF2	0	Detected#	1	Detected#	2	Detected#	1
IFNG	4	0.13±1.15	4	0.60±1.18	4	3.27±0.24 *	2
IL10	2	3.04±0.99 *	6	4.47±0.57 *	4	4.06±1.20 *	6
IL6	0	Detected#	1	Detected#	2	ND	6
IL8	1	2.63±0.85 *	5	4.39±1.69	3	4.08±1.80	5
MMP8	1	1.95	1	0.71±0.80	2	1.33	1
MMP9	2	8.98±2.05 *	6	8.76±1.91 *	4	7.21±2.15 *	5
TNF	5	0.64±1.42	5	3.07±1.34	4	3.49±0.98 *	5

Table 5.2 Fibroblast PCR Array Results. A one-way ANOVA test was used to determine statistical significance against a referent control (RC) ($p<0.05$, *) or against MI only ($p<0.05$, +)

Gene	RC Detected n	MI Only	n	MI/Gel	n	MI/Gel/SD7300	n
ACTA2	5	4.67±1.12*	4	4.42±0.72*	4	3.93±1.23*	6
CCN2	5	5.23±0.46*	5	4.56±0.62*	4	4.67±0.87*	6
COL1A1	5	7.36±0.26*	5	7.02±0.73*	4	6.24±1.11*	6
COL6A	4	4.11±0.90*	5	3.71±1.07*	4	1.40±1.89	6
EDA FN	4	8.76±1.36*	6	7.76±0.92*	4	7.74±1.04*	6
ITGA3	3	4.28±1.17*	5	4.58±0.88*	4	3.58±0.91*	5
LOX	4	5.20±0.99*	6	5.64±0.49*	4	5.08±1.08*	6
MYH14	5	0.81±0.47*	6	1.08±0.27*	4	0.77±0.34	6
P311	4	2.71±0.46*	5	2.92±0.66*	4	2.55±0.81*	6
SPP1	4	7.61±1.49*	6	6.18±1.52*	4	6.28±1.16*	6
TGFB	5	3.93±0.70*	6	3.48±0.61*	4	3.12±0.81*	6
VIM	4	5.24±0.45*	5	4.38±0.48*	4	3.12±0.61*+	5

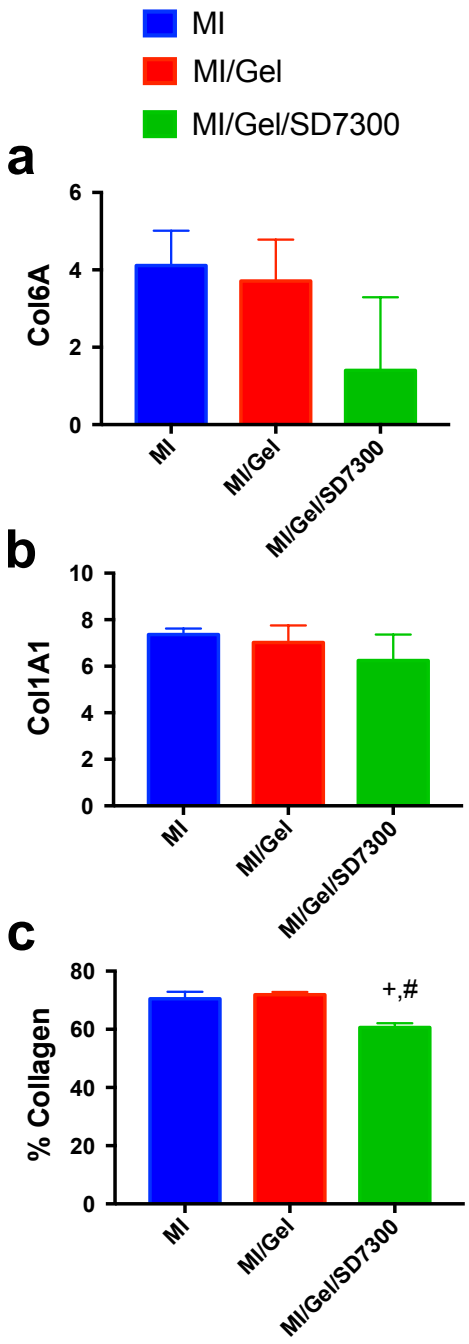

Figure 5.12. Collagen PCR and picrosirius red staining. PCR gene array samples for (a) Col6A and (b) Col1A1 and percentage of infarct containing collagen determined through picrosirius red staining for animals treated with MI (blue, n=8), MI/Gel (red, n=4), and MI/Gel/SD7300 (green, n=7) at 28 days. Animals treated with MI/Gel/SD7300 had a trend for lower Col6A and Col1A1 gene expression that was carried forward to significantly lower collagen percentages in the infarct. Statistics were determined using one-way ANOVA, with + representing $p<0.05$ in comparison to MI group and # representing $p<0.05$ in comparison to MI/Gel group.

5.4 CONCLUSIONS

This study has shown the development of an injectable, self-assembled hydrogel formulation for the delivery of the small molecule MMP inhibitor SD-7300. These materials provided month-long sustained release and activity of SD-7300 *in vitro*, and were able to localize small molecules to the myocardium *in vivo.* Hydrogels delivering SD-7300 were delivered in an ischemia-reperfusion, delayed injection model of MI and provided improved functional and structural benefit over hydrogel alone and saline controls. Finally, we observed that mechanistically, these systems may be exerting their effect on collagen production and regulation in the myocardium. Moving forward, these materials have broad impact on MMP inhibition therapies, as they solve key problems associated with systemic administration of these pharmacologics through local and sustained delivery.

5.5 REFERENCES

1. White HD, Chew DP. Acute myocardial infarction. The Lancet. 2008;372(9638):570-84.
2. Benjamin EJ, Blaha MJ, Chiuve SE, Cushman M, Das SR, Deo R, et al. Heart disease and stroke statistics-2017 update: a report from the American Heart Association. Circulation. 2017;135(10):e146-e603.
3. French BA, Kramer CM. Mechanisms of Post-Infarct Left Ventricular Remodeling. Drug discovery today Disease mechanisms. 2007;4(3):185-96.
4. Vanhoutte D, Schellings M, Pinto Y, Heymans S. Relevance of matrix metalloproteinases and their inhibitors after myocardial infarction: a temporal and spatial window. Cardiovasc Res. 2006;69(3):604-13.

5. Mukherjee R, Brinsa TA, Dowdy KB, Scott AA, Baskin JM, Deschamps AM, et al. Myocardial infarct expansion and matrix metalloproteinase inhibition. Circulation. 2003;107(4):618-25.
6. Prabhu SD, Frangogiannis NG. The biological basis for cardiac repair after myocardial infarction: from inflammation to fibrosis. Circ Res. 2016;119(1):91-112.
7. Dobaczewski M, Gonzalez-Quesada C, Frangogiannis NG. The extracellular matrix as a modulator of the inflammatory and reparative response following myocardial infarction. J Mol Cell Cardiol. 2010;48(3):504-11.
8. Yabluchanskiy A, Li Y, Chilton RJ, Lindsey ML. Matrix metalloproteinases: drug targets for myocardial infarction. Curr Drug Targets. 2013;14(3):276-86.
9. Phatharajaree W, Phrommintikul A, Chattipakorn N. Matrix metalloproteinases and myocardial infarction. Can J Cardiol. 2007;23(9):727-33.
10. Mukherjee R, Mingoia JT, Bruce JA, Austin JS, Stroud RE, Escobar GP, et al. Selective spatiotemporal induction of matrix metalloproteinase-2 and matrix metalloproteinase-9 transcription after myocardial infarction. Am J Physiol-Heart C. 2006;291(5):H2216-H28.
11. Rohde LE, Ducharme A, Arroyo LH, Aikawa M, Sukhova GH, Lopez-Anaya A, et al. Matrix metalloproteinase inhibition attenuates early left ventricular enlargement after experimental myocardial infarction in mice. Circulation. 1999;99(23):3063-70.
12. Tao ZY, Cavasin MA, Yang F, Liu YH, Yang XP. Temporal changes in matrix metalloproteinase expression and inflammatory response associated with cardiac rupture after myocardial infarction in mice. Life sciences. 2004;74(12):1561-72.
13. Wagner DR, Delagardelle C, Ernens I, Rouy D, Vaillant M, Beissel J. Matrix metalloproteinase-9 is a marker of heart failure after acute myocardial infarction. J Card Fail. 2006;12(1):66-72.

14. Wilson EM, Moainie SL, Baskin JM, Lowry AS, Deschamps AM, Mukherjee R, et al. Region- and type-specific induction of matrix metalloproteinases in post-myocardial infarction remodeling. Circulation. 2003;107(22):2857-63.
15. Ducharme A, Frantz S, Aikawa M, Rabkin E, Lindsey M, Rohde LE, et al. Targeted deletion of matrix metalloproteinase-9 attenuates left ventricular enlargement and collagen accumulation after experimental myocardial infarction. The Journal of clinical investigation. 2000;106(1):55-62.
16. Su H, Spinale FG, Dobrucki LW, Song J, Hua J, Sweterlitsch S, et al. Noninvasive Targeted Imaging of Matrix Metalloproteinase Activation in a Murine Model of Postinfarction Remodeling. 2005.
17. Fedak PWM, Smookler DS, Leco KJ, Mickle DAG, Watson KL, Hojilla CV, et al. TIMP-3 deficiency leads to dilated cardiomyopathy. Circulation. 2004.
18. Tian H, Cimini M, Fedak PWM, Altamentova S, Fazel S, Huang M-L, et al. TIMP-3 deficiency accelerates cardiac remodeling after myocardial infarction. J Mol Cell Cardiol. 2007;43(6):733-43.
19. Kassiri Z, Defamie V, Hariri M, Oudit GY, Anthwal S, Dawood F, et al. Simultaneous transforming growth factor β-tumor necrosis factor activation and cross-talk cause aberrant remodeling response and myocardial fibrosis in Timp3-deficient heart. J Biol Chem. 2009;284(43):29893-904.
20. Spinale FG, Villarreal F. Targeting matrix metalloproteinases in heart disease: lessons from endogenous inhibitors. Biochemical pharmacology. 2014;90(1):7-15.
21. Peterson JT. Matrix metalloproteinase inhibitor development and the remodeling of drug discovery. Heart failure reviews. 2004;9(1):63-79.
22. Fingleton B. Matrix metalloproteinases as valid clinical target. Current pharmaceutical design. 2007;13(3):333-46.

23. Eckhouse SR, Purcell BP, McGarvey JR, Lobb D, Logdon CB, Doviak H, et al. Local hydrogel release of recombinant TIMP-3 attenuates adverse left ventricular remodeling after experimental myocardial infarction. Science translational medicine. 2014;6(223):223ra21-ra21.

24. Gaffey AC, Chen MH, Venkataraman CM, Trubelja A, Rodell CB, Dinh PV, et al. Injectable shear-thinning hydrogels used to deliver endothelial progenitor cells, enhance cell engraftment, and improve ischemic myocardium. J Thorac Cardiovasc Surg. 2015;150(5):1268-76.

25. Rodell CB, Lee ME, Wang H, Takebayashi S, Takayama T, Kawamura T, et al. Injectable Shear-Thinning Hydrogels for Minimally Invasive Delivery to Infarcted Myocardium to Limit Left-Ventricular Remodeling. Circulation Cardiovascular interventions. 2016;9(10).

26. Rodell CB, MacArthur JW, Dorsey SM, Wade RJ, Wang LL, Woo YJ, et al. Shear-Thinning Supramolecular Hydrogels with Secondary Autonomous Covalent Crosslinking to Modulate Viscoelastic Properties In Vivo. Adv Funct Mater. 2015;25(4):636-44.

27. Tous E, Purcell B, Ifkovits JL, Burdick JA. Injectable acellular hydrogels for cardiac repair. J Cardiovasc Transl Res. 2011;4(5):528-42.

28. Hoare TR, Kohane DS. Hydrogels in drug delivery: Progress and challenges. Polymer. 2008;49(8):1993-2007.

29. Li J, Mooney DJ. Designing hydrogels for controlled drug delivery. Nature Reviews Materials. 2016;1(12):16071.

30. Purcell BP, Lobb D, Charati MB, Dorsey SM, Wade RJ, Zellars KN, et al. Injectable and bioresponsive hydrogels for on-demand matrix metalloproteinase inhibition. Nat Mater. 2014;13(6):653-61.

31. SD-7300 Investigator's Brochure. 2003.

32. Rodell CB, Kaminski AL, Burdick JA. Rational design of network properties in guest-host assembled and shear-thinning hyaluronic acid hydrogels. Biomacromolecules. 2013;14(11):4125-34.

33. Mealy J, Rodell C, Burdick JA. Sustained Small Molecule Delivery from Injectable Hyaluronic Acid Hydrogels through Host-Guest Mediated Retention. Journal of Materials Chemistry B. 2015.

34. Loftsson T, Brewster ME. Pharmaceutical applications of cyclodextrins: basic science and product development. J Pharm Pharmacol. 2010;62(11):1607-21.

35. Hyabell Professionals Hyabell. Available from: https://http://www.hyabell.com/professionals.php.

36. Rohde LE, Ducharme A, Arroyo LH, Aikawa M, Sukhova GH, Lopez-Anaya A, et al. Matrix metalloproteinase inhibition attenuates early left ventricular enlargement after experimental myocardial infarction in mice. Circulation. 1999;99(23):3063-70.

37. Turk B. Targeting proteases: successes, failures and future prospects. Nat Rev Drug Discov. 2006;5(9):785-99.

38. Yoshizumi T, Zhu Y, Jiang H, D'Amore A, Sakaguchi H, Tchao J, et al. Timing effect of intramyocardial hydrogel injection for positively impacting left ventricular remodeling after myocardial infarction. Biomaterials. 2016;83:182-93.

Chapter 6

INJECTABLE GRANULAR HYDROGELS WITH MULTIFUNCTIONAL PROPERTIES FOR BIOMEDICAL APPLICATIONS

Adapted from:

Mealy JE, Chung JJ, Jeong HH, Issadore D, Lee D, Atluri P, Burdick JA. Injectable Granular Hydrogels with Multifunctional Properties for Biomedical Applications. Advanced Materials. 2018 May;30(20):1705912.

6.1. INTRODUCTION

Biomaterials are being developed as useful therapeutic modalities for a wide range of applications, including for the delivery of cells and molecules (e.g. pharmacologics, cytokines, growth factors), as cell scaffolds for tissue engineering and regenerative medicine, and for mechanical support and tissue bulking.[1,2] Many biological contexts such as development, inflammation, and tissue repair are quite complex and would benefit from multiplexed functionality (e.g. multiple independent drug delivery rates, multi-modal degradation behavior, hierarchical mechanical properties) in therapeutic design.

To address this, biomaterials are now evolving beyond simple static and uniform materials to incorporate and harness this complexity through advanced material design. As examples, approaches to introduce multiplexed functionality in molecule delivery have included composite embedding techniques, layer by layer design, or simple co-encapsulation of multiple factors within a single material.[3-6] Furthermore, techniques such as photolithography and 3D printing are emerging to improve the spatial design of

multifunctional materials.[7,8] Despite these advances, there is a disparity between creating highly complex materials and doing so in a manner that is broadly amenable to clinical translation, such as with the use of injectable materials.

Injectable materials – commonly hydrogels - can be introduced into tissues via percutaneous procedures using syringes and catheters and have been used in numerous biomedical applications.[9-14] Traditionally, these materials are isotropic and homogeneous, frequently designed with a single set of input parameters governing the material function. Self-assembled hydrogels are a subset of these materials, where crosslinking chemistry is derived from non-covalent interactions including hydrophobic, ionic, and guest-host binding.[15] These materials are often both shear-thinning and self-healing, which permits ease of injection and then stabilization upon reaching the injection site. For example, we developed a hydrogel system based on the guest-host assembly of polymers modified with cyclodextrin and adamantane that exhibited these properties and could be injected into tissues.[16-18] Thus, there is a need for materials that are injectable and can be engineered to meet the complex demands of tissue repair.

To meet this challenge, we developed a granular hydrogel system, based on the interactions of modular microgel components via guest-host interactions. Particulate assemblies are commonly designed through the association of nano- and micro-scale components and have recently found utility as cell culture platforms, wound healing aids, and drug delivery systems.[4,19-22] Guest-host interactions have not been previously used for the formation of granular systems and our design provides a high level of control over the hydrogel properties through the combination of microgels, including controlled drug delivery and porosity for cell invasion. Specifically, we fabricated crosslinked hyaluronic acid (HA) microgels with modular *intra-particle* covalent crosslinking that were formed into an injectable granular hydrogel through the use of cyclodextrin and adamantane guest-host *inter-particle* crosslinking. Here, we explored these materials for application in

the treatment of cardiac tissue after injuring, by introducing temporally controlled porosity and drug delivery.

6.2. METHODS

6.2.1. MATERIAL SYNTHESIS

All materials were purchased from Sigma unless otherwise noted. Sodium hyaluronate (HA, 75 kDa, Lifecore) was first converted to a tetrabutylammonium salt (HA-TBA) through the use of an ion exchange resin (Dowex50Wx4) to facilitate further modification. Briefly, HA was dissolved in aqueous solution and mixed with resin for 4 h, after which the resulting solution was neutralized with tetrabutylammonium hydroxide. The resulting aqueous solution was frozen and lyophilized to yield dried HA-TBA. ^{1}H-NMR (360 MHz, Bruker) was used to characterize the final product.

CD-HA was synthesized using previously described protocols.[17] Briefly, an aminated β-cyclodextrin was coupled to HA-TBA in a solution of dimethyl sulfoxide (DMSO) containing (benzotriazol-1-ylozy)tris(dimethylamino)phosphonium catalyst and allowed to proceed for 3h at room temperature. The resulting macromer was purified through precipitation in cold acetone, followed by dialysis against water for 2 weeks. The CD-HA solution was then frozen, lyophilized, and characterized via ^{1}H-NMR to yield ~25% modified CD-HA (**Figure 6.1a**).

Ad-NorHA was synthesized using a one-pot esterification reaction. HA-TBA, 1-adamantane acetic acid (TCI America) and 5-norbornene-2-carboxylic acid were dissolved in DMSO containing 4-methylaminopyridine and di-tertbutyl dicarbonate catalysts. The reaction was allowed to proceed for 20 h at 45 °C. The resulting product was purified via precipitation in cold acetone, and dialysis against water for two weeks. Ad-NorHA was then frozen, lyophilized, and characterized via ^{1}H-NMR to yield ~40%

norbornene and ~40% adamantane modified HA (**Figure 6.1b**). NorHA was synthesized in a similar protocol, excluding the adamantane reactants, to yield ~35% norbornene modified HA (**Figure 6.1c**).[23]

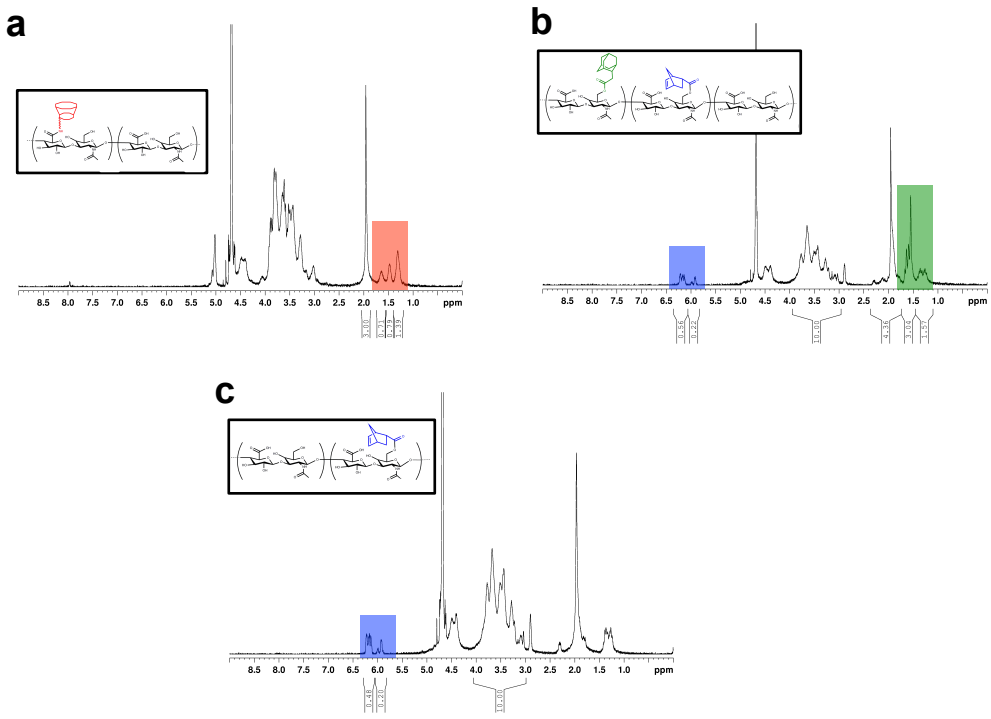

Figure 6.1. NMR spectra for modified HA macromers. ^{1}H-NMR (360MHz, D_2O) of modified hyaluronic acid polymers. (a) NMR spectrum for CD-HA with peaks from δ ~ 1.35 – 1.85 ppm used for determination of relative modification of cyclodextrin. (b) NMR spectrum for AdNorHA with peaks at δ ~ 6.3 ppm and δ ~ 6.0 ppm used for determination of relative modification of norbornene and peaks at δ ~ 1.6 ppm and δ ~ 1.4 ppm used for determination of relative modification of adamantane. (c) NMR spectrum for NorHA with integrated peaks at δ ~ 6.3 ppm and δ ~ 6.0 ppm used for determination of relative modification of norbornene.

6.2.2. PEPTIDE SYNTHESIS

Peptides were synthesized via fluorenylmethyloxycarbonyl (FMOC) solid phase peptide synthesis and glycanol 2-chlorotrityl substrate (GCKK-RHO, GCNSVPMSMRGGSNCG) or a 1,6 diaminohexane trityl resin (GCKK-FITC). Peptides were cleaved from the resin in a mixture of trifluoroacetic acid, triisopropylsilane, and water (95:2.5:2.5) and then purified by precipitation in cold diethyl ether. Peptides were

then dissolved in water, frozen, and lyophilized. Peptides were then characterized via MALDI-TOF spectroscopy (Multiflex, Bruker).

6.2.3. DEVICE MANUFACTURE

As described previously, a three-dimensional monolithic elastomer device (3D MED) was used for scale-up of liquid droplets.[24] A 3D MED was fabricated with poly dimethyl siloxane using a double-sided imprinting method with a hard and soft master. The fabrication of hard and soft master was formed by conventional photo- and soft-lithography.

6.2.4. MICROGEL SYNTHESIS

A dispersed phase consisting of 3 wt% aqueous macromer (Ad-NorHA, NorHA) 0.05 wt% I2959, thiol crosslinker, and payload (FITC-BSA, 70kDa RHO-Dextran) pumped at 0.6 mL/h was focused into droplets using a dispersed phase of hexadecane containing 2 wt% Span80 flowed at 3.5 mL/h. Thiolated crosslinkers were included to consume 15% of norbornene units in the case of stable (DTT) and to consume 7.5% of norbornene groups in the case of cleavable microgels (GCNSVPMSMRGGSNCG), due to increased solution viscosity caused by charge interactions from the peptide. Droplets were collected and cured off chip using 365 nm UV light (Omnicure S1500, Excelitas Technologies) at approximately 10mW cm^{-2}.

For covalently-labeled materials, thiolated fluorophores (GCKK-FITC and GCKK-RHO) were included in the dispersed phase and coupled to microgels via thiol-norbornene photochemistry during curing. Crosslinked microgels were then purified by precipitation in cold acetone, followed by washing with isopropyl alcohol, then subsequent drying under vacuum to yield dried microgel product. Microgels were characterized using fluorescent and confocal microscopy, and microgel size was

calculated using ImageJ particle tracker on an analysis of ~50 microgels. To prepare granular hydrogels, microgels and CD-HA were dissolved at 10 wt% in phosphate buffered saline. For mixed microgels, the dried microgel powders were mixed prior to hydration.

6.2.5. IN VITRO MATERIAL CHARACTERIZATION

Granular hydrogels were imaged using a Leica TCSP5 confocal microscope and 3D reconstructions were rendered using ImageJ. Hydrogel mechanics were assessed using a stress-controlled rheometer (AR2000, TA) fitted with a 20 mm diameter flat plate geometry and a 300 μm gap height. Oscillatory frequency sweeps were conducted ranging from 0.01 to 100 Hz, while cyclic strain experiments were conducted by cycling between 1% and 500% strain at 1 Hz. Drug release was assessed using custom designed erosion cells in which 30 μL of gel was placed in a 4.3 mm diameter depression in a 1.6 cm diameter supernatant chamber. The chamber was filled with 1 mL PBS supplemented with 1 mM $CaCl_2$ containing either 200 U/mL Type IV collagenase or 0 U/mL collagenase. Releaseate was collected and analyzed for FITC-BSA release at $\lambda_{ex} = 490$, $\lambda_{em} = 525$ or for RHO-Dextran release at $\lambda_{ex} = 544$, $\lambda_{em} = 576$. Material degradation was assessed using a colorimetric uronic acid assay, as performed previously.[18]

6.2.6. IN VIVO MYOCARDIAL INFARCTION STUDIES OF MATERIAL DEGRADATION

The *in vivo* studies included an infarction and non-infarcted group to investigate differential degradation patterns under these two conditions. Using an established protocol of myocardial infarction (MI) in a rat model, 8-9 week old male Wistar rats were anesthetized, mechanically ventilated and underwent permanent ligation of the left

anterior descending artery to produce a 30-40% infarction of the left ventricle, confirmed by blanching of the myocardium in the appropriate distribution. Using a 27 G needle on a 0.5 mL syringe, labeled granular hydrogel containing equal masses of cleavable and stable microgels was delivered directly into the infarcted myocardium, as five discrete 10 μL injections. Care was taken to avoid intraventricular delivery of the hydrogel and the formation of visible hydrogel pockets confirmed containment within the myocardial tissue. The no MI group received the same 5 x 10 μL injections of gel into healthy myocardium corresponding to the infarcted region of the MI group. Due to the nature of the procedure, the surgeon was not blinded, although the treatment groups were randomly assigned. At pre-assigned timepoints of 1, 2, and 3 weeks, the rats were sacrificed and the hearts were explanted, flushed with PBS and preserved in OCT at -80°C for histologic analysis. 10 μm transverse sections were taken through the area of infarct. Sections were stained using hematoxylin and eosin (Sigma) and DAPI (Thermo Fisher) staining. Sections were stained using DAPI and hematoxylin and eosin staining.

6.2.7. IMAGE ANALYSIS FROM IN VIVO DEGRADATION STUDIES

Hearts from MI and non-MI groups (n=3) after 2 weeks were sectioned and three sections per animal were analyzed. Injection site area was estimated by the minimum region including all microgels (**Figure 6.2a**). For each section, red and green channel images were split (**Figure 6.2b**) and thresholded with a minimum intensity of 20 and maximum intensity of 255 to form a binary mask (**Figure 6.2c**). Masked areas were computed using the "measure" function in ImageJ. Areas of cleavable and stable microgels were then normalized to the total injection site area, to yield an area fraction:

$$Normalized\ Microgel\ Area = Total\ Microgel\ Area / Injection\ Site\ Area$$

Intensity density was calculated by summing the total pixel intensity in either the red or green channel, then dividing by the estimated injection site area:

$$Normalized\ Microgel\ Fluorescence = \frac{Total\ Microgel\ Fluorescence}{Injection\ Site\ Area}$$

Area fractions and intensity densities for each animal were determined, then averaged for three biological replicates in each group.

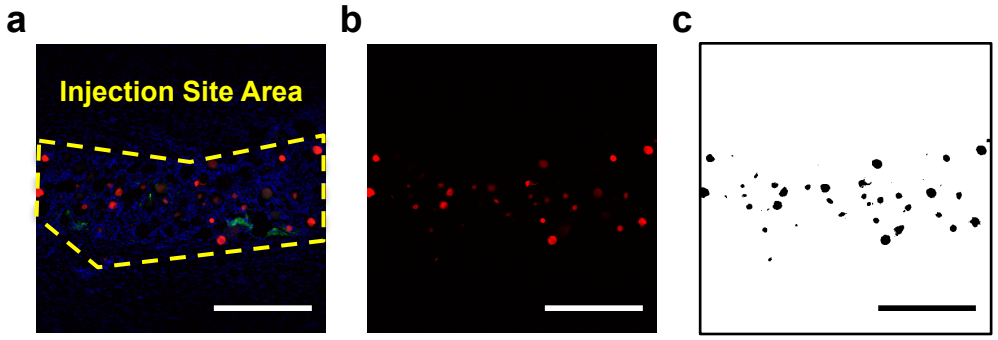

Figure 6.2. Example image series from image analysis on *in vivo* studies. (a) Composite image showing cleavable microgels (green), stable microgels (red), and cell nuclei (blue), and the estimated injection site area (yellow). (b) Red channel image of stable microgels. (c) Thresholded mask of (b) used for computing stable microgel areas used in area fraction calculations.

6.2.8. IN VIVO FUNCTIONAL STUDIES

To investigate the potential of the granular hydrogel for the delivery of therapeutic molecules, stromal-derived factor 1-alpha (SDF-1α) was encapsulated into the cleavable microgel portion of the injectable hydrogel. Encapsulation was performed as above, using DTT as the crosslinker. The release of SDF-1α from the hydrogel composite was investigated as described above, using an ELISA for SDF-1α to quantify release over time.

Using the previously described protocol, MI was generated in Wistar rats via ligation of the left anterior descending artery accessed using a left lateral thoracotomy. Animals were randomly assigned to three groups: PBS injections, granular hydrogels without SDF-1α, and granular hydrogels containing SDF-1α encapsulated in cleavable particles at approximately 0.33 μg/mg HA. Similar to degradation studies, materials were injected into the border zone region through 5x10 μL, with a final SDF-1α content of

approximately 1 μg per animal. Prior to tissue explant at 4 weeks, cardiac function was determined using a 12-mm pressure-volume loop catheter (Millar).

6.2.9. IMMUNOHISTOCHEMISTRY

Using a cryostat, 10 μm tissue sections were obtained from explanted hearts that had been washed in PBS, and frozen in OCT. For analysis of microvasculature, tissues were stained with primary antibodies for isolectin, α-smooth muscle actin (α-SMA-AF594, Abcam, 1:400), wheat germ agglutinin (WGA-AF647, 1:300), and DAPI (D1306 ThermoFisher Scientific, 1:1000). Images were collected using a Leica DM5000b fluorescent microscope with a DFC350 FX monochrome camera at 10x magnification. Isolectin area and isolectin co-localized α-SMA area were quantified using ImageJ. At least two images collected at the border zone were analyzed and averaged for each biological replicate (n=3 for PBS, gel, and gel/SDF groups).

To determine the effect of granular systems on macrophage response, tissue sections were stained for CD68 (MCA341GA, Bio-Rad, 1:300) and with goat anti-mouse AF647 secondary antibody (ab150115, Abcam, 1:300) as well as DAPI to visualize cellularization. Image analysis of CD68+ area fraction was conducted in ROIs at the border zone, in the vicinity of (but not including) microgel injections, determined by the absence of significant DAPI staining. Images were thresholded to form a binary mask, which was used to determine CD68+ area for at least 4 images per biological replicate (n=3 for each group). Finally, to determine the effect of SDF, cells were stained for the SDF receptor, CXCR4 using with a goat anti-CXCR4 primary antibody (ab1670, Abcam, 1:300) and a FITC donkey anti-goat secondary antibody (Abcam 7121, 1:1000). Images were thresholded to form a binary mask, over which particle counts were conducted to determine CXCR4+ cells for each high powered field. At least four images were analyzed and averaged for each biological replicate.

6.2.10. STATISTICAL ANALYSIS

Data is presented as mean ± standard deviation. Statistical analysis was conducted using ANOVA and a post hoc Tukey's Honestly Significant Difference test ($p<0.05$, $p<0.005$) on mechanical time sweeps, and a two-tailed student t-test on quantified tissue section data ($p<0.05$).

6.3. RESULTS AND DISCUSSION

A granular hydrogel system was developed that involved crosslinked hyaluronic acid (HA) microgels with modular *intra-particle* covalent crosslinking that were formed into an injectable granular hydrogel through the use of cyclodextrin and adamantane guest-host *inter-particle* crosslinking (**Figure 6.3a**). These materials were evaluated for modular, multiplexed functionality *in vitro* and *in vivo,* and then applied as a therapeutic system in a rat model of MI.

6.3.1. MICROGEL AND GRANULAR HYDROGEL FABRICATION

To fabricate microgels, we used a novel poly dimethyl siloxane (PDMS) microdevice to provide high throughput droplet generation (**Figure 6.3b**).[24] Droplets contained norbornene modified hyaluronic acid (**Figure 6.3a**) or adamantane and norbornene modified hyaluronic acid (AdNor-HA, **Figure 6.3a**), di-thiol crosslinkers (e.g., dithiotritiol (DTT), peptides), and a photoinitator, as well as fluorescein isothiocyanate (FITC) labeled bovine serum albumin (BSA) to image microgels. The droplets were crosslinked using a photoinitiated thiol-ene reaction to form microgels having diameters of 43 ± 10μm and 46 ± 12μm, depending on the crosslinker used (**Figure 6.4**). While some size dispersity was observed, potentially due to the drying and hydration process,

we were able to manufacture droplets at 0.6 mL of hydrogel precursor per hour through the use of 8 parallel droplet generators on a single device. This enabling technology is particularly useful when considering scale up of such systems for translation and this design has used up to hundreds of parallel droplet generators on a single device, processing solutions at rates as high as 1.5 L/h.[24]

In order to form and visualize the material microstructure, dry FITC-BSA loaded microgels were reconstituted in phosphate buffered saline (PBS) and combined with rhodamine (RHO) labeled cyclodextrin modified HA (CD-HA, **Figure 6.3c**). Gelation occurred instantly upon mixing of these two components to form the granular hydrogel. Confocal imaging of the hydrogel showed a clear "brick and mortar" structure, where distinct regions of FITC labeled microgels were interconnected by a web of RHO labeled CD-HA (**Figure 6.3c**). These images highlight the hierarchical structure of the material, which can be exploited to introduce functionality.

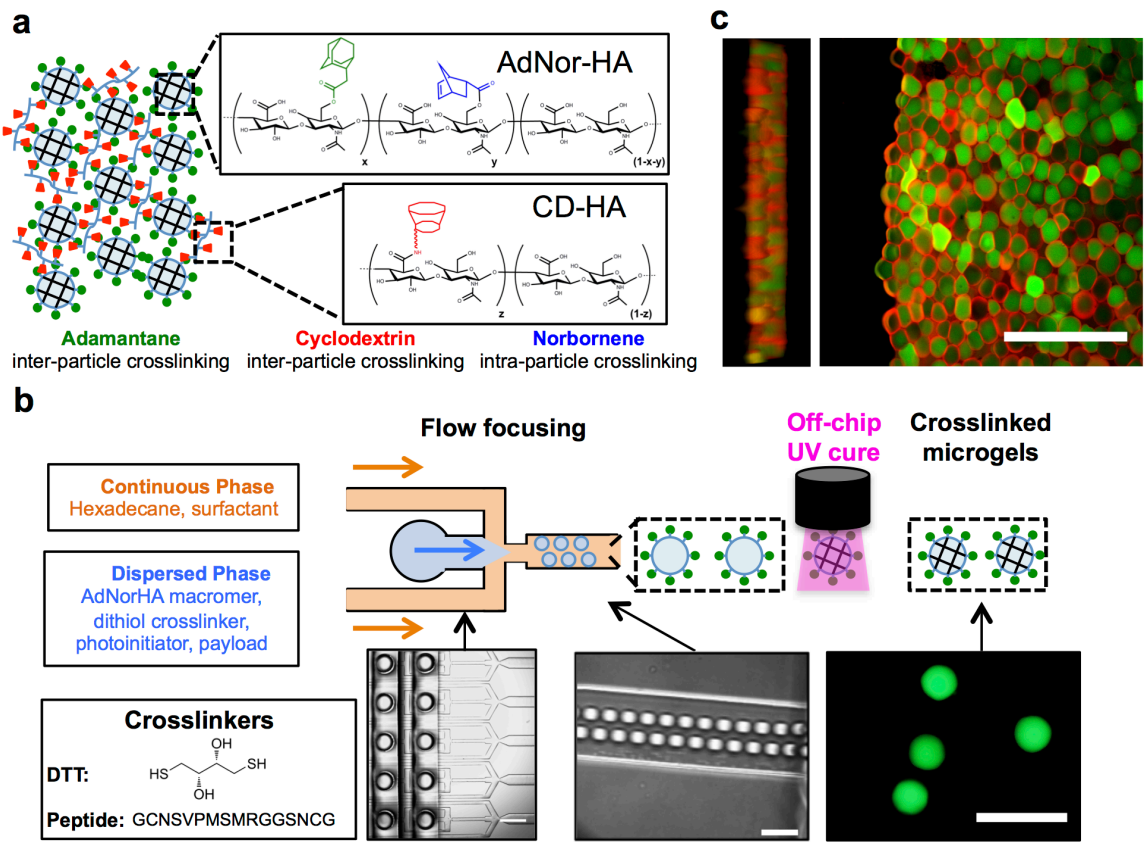

Figure 6.3. Guest-host granular hydrogel fabrication. (a) Schematic representation of guest-host granular hydrogel formation via the mixing of crosslinked adamantane (green) and norbornene (blue) modified hyaluronic acid (AdNor-HA) microgels and cyclodextrin (red) modified HA (CD-HA). (b) Schematic representation of the microgel fabrication process by which macromer droplets (containing AdNor-HA, di-thiol crosslinker, photoinitiator) are formed using a high throughput microfluidic device and stabilized through a photoinitiated thiol-ene reaction to form stable microgels that averaged ~43 μm in diameter. Scale bars from left to right are 500, 100, and 100 μm. (c) Confocal image (cross-sectional (left) and top (right) views) of a guest-host granular hydrogel formed with rhodamine labeled CD-HA and fluorescein labeled microgels. Scale bar = 200 μm.

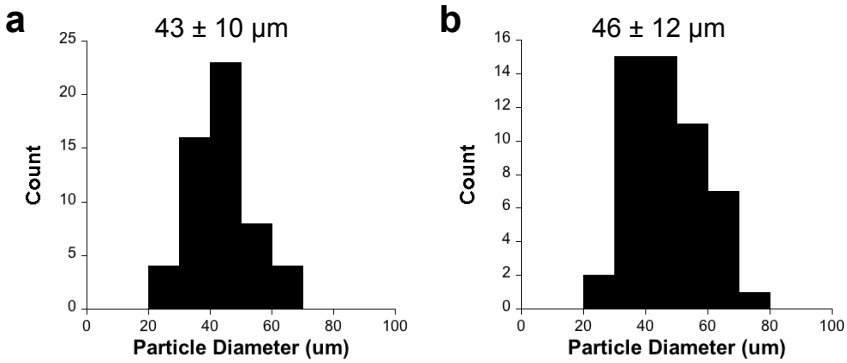

Figure 6.4. Size distributions of hydrated microgels. Sizing was assessed through fluorescent imaging for (A) microgels crosslinked using DTT (n=55) and (B) microgels crosslinked using an MMP cleavable peptide (n=49).

6.3.2. GRANULAR HYDROGEL MECHANICAL PROPERTIES

The mechanical properties of granular guest-host hydrogels were investigated using stress controlled shear oscillatory rheology. A series of three formulations was investigated: a "granular hydrogel" group containing 5wt% AdNorHA microgels crosslinked with DTT and mixed with 5wt% CD-HA, a "microgel control" group containing 5wt% NorHA microgels crosslinked with DTT and mixed with 5wt% CD-HA (i.e. no adamantane guest for inter-particle crosslinking), and a "polymer control" group containing 5wt% AdNorHA microgels crosslinked with DTT and mixed with 5wt% HA (i.e. no cyclodextrin host for inter-particle crosslinking) (**Figure 6.5a**). Across frequencies ranging from 0.01 Hz to 100 Hz, the granular hydrogel group maintained the highest mechanics of all three groups, with the microgel control group having an intermediate level of mechanics, and the polymer control group having the lowest mechanics (**Figure 6.5b**). Furthermore, when 1 Hz and 10 Hz frequencies were probed in time sweeps, the granular hydrogel was significantly higher ($p<0.05$) than either control system in both storage and loss moduli. All groups, however, did behave rheologically as hydrogels (i.e. G' > G"), potentially as a result of dense microgel packing in all conditions (**Figure 6.5c**). It is likely that the high mechanical properties observed in the granular hydrogel system

are a result of the guest-host inter-particle crosslinking, while the intermediate mechanics in the microgel control could be a result of promiscuous interactions between cyclodextrin and unreacted norbornenes, as well as molecule hydrophobicity.[25]

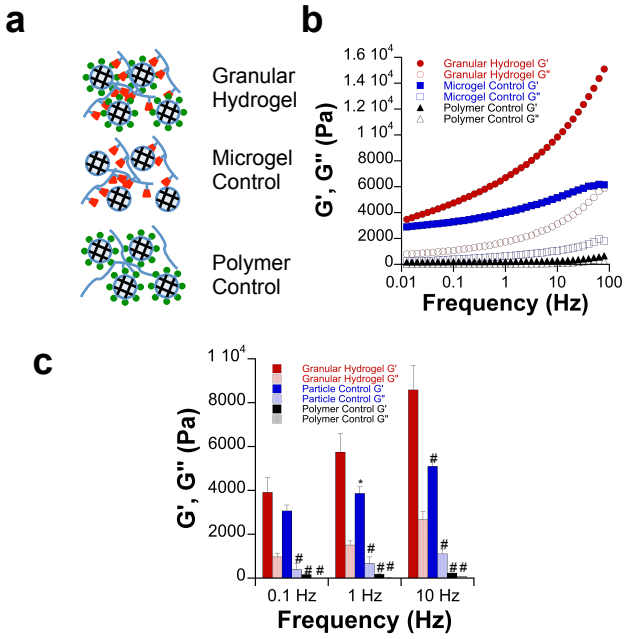

Figure 6.5. Rheological properties of guest-host granular hydrogels. (a) Schematic, (b) frequency sweeps and (c) average storage (G') and (G'') across a range of frequencies for granular hydrogels (red), microgel controls where cyclodextrin is omitted (blue), and polymer controls where the adamantane is omitted (black). Statistical significance was assessed relative to the granular hydrogel for the corresponding modulus and frequency with * denoting $p < 0.05$ and # denoting $p < 0.005$.

In previously developed hydrogels, guest-host crosslinking imparted shear-thinning and self-healing properties rendering them injectable; thus, we investigated the granular hydrogel behavior using a series of high (500%) and low (1%) strain cycles to simulate the conditions of injection (**Figure 6.6a**). Granular hydrogels maintained high mechanics (G' ~6 kPa) under low strain conditions and then rapidly adopted fluid-like, low mechanics (G' ~100 Pa) under high strain. After returning to low strain, the hydrogel returned to the initial, solid-like state before the next measurable time point (i.e. < 6 s)

with similar mechanics (G' ~6 kPa). This suggests that these materials undergo shear-thinning and self-healing that makes them amenable for syringe injections.

This behavior was also observed in strain sweeps where increasing strain transitioned the hydrogel from a more elastic solid to more viscous liquid behavior (**Figure 6.6b**). Interestingly, a peak in the loss modulus was observed for the granular hydrogel during yield (~30%) strain. We hypothesize that this is related to a rearrangement of microgels as the material transitions towards a more fluid-like state. Functionally, these granular hydrogels could be injected via needles as small as 27 G (~210 μm inner diameter) into dry or aqueous environments with minimal extravasation and without the need for long cure times or other stabilizing reactions (**Figure 6.6c**).

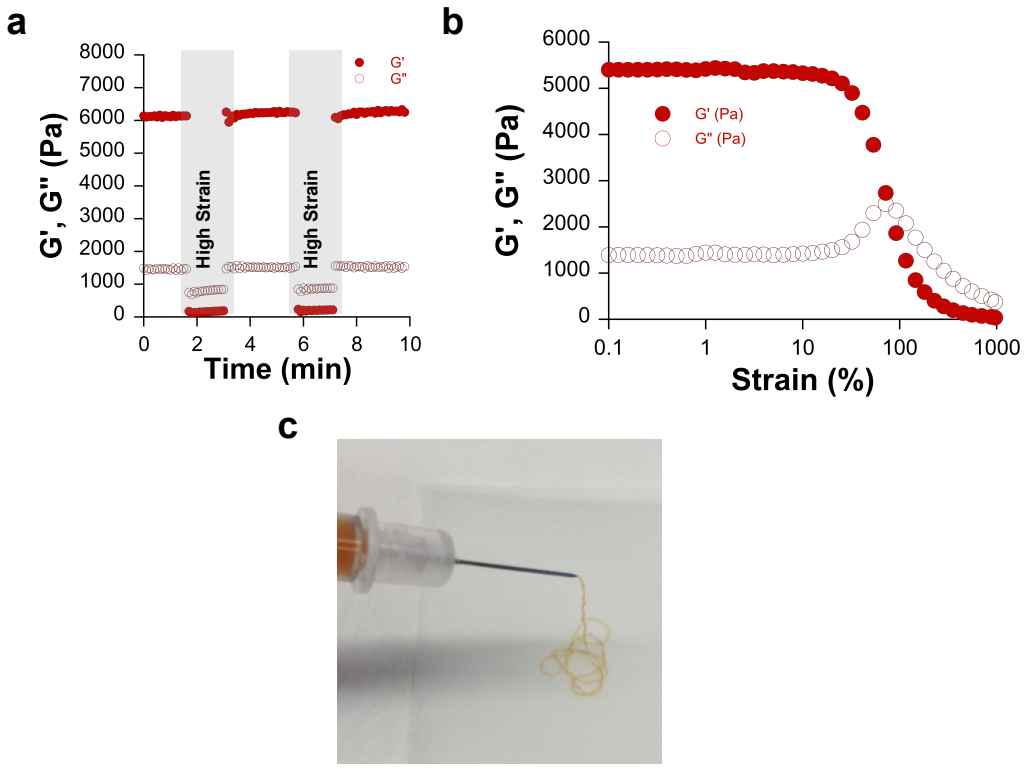

Figure 6.6. Shear-thinning behavior of granular hydrogels. (a) Strain-cycle experiment for granular hydrogels, whereby materials are cycled between 1% and 500% (shaded) strains. (b) Strain sweep analysis of granular hydrogels, indicating yielding behavior at high strains. (c) Ejection of a guest-host granular hydrogel from a syringe through a 27 G needle onto a dry surface.

6.3.3. MULTIPLEXED, MULTIFUNCTIONAL PROPERTIES OF GRANULAR HYDROGELS

One advantage to the design of the granular hydrogels is that microgels of various compositions (e.g., degradation, release profiles of encapsulated molecules) can be included, either as separate formulations or even combined into a single injectable system. Generally, the variable properties of the microgels can be tailored through altering the crosslinker chemistry. To explore this, we altered the di-thiol crosslinker used for intra-particle covalent crosslinking to be either non-degradable (DTT), to generate microgels that will subsequently be referred to as stable microgels, or matrix metalloproteinase (MMP) cleavable through inclusion of a peptide (GCNSGGRMSMPVSNCG, **Figure 6.7a**) that incorporates multiple cysteines to present thiols and an MMP-cleavable domain, to generate microgels that will subsequently be referred to as cleavable microgels.

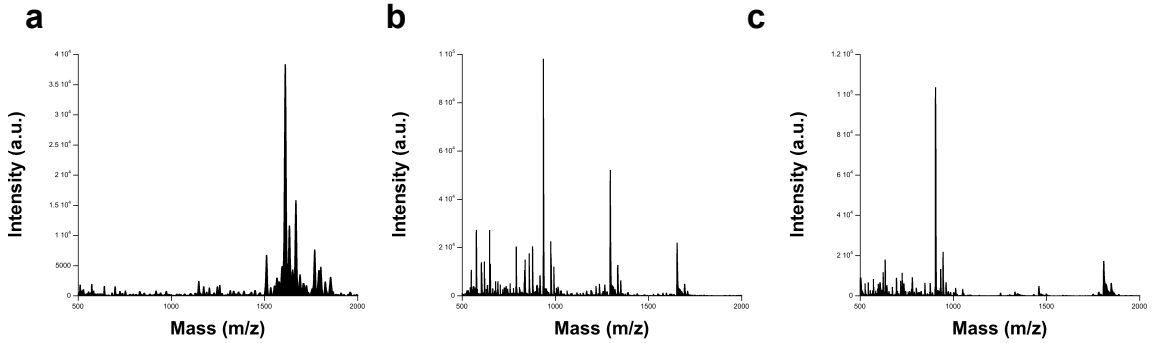

Figure 6.7. MALDI-TOF spectroscopy of synthesized peptides. (a) MMP cleavable peptide (GCNSVPMSMRGGSNCG) m/z: expected 1601, found 1611. (b) Fluorescein peptide (GCKK-FITC) m/z: expected 890, found 935 (corresponding to two Na ion complex). (c) Rhodamine peptide (GCKK-RHO) m/z: expected 903, found 904.

Stable or cleavable microgels containing a rhodamine labeled dextran (RHO-DEX) or FITC-BSA payload, respectively, were formed into single-component granular hydrogels and release of the payload and the hydrogel degradation (via uronic acid

assay) were monitored over two weeks. Studies were performed either in PBS buffer alone or containing 200U/mL collagenase to investigate the microgel response to proteases. Single component stable and single component cleavable hydrogels appeared as a mosaic of red or green microgels, respectively, when imaged on confocal microscopy. Some non-uniformity in microgel fluorescence was observed, likely a result of diffusion of the fluorescent materials. Over the course of two weeks, the cleavable granular gels released their payload significantly faster in the presence of collagenase (**Figure 6.8a**) and degraded more quickly (**Figure 6.8b**) when compared to the same formulation in buffer alone. Comparatively, the stable formulation maintained similar release profiles (**Figure 6.8c**) and degradation behavior (**Figure 6.8d**) regardless of inclusion of collagenase in the release buffer. These data suggest that the choice of microgel crosslinker provides a simple approach to control granular gel response and encapsulated molecule release behavior.

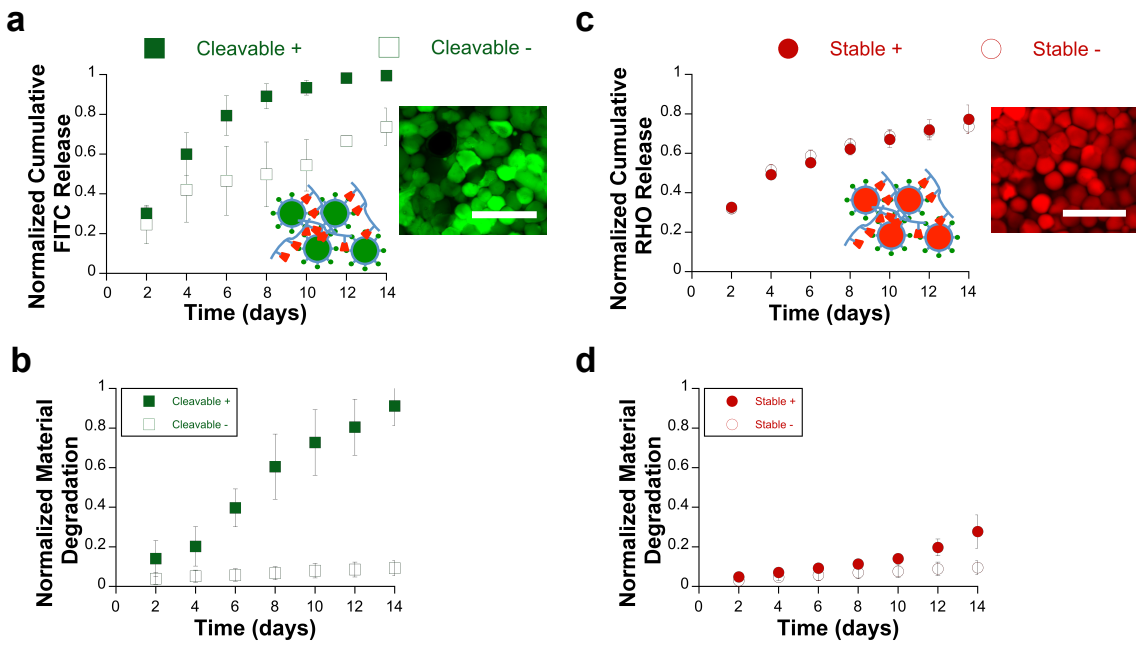

Figure 6.8. Molecule release and degradation of single-component granular hydrogels. (a) FITC-BSA release and (b) degradation of granular hydrogels fabricated from cleavable microgels with (+) or without (-) 200 U/ml collagenase included in the buffer. (c) RHO-DEX release and (d) degradation of granular hydrogels fabricated from stable microgels with (+) or without (-) 200 U/ml collagenase included in the buffer. Degradation behavior was monitored through uronic acid release (n=3). Scale bar =100 μm.

We then sought to investigate more complex hydrogels by combining multiple microgels into a single granular hydrogel. The advantage of the mixed microgel system is the complexity that is obtained through the design, where features such as controlled release of multiple factors and controlled cellular invasion are obtained with a single hydrogel. We created a two-component granular hydrogel by mixing equal amounts of stable and cleavable microgels containing RHO-DEX and FITC-BSA, respectively. Microgels of varied composition were fabricated on separate devices, but potentially devices could be generated in the future to simultaneously fabricate and mix microgel populations on-chip. Visually, these materials contained distinct red, stable microgels and green, cleavable microgels mixed together in a mosaic pattern (**Figure 6.9a**).

When two-component hydrogels were probed for release, an accelerated rate of FITC-BSA release was observed in the presence of collagenase, while profiles of RHO-DEX remained approximately similar either with or without collagenase (**Figure 6.9b**). This result is in agreement with how each of the individual microgels behaved in single-component systems. Furthermore, material degradation rates in the two-component systems in the presence of collagenase fell in between single component stable and single component cleavable systems, as expected due to the combination of microgel populations (**Figure 6.9c**). Taken together, these data showed both visually and functionally, that two-component systems combined the properties of each of the previous single-component systems, suggesting that modular exchange of microgel types is a successful means to independently multiplex functionality into these granular hydrogels. Although only two components were investigated here, a higher number of microgel compositions could be easily introduced. Additionally, passive release of encapsulated molecules could be minimized with alterations in microgel crosslink density or through the incorporation of binding agents between the microgel and entrapped molecule. The specific molecules and release profiles incorporated into the design will depend on the biomedical application targeted.

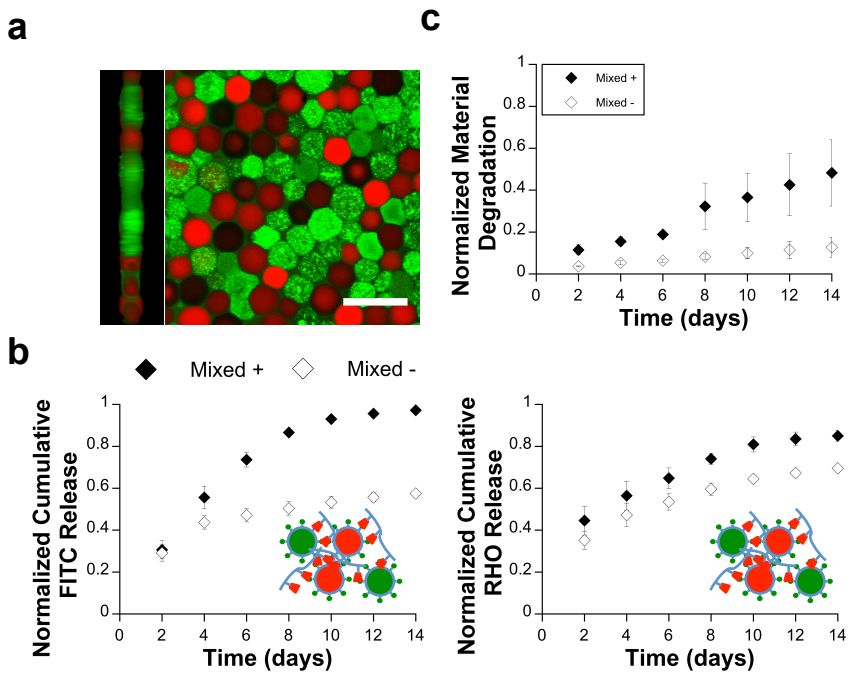

Figure 6.9. Molecule release and degradation of multi-component granular hydrogels. (a) Confocal image (cross-sectional (left) and top (right) views) of two-component granular hydrogels containing cleavable microgels with encapsulated FITC-BSA (green) and stable microgels containing RHO-DEX (red). (b) FITC-BSA and RHO-DEX release and (c) degradation of two-component granular hydrogels with (+) or without (-) 200 U/ml collagenase included in the buffer. Degradation behavior was monitored through uronic acid release (n=3). Scale bar =100 μm.

6.3.4. IN VIVO DEGRADATION AND CELL INVASION OF GRANULAR HYDROGELS

Myocardial infarction (MI) involves a complex sequence of tissue level changes, including inflammation and elevated protease activity, cell death, and fibrosis.[26,27] These processes ultimately contribute to expansion of the left ventricle, thinning of the myocardial wall, a loss of efficient ventricular mechanics and eventual heart failure.[28] Injectable hydrogels are finding widespread use for the treatment of MI, particularly to provide mechanical support or deliver therapeutics (e.g., drugs, cells) to the myocardium during the remodeling process to improve outcomes.[29,30] Emerging knowledge in this field suggests that this manner of intervention can be time and disease dependent, requiring control over material presence and drug release to optimally address

therapeutic and mechanical targets.[10,31] Multifunctional materials may be able to address this cascade of events, through multiplexing properties that facilitate spatiotemporal delivery of a variety of drugs and/or the manipulation of appropriate cell infiltration.

As elevated protease activity is a hallmark of MI, we sought to utilize disease-state protease levels within MI to investigate a responsive two-component granular hydrogel. In order to track these materials without the limitations of using encapsulated fluorophores, we covalently labeled MMP-cleavable microgels with a FITC-tagged thiolated peptide (GCKK-FITC,) and stable microgels with a RHO-tagged thiolated peptide (GCKK-RHO) *in situ* during the microdevice-based microgel synthesis (**Figure 6.7b,c**). Granular hydrogels were then formed containing equal amounts of cleavable and stable microgels and injected into the myocardial wall of either healthy rats or rats having undergone MI. Animals were serially sacrificed after one, two, or three weeks, at which point the hearts were explanted and preserved in optimal cutting temperature compound. Cardiac tissue was sectioned and imaged using a confocal microscope (**Figure 6.10**).

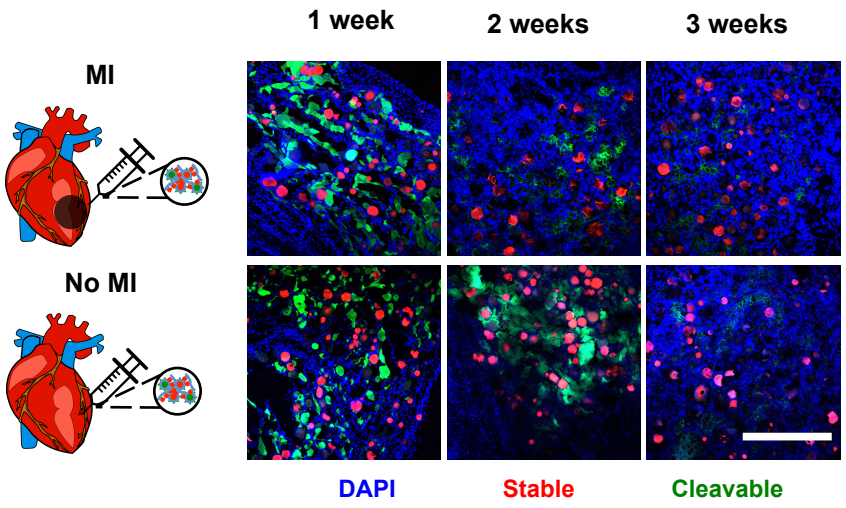

Figure 6.10. Disease dependent behavior of two-component granular hydrogels. Two-component granular hydrogels labeled with FITC for cleavable microgels and rhodamine for stable microgels were injected into rat hearts either without myocardial infarction (no MI) or with MI. Representative images of microgels and cell nuclei (blue) at one, two, and three weeks after injection (scale bar = 500 μm).

At one week, cleavable microgels in tissue sections were a mixture of spherical and degraded morphologies, with the MI group displaying more advanced degradation in microgel morphology (**Figure 6.10**). At two weeks, much of the cleavable material was cleared in the MI condition, while large aggregates of partially degraded microgels remained in the healthy condition. Finally, at the three-week time point, there was little remaining cleavable material in either condition. Across all conditions, stable microgels remained present with spherical, non-degraded morphologies throughout the duration of the three-week study.

Microgel presence was quantified at the two week timepoint, due to stark visual differences in microgels at this timepoint, by measuring the fluorescence intensity and area of both microgel types and normalizing to the total injection site area, in order to provide a metric of material mass and volume in the injection site (**Figure 6.11a**). Cleavable material normalized fluorescence intensity in the MI condition was ~40% of the no MI condition and cleavable material normalized area was ~20% of the normalized

area in the no MI condition. This indicated preferential degradation of cleavable microgels in the MI condition. There were no significant differences in stable microgel fluorescence intensity in the no MI condition. Relative to the no MI condition, there was a small decrease in the amount of stable normalized microgel area in the MI group, possibly indicating increased dispersion of the stable microgels in the tissue after MI, likely due to increased cellular invasion as the cleavable microgels were degraded (**Figure 6.11b**).

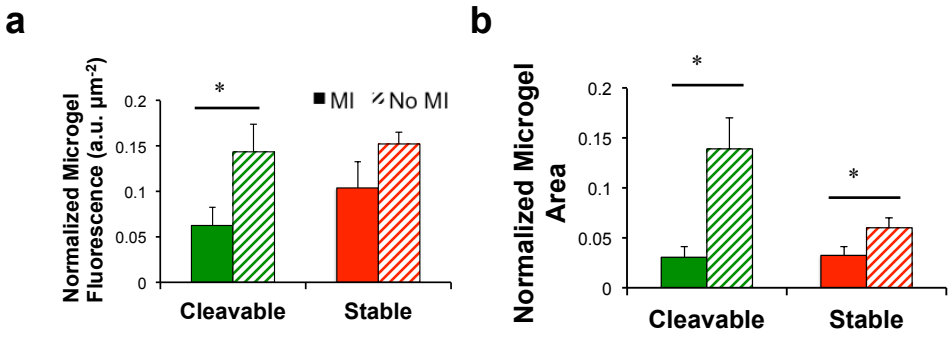

Figure 6.11. Quantification of microgel degradation in vivo. (a) Quantification of remaining microgels at 2 weeks, as (a) fluorescence intensity normalized to the injection site area or (b) area of microgel to injection site area (n=3). Statistical significance was assessed relative to healthy controls with $p < 0.05$.

Because proteases are elevated during MI, but still maintain a baseline presence in healthy tissue, we would expect that protease degradable microgels would eventually degrade in both healthy and MI conditions; however, the rates would be significantly different. These data suggest that the elevated MMP activity following an infarction is responsible for significantly accelerating the degradation of the protease cleavable microgels in the two-component granular hydrogel.

Further to differences in degradation, these materials facilitated cell infiltration, due to their highly porous, dynamic nature and this is in agreement with other results found in granular systems.[22] Through both DAPI (**Figure 6.10**) and hematoxylin and eosin staining (**Figure 6.12**), we observed cellularization within all conditions across the

timepoints; however, accelerated cellularization was observed at earlier time points in the MI condition concomitant with the more rapid degradation of the cleavable component of the dual-microgel system. For the MI conditions, large, vacated pores that we believe are a result of cleavable microspheres degrading were observed as early as one week and cellularity then increased with time. For the no MI condition, less cellularization was observed at the early times, but cellularity also increased with time, albeit at a slower pace when compared to the MI condition with elevated protease levels. In the context of MI, these findings are important as protease activity is a significant biological handle to signal disease-dependent material response. Beyond MI, elevated MMP activity is a key signal for smart biomaterial approaches during other conditions such as inflammation and cancer, making this approach broadly impactful in a number of diseases.

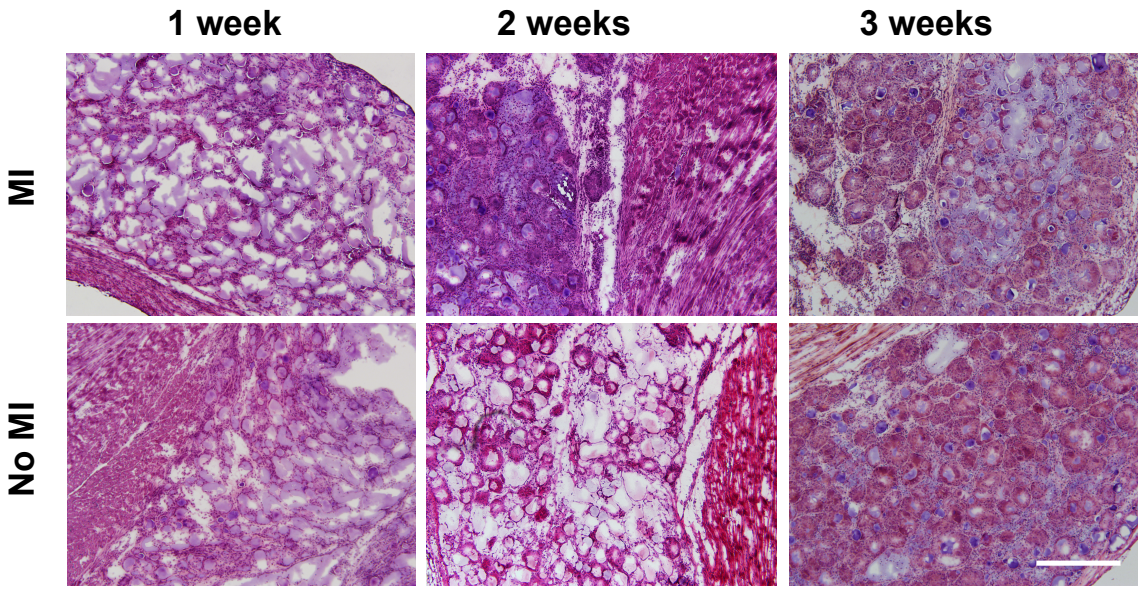

Figure 6.12. Hematoxylin and eosin staining. Hematoxylin and eosin staining of MI and no MI tissue sections at one week, two weeks, and three weeks. Scale bar = 500 μm.

6.3.5. FUNCTIONAL STUDIES OF GRANULAR HYDROGELS DELIVERING SDF-1α

As we observed controllable degradation and cellular invasion in these materials in response to disease states, we considered that granular hydrogel injection may also influence cardiac function. Indeed, it has been observed previously that particle-based systems in the myocardium can influence functional outcomes in the myocardium through tissue bulking and alteration of the inflammatory response. [32,33] Additionally, towards controlling cell type in the myocardium, and providing therapeutic delivery, we designed the granular hydrogel system for the delivery of therapeutics; specifically, SDF-1α was encapsulated into microgels, as SDF-1α has been previously shown to be useful in the myocardium as a therapeutic for recruiting stem cells and influencing biological outcomes such as vascularization. [34]

SDF-1α was encapsulated in cleavable microgels to provide early, disease dependent delivery to recruit stem cells to the infarct. We assayed release of SDF-1α using an ELISA kit in the presence of 500 U/mL collagenase, and observed release of SDF-1α over approximately two weeks (**Figure 6.13**). This aligned well with the goal of early recruitment of cells. Because stable particles themselves have previously shown functional benefit in MI models, we formulated a granular system as done previously, containing cleavable particles either empty or loaded with SDF-1α, as well as stable particles. Wistar rats received infarcts and were treated with either PBS (PBS, n = 15), blank granular gels (Gel, n = 7), or granular gels loaded with SDF-1α (Gel/SDF, n = 7).

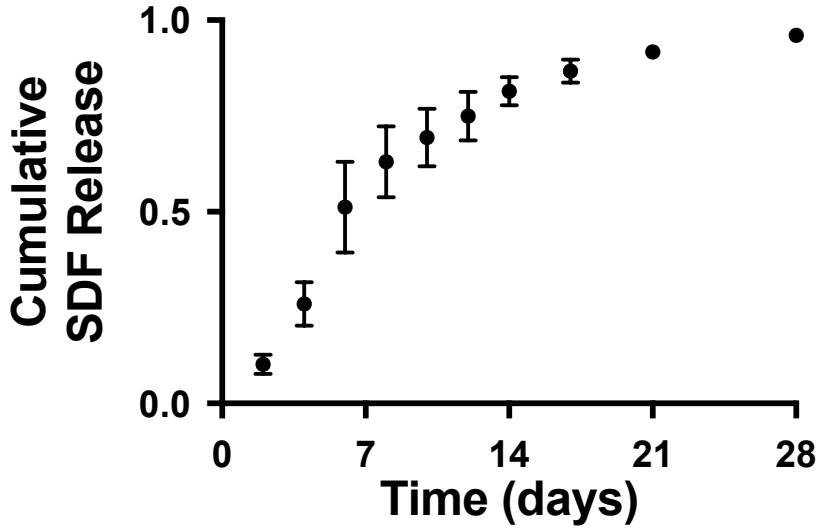

Figure 6.13. Release of SDF-1α from granular hydrogels. Granular hydrogels of the formulation investigated previously loaded with SDF-1α contained in cleavable microgels were incubated in the presence of 200 U/mL collagenase as a means to replicate the proteolytic infarcted myocardium. Supernatant was sampled and collected over 4 weeks, and releaseates were analyzed for SDF-1α content using an ELISA kit.

When investigating the functional outcomes, it was observed that only the granular hydrogel delivering SDF-1α had a significantly improved ejection fraction over the PBS control (**Figure 6.14a**). Both granular hydrogel groups (with and without SDF-1α) groups showed significant improvements in cardiac output, as well as dP/dt_{max}, a measure of cardiac contractility as compared to PBS controls (**Figure 6.14b,c**). Surprisingly, the granular hydrogel treatments did not improve volumes after treatment (**Figure 6.14d,e**). It is likely that both granular materials are influencing the myocardium by providing a means of cellular invasion and bulking, as has been demonstrated previously with numerous hydrogel systems and one treatment group improved outcomes with SDF delivery by altering local cellularity.

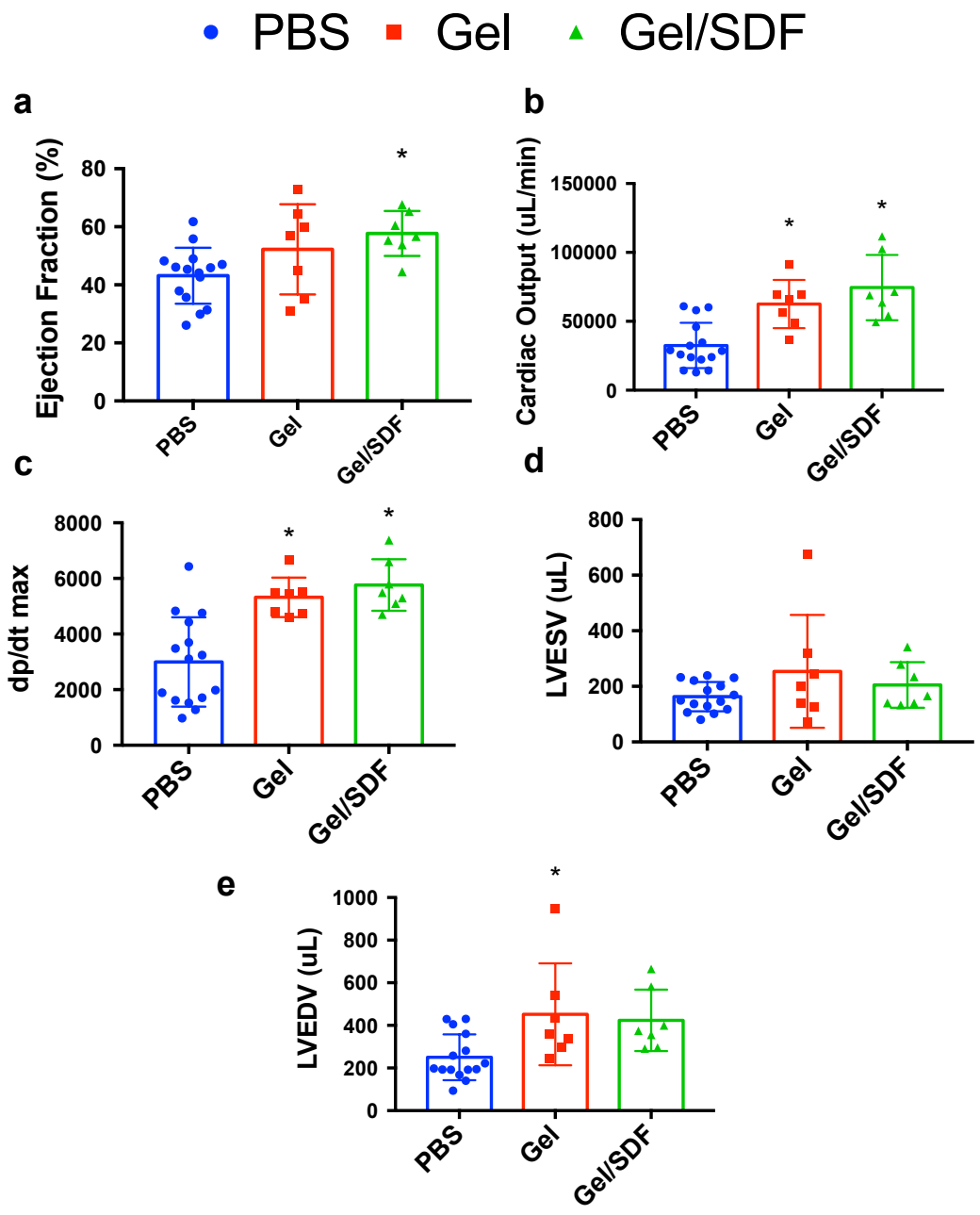

Figure 6.14 Functional outcomes at 4 weeks after MI. (a) Ejection fraction, (b) cardiac output, (c) dp/dt_{max}, (d) left ventricle end-systolic volume (LVESV), and (e) left ventricle end-diastolic volume (LVEDV) for animals treated with PBS (n=15, blue), granular hydrogels (gel, n=7, red), or granular hydrogels loaded with SDF (gel/SDF, n=7, green). Statistical significance was assessed using a one-way ANOVA with post hoc Tukey testing with * representing $p<0.05$ against PBS control group.

The biological role of particle based material systems in the myocardium has been investigated through the implantation of dermal fillers, as well as hyaluronic

acid/PLGA microsphere composites. [32,33] These systems have been shown to stimulate the inflammatory response in a unique way to induce beneficial stabilization to the infarct through ECM production as well as vasculogenesis, ultimately leading to improved outcomes including scar fraction and functional benefits. Particles in these systems fell into a unique size regime (>10μm, <100μm) that mitigates fibrous capsule formation, but prevents macrophage phagocytosis. Granular hydrogels developed here utilized microgels of a similar size regime to microgels. To better understand the biological response to the injected granular hydrogels, markers for inflammation, cell receptors, and vascularization were investigated using immunohistochemical analysis (**Figure 6.15a)**. Analysis of the inflammatory state of the myocardium local to injection sites shows that both gel groups and gel/SDF groups have significantly elevated macrophage levels as compared to PBS control groups (**Figure 6.15b**). This is likely a result of the granular nature of these materials, as previous studies investigating PLGA microsphere implants in the myocardium have shown elevated pro-healing, and overall inflammatory response. [33] While elevated inflammatory response is often thought to be detrimental in implanted materials, the potential for increased collagen deposition and vascularization generating stabilization of the infarcted tissue in the myocardium could provide significant benefit in acute phase MI.

We further explored the biological function of SDF-1α delivery from granular hydrogels. To this end, we stained tissue sections for the presence of CXCR4, the cell receptor for SDF that is often present on recruited cells. Gel/SDF treatment groups showed significantly higher CXCR4+ cell counts as compared to either PBS or gel treatments without SDF, suggesting that SDF delivery was in fact localizing stem cells to the myocardium in this system (**Figure 6.15c**).

Finally, we evaluated vascularization as a further downstream biological process of both macrophage invasion and stem cell recruitment. Areas of colocalized regions

staining positive for isolectin and αSMA were quantified. Only the Gel/SDF treatment group showed significant increase in this area as compared to PBS controls, indicating that SDF was critical to stimulating vasculogenesis in these systems. (**Figure 6.15d**). In summary, it is clear that granular hydrogels provide improved functional benefits to the myocardium, play a role in altering macrophage response, and that SDF delivery from these systems provides synergistic effect through the recruitment of stem cells to and generation of microvasculature in the infarcted tissue.

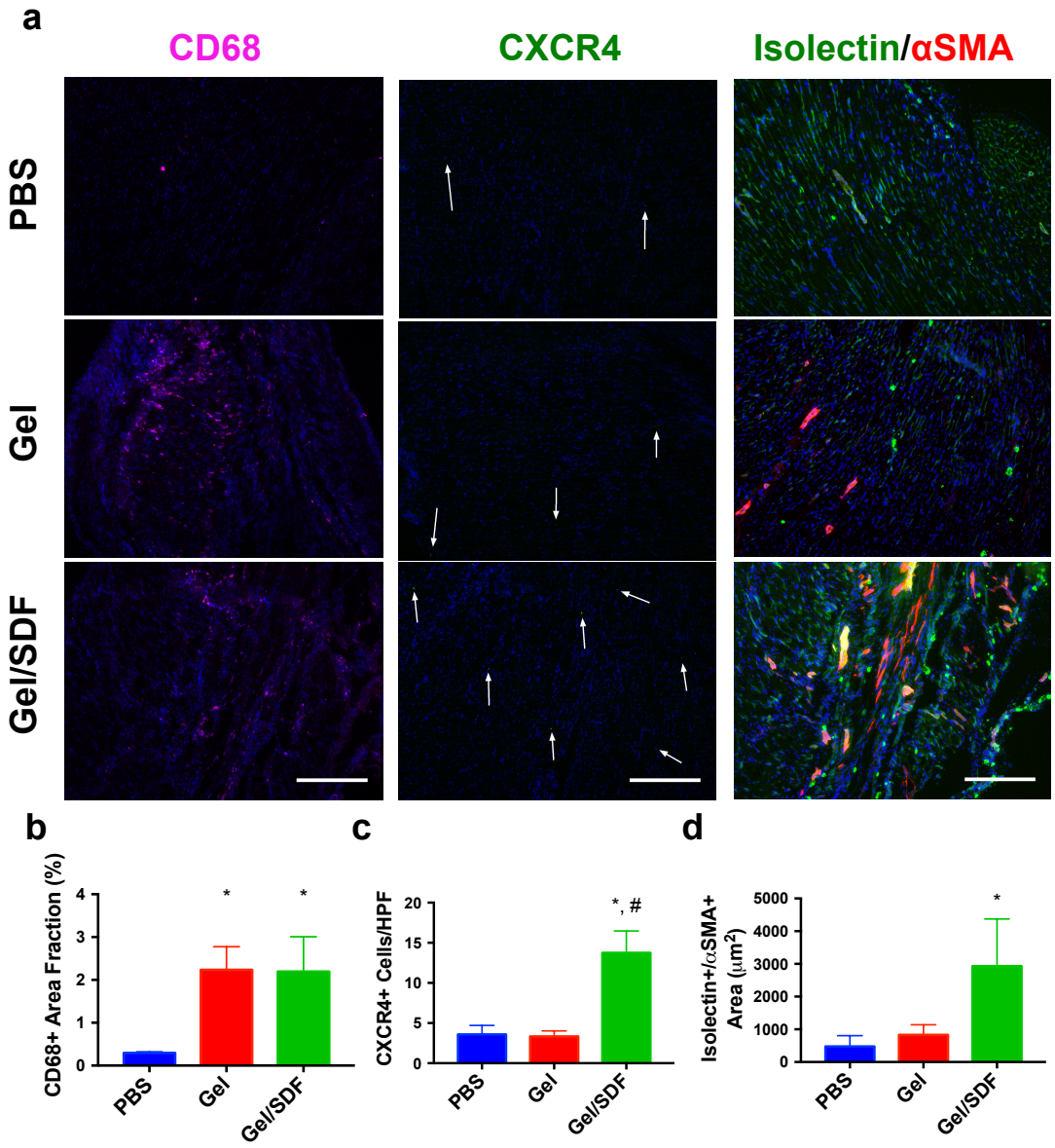

Figure 6.15. Immunohistochemistry for myocardial sections at 4 weeks after MI. (a) Representative images of macrophage (CD68, magenta), migratory stem cells (CXCR4, green), and vascular (isolectin, green and αSMA, red) staining. All images are co-stained with DAPI (blue). Scale bar represents 200μm. (b) CD68+ area fraction, a marker of macrophage activity, (c) CXCR4+ cells, a marker of miratory stem cells induced by SDF, and (d) isolectin/ αSMA co-stained area, a marker of microvasculature determined in regions local to microparticle injections at the border zone of MI. Statistical significance was assessed using a one-way ANOVA with post hoc Tukey testing with * representing $p<0.05$ against PBS control group, and # representing $p<0.05$ against Gel group.

6.4. CONCLUSIONS

In conclusion, we developed an injectable granular hydrogel, using guest-host interactions. This hydrogel displayed shear-thinning and self-healing properties that rendered it amenable to injection into dynamic environments and abrogated the need for controlled working/cure times that are often associated with other crosslinking mechanisms. The granular structure of this material allowed for multiplexing of complex release and degradation profiles that could be adjusted through modular exchange of intra-particle crosslinking or through combining multiple microgel types. The multiplexed material properties and high porosity of two-component granular hydrogels provided for unique disease-dependent behavior and high levels of cell invasion after injection into myocardial tissues. Finally, these materials were able to deliver the chemokine SDF-1α to improve cardiac function and biological outcomes.

6.5 REFERENCES

1. Kohane DS, Langer R. Polymeric biomaterials in tissue engineering. Pediatric research. 2008;63(5):487-91.
2. Tibbitt MW, Rodell CB, Burdick JA, Anseth KS. Progress in material design for biomedical applications. Proceedings of the National Academy of Sciences. 2015;112(47):14444-51.
3. Awada HK, Johnson NR, Wang Y. Sequential delivery of angiogenic growth factors improves revascularization and heart function after myocardial infarction. J Control Release. 2015;207:7-17.
4. Han LH, Yu S, Wang T, Behn AW, Yang F. Microribbon-Like Elastomers for Fabricating Macroporous and Highly Flexible Scaffolds that Support Cell Proliferation in 3D. Adv Funct Mater. 2013;23(3):346-58.

5. Min J, Choi KY, Dreaden EC, Padera RF, Braatz RD, Spector M, et al. Designer dual therapy nanolayered implant coatings eradicate biofilms and accelerate bone tissue repair. Acs Nano. 2016;10(4):4441-50.
6. Richardson TP, Peters MC, Ennett AB, Mooney DJ. Polymeric system for dual growth factor delivery. Nature biotechnology. 2001;19(11):1029-34.
7. DeForest CA, Polizzotti BD, Anseth KS. Sequential click reactions for synthesizing and patterning 3D cell microenvironments. Nature materials. 2009;8(8):659.
8. Highley CB, Rodell CB, Burdick JA. Direct 3D printing of shear‐thinning hydrogels into self‐healing hydrogels. Adv Mater. 2015;27(34):5075-9.
9. Gaffey AC, Chen MH, Venkataraman CM, Trubelja A, Rodell CB, Dinh PV, et al. Injectable shear-thinning hydrogels used to deliver endothelial progenitor cells, enhance cell engraftment, and improve ischemic myocardium. The Journal of thoracic and cardiovascular surgery. 2015;150(5):1268-77.
10. Purcell BP, Lobb D, Charati MB, Dorsey SM, Wade RJ, Zellers KN, et al. Injectable and bioresponsive hydrogels for on-demand matrix metalloproteinase inhibition. Nature materials. 2014;13(6):653.
11. Rodell CB, Lee ME, Wang H, Takebayashi S, Takayama T, Kawamura T, et al. Injectable shear-thinning hydrogels for minimally invasive delivery to infarcted myocardium to limit left ventricular remodeling. Circulation: Cardiovascular Interventions. 2016;9(10):e004058.
12. Singelyn JM, Christman KL. Injectable materials for the treatment of myocardial infarction and heart failure: the promise of decellularized matrices. Journal of cardiovascular translational research. 2010;3(5):478-86.

13. Singelyn JM, DeQuach JA, Seif-Naraghi SB, Littlefield RB, Schup-Magoffin PJ, Christman KL. Naturally derived myocardial matrix as an injectable scaffold for cardiac tissue engineering. Biomaterials. 2009;30(29):5409-16.

14. Yang J-A, Yeom J, Hwang BW, Hoffman AS, Hahn SK. In situ-forming injectable hydrogels for regenerative medicine. Progress in Polymer Science. 2014;39(12):1973-86.

15. Rodell CB, Mealy JE, Burdick JA. Supramolecular guest–host interactions for the preparation of biomedical materials. Bioconjugate chemistry. 2015;26(12):2279-89.

16. Mealy JE, Rodell CB, Burdick JA. Sustained small molecule delivery from injectable hyaluronic acid hydrogels through host–guest mediated retention. Journal of Materials Chemistry B. 2015;3(40):8010-9.

17. Rodell CB, Kaminski AL, Burdick JA. Rational design of network properties in guest-host assembled and shear-thinning hyaluronic acid hydrogels. Biomacromolecules. 2013;14(11):4125-34.

18. Rodell CB, MacArthur JW, Dorsey SM, Wade RJ, Wang LL, Woo YJ, et al. Shear-Thinning Supramolecular Hydrogels with Secondary Autonomous Covalent Crosslinking to Modulate Viscoelastic Properties In Vivo. Adv Funct Mater. 2015;25(4):636-44.

19. Appel EA, Tibbitt MW, Webber MJ, Mattix BA, Veiseh O, Langer R. Self-assembled hydrogels utilizing polymer–nanoparticle interactions. Nat Commun. 2015;6:6295.

20. Bruzewicz DA, McGuigan AP, Whitesides GM. Fabrication of a modular tissue construct in a microfluidic chip. Lab Chip. 2008;8(5):663-71.

21. Du Y, Lo E, Ali S, Khademhosseini A. Directed assembly of cell-laden microgels for fabrication of 3D tissue constructs. Proceedings of the National Academy of Sciences. 2008;105(28):9522-7.

22. Griffin DR, Weaver WM, Scumpia P, Di Carlo D, Segura T. Accelerated wound healing by injectable microporous gel scaffolds assembled from annealed building blocks. Nature materials. 2015;14(7):737.

23. Gramlich WM, Kim IL, Burdick JA. Synthesis and Orthogonal Photopatterning of Hyaluronic Acid Hydrogels with Thiol-Norbornene Chemistry. Biomaterials. 2013;34(38).

24. Jeong H-H, Yelleswarapu VR, Yadavali S, Issadore D, Lee D. Kilo-scale droplet generation in three-dimensional monolithic elastomer device (3D MED). Lab Chip. 2015;15(23):4387-92.

25. Rekharsky MV, Inoue Y. Complexation Thermodynamics of Cyclodextrins. Chem Rev. 1998;98(5):1875-918.

26. Jessup M, Brozena S. Medical progress: Heart failure. New Engl J Med. 2003;348(20):2007-18.

27. Mozaffarian. Heart Disease and Stroke Statistics-2015 Update: A Report From the American Heart Association (vol 131, pg e29, 2015). Circulation. 2015;131(24):E535-E.

28. Dobaczewski M, Gonzalez-Quesada C, Frangogiannis NG. The extracellular matrix as a modulator of the inflammatory and reparative response following myocardial infarction. J Mol Cell Cardiol. 2010;48(3):504-11.

29. Tous E, Purcell B, Ifkovits JL, Burdick JA. Injectable acellular hydrogels for cardiac repair. J Cardiovasc Transl Res. 2011;4(5):528-42.

30. Ye Z, Zhou Y, Cai H, Tan W. Myocardial regeneration: Roles of stem cells and hydrogels. Adv Drug Deliver Rev. 2011;63(8):688-97.

31. Yoshizumi T, Zhu Y, Jiang H, D'Amore A, Sakaguchi H, Tchao J, et al. Timing effect of intramyocardial hydrogel injection for positively impacting left ventricular remodeling after myocardial infarction. Biomaterials. 2016;83:182-93.

32. Ryan LP, Matsuzaki K, Noma M, Jackson BM, Eperjesi TJ, Plappert TJ, et al. Dermal Filler Injection: A Novel Approach for Limiting Infarct Expansion. Ann Thorac Surg. 2009;87(1):148-55.

33. Tous E, Weber HM, Lee MH, Koomalsingh KJ, Shuto T, Kondo N, et al. Tunable hydrogel-microsphere composites that modulate local inflammation and collagen bulking. Acta Biomater. 2012;8(9):3218-27.

34. Purcell BP, Elser JA, Mu A, Margulies KB, Burdick JA. Synergistic effects of SDF-1α chemokine and hyaluronic acid release from degradable hydrogels on directing bone marrow derived cell homing to the myocardium. Biomaterials. 2012;33(31):7849-57.

CHAPTER 7

CONCLUSIONS, LIMITATIONS, AND FUTURE DIRECTIONS

7.1. OVERVIEW

Work presented in this dissertation shows the development, characterization, and application of guest-host (GH) interactions in designing hydrogels with properties that are appropriate for biomedical applications. As described in Chapter 3, biomaterial systems based on this class of interactions are finding broad use in the fields of drug delivery, cell delivery, material implants, and even towards basic science applications.[1] Specifically, hydrogels engineered with GH interactions have been useful in the context of myocardial infarction (MI), as outlined in Chapter 1, largely due to their ability to be injected into tissues.[2-4] Through further engineering, this thesis expands the application of GH hydrogels to MI, by incorporating small molecule delivery or through multiplexing design where properties such as degradation, delivery, and cell invasion are included in a single system.[5]

More specifically, Chapter 4 described utilizing the reversible nature of cyclodextrin GH chemistry to tune small molecule sustained release for a number of model payloads as well as representative small molecule pharmaceuticals.[6] Chapter 6 described the development of granular hydrogels, formed through GH mediated assembly of microgel components, that allowed for the modular combination of different populations of microgels (each with different material design parameters, e.g. degradation, payload, etc) into a single bulk, injectable material with multifunctional properties.[7] Both of these advances in material design were then applied in models of MI. Chapter 5 described the design of GH hydrogels for the sustained release of

SD7300, an MMP inhibitor that requires local delivery, and the application of the hydrogel system to a porcine model of MI with clinically relevant timing and percutaneous delivery. Additionally, work at the end of Chapter 6 outlined the potential efficacy of multifunctional granular materials in treatment of MI, with a capacity for disease responsive behavior and tunable cell invasion properties. The remainder of this chapter will focus on the main conclusions, limitations, and future directions associated with each of these aims.

7.2. SPECIFIC AIM 1

DESIGN AN EASILY INJECTABLE GUEST-HOST HYDROGEL FORMULATION FOR SUSTAINED SMALL MOLECULE DELIVERY

7.2.1. CONCLUSIONS

In this aim, we were able to demonstrate the ability of cyclodextrin to modify the affinity of HA polymers for small molecules through the use of analytical calorimetric methods. When assembled into hydrogels through GH interactions, the inclusion of cyclodextrin altered the diffusion and bulk release of encapsulated peptides. We determined that these outcomes were tunable based on two key parameters: the level of cyclodextrin content in the GH hydrogels and the payload affinity for cyclodextrin. The mechanical properties of these materials were not greatly influenced by the encapsulation of small molecules, likely due to the higher relative affinity of cyclodextrin for adamantane, the interaction driving polymer association in this system. Ultimately, we were then able to use these parameters as a means to provide tunable sustained release of small molecule antibiotics and chemotherapeutics. This work has expanded the capabilities of injectable hydrogel systems to easily incorporate small molecule

sustained release, an important class of therapeutics that frequently require carriers such as these injectable hydrogels for efficacy.

7.2.2. LIMITATIONS AND FUTURE DIRECTIONS

Material systems developed in this chapter lay a foundation for simple strategies to provide sustained small molecule release from biomaterials; however, there are numerous instances where the findings could be expanded with further material iteration. Specifically, the studies were confined to the investigation of one host molecule (cyclodextrin) and only a handful of different guest molecules. Thus, the observed scope of the effects on sustained release remains somewhat limited. While this selection of host molecule was highly useful, due to the GRAS classification of cyclodextrin and its general use as a pharmaceutical excipient, it is possible that investigation of other host molecules such as cucurbits, etc could provide an even more pronounced effect on sustained release.[8,9] Furthermore, while we observed no significant effects of molecule encapsulation on material mechanics in the system investigated, it is possible that through competitive binding, small molecules with high affinity for cyclodextrin (i.e. approaching that of adamantane) could alter hydrogel mechanical properties.

Towards future studies, one important advance would be modeling to predict release profiles for small molecules encapsulated in GH hydrogels. In the case of other material systems such as PLGA microspheres, it is often simple to predictively generalize release profiles since release is largely controlled by material degradation and structure, and is largely independent of the nature of the selected payload.[10,11] Our experience with these systems is that release is not only controlled by material parameters (e.g., concentration, extent of modification), but also the specific interaction between material and payload, making it difficult to predictively generalize release profiles, although some groups have taken steps towards this in protein-based

systems.[12] Particularly with cyclodextrins, there is a wealth of molecule affinity data that could be directly integrated to a predictive modeling approach, or data that could be gathered using modeling software of molecular interactions.[13] Within models, variations in parameters such as host (cyclodextrin) concentration, guest (adamantane) concentration, drug concentration, and drug-host affinity, would be useful to quantitatively determine their effect on release *in silico* to guide the design of GH hydrogel formulations for future small molecule release.

7.3. SPECIFIC AIM 2

RELEASE A SMALL MOLECULE PROTEASE INHIBITOR FROM AN INJECTABLE GH HYDROGEL FOR TREATMENT OF MI

7.3.1. CONCLUSIONS

In this aim, we were able to design GH hydrogels as easily injectable materials for sustained SD-7300 release. First, we screened material formulations to assess shear-thinning properties to determine a formulation that balanced shear-thinning for injection, mechanical properties for deposition into tissue, and cyclodextrin content for SD-7300 retention. We determined a formulation that was easily injectable based on injection force testing, and assayed it for SD-7300 release. Hydrogels with encapsulated SD-7300 had sustained release over several weeks and showed MMP-2 inhibitory activity over this entire period, a timeline that is concurrent with the acute phase of MI. When investigated in a porcine MI model of ischemia-reperfusion, GH hydrogels could be injected and retained in the myocardial wall and localized small molecules to this region Animals received injections 3-5 days after MI of hydrogels containing SD-7300 with hydrogels or PBS injections alone used as controls. Gel/SD7300 treatment

improved functional outcomes such as ejection fraction, as well as histological outcomes including MI area and collagen content when compared to hydrogel or PBS injection alone. Thus, GH hydrogels were able to successfully sustain the release of SD-7300 to provide therapeutic efficacy in a clinically relevant, delayed injection animal model.

7.3.2. LIMITATIONS AND FUTURE DIRECTIONS

This study showed the development of GH hydrogels for the sustained release of SD-7300, and application in a porcine model of MI. As a pre-clinical model, this study was translationally focused, incorporating an ischemia-reperfusion infarct as well as delayed injection of hydrogels, both features that represent more common infarct and treatment scenarios in patients. This study, however, is not without limitations. This study was limited through necessary design choices in both materials and animal models. While logistically challenging to complete, a number of dosing studies are necessary to optimize both drug dosing and material volumes in the myocardium for specific drugs and material formulations. In depth clarification of these parameters will help to clarify the interplay between material bulking, and the biological effects targeted by therapeutic payloads such as SD-7300. Further developments of catheter/injection systems are needed, to provide assurance in the safety of material injection, to limit any risk of embolism upon ventricular injection of this material. This could include catheter-based or helical needle injections to afford surgeons increased control over material placement in the myocardial wall. Further, the scope of this project was confined to one inhibitor at a 3-day delayed timepoint.

Both timing of material injections and MMP inhibitor subtype have been shown to play a critical role in MI, often with optimal windows for material injection and specific MMP inhibition.[14-16] Future directions for this work could investigate the inhibitor treatment at a range of different injection time-points, to evaluate further efficacy of the

therapy. All studies completed here evaluated relatively short (~4 weeks) time points after infarct and administration of treatment for structure and function. As the effects of these therapies influence the long term progression of heart failure, it is important to consider analysis of much longer time points (i.e. months to years) after MI and treatment to gain a full understanding of the impact of these systems.

7.4. SPECIFIC AIM 3

DEVELOP AN INJECTABLE GRANULAR HYDROGEL SYSTEM FOR TREATMENT OF MI

7.4.1. CONCLUSIONS

In this aim, we showed the design of granular hydrogel systems that were injectable through the incorporation of GH chemistry. Microgels with adamantane chemistry were formed using a microfluidic approach that is scalable to high throughput production. These particles were assembled using CD-HA into brick and mortar type structures that were visualized using confocal microscopy. Furthermore, the mechanical properties of these systems were dependent on GH interactions between particles and CD-HA polymer incorporated into the system. Granular hydrogels developed in this aim were shear-thinning and self-healing, and were injectable through needles as small as 28 G. Through the design of intra-particle covalent crosslinking chemistry and payload encapsulation, particles were designed to encapsulate a range of payloads that released under a variety of conditions. These particle populations were combined into a single granular hydrogel, which represented the behavior of the specific microgel compositions (payload, release profile).

Multifunctional granular hydrogels were injected into infarcted and healthy myocardium in rats, and displayed disease responsive and disease independent

behavior in subpopulations of microgels in these systems. Furthermore, the granular nature of these materials allowed for high degrees of cell invasion, which is also dependent on particle design and disease interaction. Cell-material interactions are critical in this context, as cell invasion and the subsequent stimulation of inflammatory processes such as collagen deposition and vasculogenesis are beneficial to stabilizing the infarcted myocardium. In rat MI studies, we showed that granular systems themselves provide functional benefits, likely by influencing macrophage response and stabilizing the infarct through this response, as has been seen in previous studies.[17] Furthermore, we controlled cells invading the myocardium, by delivering the chemokine SDF-1α from an individual microgel component. Materials loaded with this chemokine were able to provide increased recruitment of CXCR4+ cells to the myocardium, and showed improved benefit in ejection fraction. This microgel system provides a platform for investigation of numerous therapeutic molecules to treat MI.

7.4.2. LIMITATIONS AND FUTURE DIRECTIONS

Materials developed in this aim provided a new avenue for material design by multiplexing material properties into a single system with controllable bulk mechanical properties for injection. Studies conducted in this aim do have several limitations. Animal studies in this aim were conducted in small animal models. While these studies are beneficial for throughput and gaining insight into material behavior in an *in vivo* context, there are limitations to testing myocardial injections in small animals. Due to the injected volumes of hydrogel in the rat myocardium, it is likely that in addition to the biological roles of these systems described in chapter 6, these granular systems are exerting a major effect through cardiac bulking. Furthermore, these systems were delivered concurrently with the generation of infract, which itself was a permanent ligation of cardiac vasculature. These approaches in an animal model are not representative of the

conditions these systems would experience in a clinical setting, in terms of both injection timing and potential tissue perfusion. Moving towards analysis in large animals can help to clarify the interplay between tissue bulking, cell invasion and vasculogenesis, and the effect of delivered payloads such as SDF.

These studies have also only shown early proof of concept for the use of granular systems as drug delivery depots. Due to the ease of combining numerous payloads, release rates, and degradation properties, these materials would make an excellent platform for complex drug delivery problems involving synergistic release of multiple payloads. Prior work has shown the benefits of delivering multiple factors to the myocardium associated with vasculogenesis, however, this could be expanded to introduce further targets such as cell recruitment and MMP inhibition.[18] Furthermore, this system lends itself to complex release profiles, which could be useful in timing-critical delivery challenges such as *in vivo* cell reprogramming, a process requiring sequential delivery of numerous factors.[19]

A final limitation of this work is that the scope of these materials was confined to the design of ~40 μm diameter microgel particles. The role of particle size could be investigated in future studies to determine the effect on both material mechanical properties, as well as induction of *in vivo* cell invasion and ECM deposition. Finally, the utility of these materials could be further expanded to basic science studies in cell culture and mechanobiology.

7.5. OVERALL SUMMARY

Overall, broad conclusions of this dissertation relate to the development of novel biomaterial function through the utilization of GH chemistry, and the application of these materials for myocardial infarction therapies. Through material design, we were able to

generate unique hydrogel systems that could deliver small molecules or provide combinatorial functionality. These platform systems are broadly compatible with a range of molecules for drug delivery, providing future potential investigating translational challenges such as the local delivery of small molecules, or more academic pursuits clarifying the nature of timing, and synergistic therapies in drug delivery strategies for MI. Hydrogel systems for drug delivery have enormous potential as an emerging class of therapeutics in the myocardium. As an understanding of the effects of biomaterials in the myocardium matures, studies and materials such as the ones of this thesis will form the groundwork for translation and solving clinical delivery challenges.

7.6. REFERENCES

1. Rodell CB, Mealy JE, Burdick JA. Supramolecular guest–host interactions for the preparation of biomedical materials. Bioconjugate chemistry. 2015;26(12):2279-89.
2. Rodell CB, Lee ME, Wang H, Takebayashi S, Takayama T, Kawamura T, et al. Injectable Shear-Thinning Hydrogels for Minimally Invasive Delivery to Infarcted Myocardium to Limit Left-Ventricular Remodeling. Circulation Cardiovascular interventions. 2016;9(10).
3. Rodell CB, MacArthur JW, Dorsey SM, Wade RJ, Wang LL, Woo YJ, et al. Shear-Thinning Supramolecular Hydrogels with Secondary Autonomous Covalent Crosslinking to Modulate Viscoelastic Properties In Vivo. Adv Funct Mater. 2015;25(4):636-44.
4. Tous E, Purcell B, Ifkovits JL, Burdick JA. Injectable acellular hydrogels for cardiac repair. J Cardiovasc Transl Res. 2011;4(5):528-42.

5. Hoare TR, Kohane DS. Hydrogels in drug delivery: Progress and challenges. Polymer. 2008;49(8):1993-2007.
6. Mealy J, Rodell C, Burdick JA. Sustained Small Molecule Delivery from Injectable Hyaluronic Acid Hydrogels through Host-Guest Mediated Retention. Journal of Materials Chemistry B. 2015.
7. Mealy JE, Chung JJ, Jeong HH, Issadore D, Lee D, Atluri P, et al. Injectable Granular Hydrogels with Multifunctional Properties for Biomedical Applications. Adv Mater. 2018;30(20):1705912.
8. Loftsson T, Brewster ME. Pharmaceutical applications of cyclodextrins: basic science and product development. J Pharm Pharmacol. 2010;62(11):1607-21.
9. Ma D, Hettiarachchi G, Nguyen D, Zhang B, Wittenberg JB, Zavalij PY, et al. Acyclic cucurbit [n] uril molecular containers enhance the solubility and bioactivity of poorly soluble pharmaceuticals. Nature Chemistry. 2012;4(6):503-10.
10. Rothstein SN, Federspiel WJ, Little SR. A unified mathematical model for the prediction of controlled release from surface and bulk eroding polymer matrices. Biomaterials. 2009;30(8):1657-64.
11. Rothstein SN, Federspiel WJ, Little SR. A simple model framework for the prediction of controlled release from bulk eroding polymer matrices. J Mater Chem. 2008;18(16):1873-80.
12. Vulic K, Pakulska MM, Sonthalia R, Ramachandran A, Shoichet MS. Mathematical model accurately predicts protein release from an affinity-based delivery system. J Control Release. 2015;197:69-77.
13. Rekharsky MV, Inoue Y. Complexation Thermodynamics of Cyclodextrins. Chem Rev. 1998;98(5):1875-918.

14. Yoshizumi T, Zhu Y, Jiang H, D'Amore A, Sakaguchi H, Tchao J, et al. Timing effect of intramyocardial hydrogel injection for positively impacting left ventricular remodeling after myocardial infarction. Biomaterials. 2016;83:182-93.
15. Iyer RP, de Castro Brás LE, Patterson NL, Bhowmick M, Flynn ER, Asher M, et al. Early matrix metalloproteinase-9 inhibition post-myocardial infarction worsens cardiac dysfunction by delaying inflammation resolution. J Mol Cell Cardiol. 2016;100:109-17.
16. Iyer RP, Patterson NL, Zouein FA, Ma Y, Dive V, de Castro Brás LE, et al. Early matrix metalloproteinase-12 inhibition worsens post-myocardial infarction cardiac dysfunction by delaying inflammation resolution. International journal of cardiology. 2015;185:198-208.
17. Tous E, Weber HM, Lee MH, Koomalsingh KJ, Shuto T, Kondo N, et al. Tunable hydrogel-microsphere composites that modulate local inflammation and collagen bulking. Acta Biomater. 2012;8(9):3218-27.
18. Awada HK, Johnson NR, Wang Y. Sequential delivery of angiogenic growth factors improves revascularization and heart function after myocardial infarction. J Control Release. 2015;207:7-17.
19. Buganim Y, Faddah DA, Jaenisch R. Mechanisms and models of somatic cell reprogramming. Nature Reviews Genetics. 2013;14(6):427.